

For Reference

NOT TO BE TAKEN FROM THIS ROOM

For Reference

NOT TO BE TAKEN FROM THIS ROOM

Ex LIBRIS
UNIVERSITATIS
ALBERTAENSIS



THESIS
1965 (F)
17 D

THE UNIVERSITY OF ALBERTA

COMPARATIVE PHYSICO-CHEMICAL STUDIES ON
CARDIAC TROPOMYOSINS

by

RUDOLPH FRANK KOUBA

A THESIS

SUBMITTED TO THE FACULTY OF GRADUATE STUDIES
IN PARTIAL FULFILMENT OF THE REQUIREMENTS FOR THE DEGREE
OF DOCTOR OF PHILOSOPHY

DEPARTMENT OF BIOCHEMISTRY

EDMONTON, ALBERTA

OCTOBER, 1965

UNIVERSITY OF ALBERTA

FACULTY OF GRADUATE STUDIES

The undersigned certify that they have read, and recommend to the Faculty of Graduate Studies for acceptance, a thesis entitled "COMPARATIVE PHYSICO-CHEMICAL STUDIES ON CARDIAC TROPOMYOSINS", submitted by Rudolph Frank Kouba in partial fulfilment of the requirements for the degree of Doctor of Philosophy.

Date

Oct. 25/65

ABSTRACT

Distinct and fundamental differences are known to exist between cardiac and skeletal muscle. These include the lesser tension generated by cardiac muscle and the relative slowness of onset of the active state of this muscle type when compared to its skeletal counterpart (31). The possibility exists that these physiological differences may well be a reflection of basic differences at the molecular level between the cardiac and skeletal muscle proteins. Experimental evidence to support this possibility has arisen from the observations that (i) the ATPase activities of cardiac actomyosin and myosin are considerably less than the corresponding activities of skeletal actomyosin and myosin (26) and (ii) the susceptibility of cardiac myosin to proteolytic hydrolysis differs from that of the homologous protein from skeletal muscle (6). Comparison of cardiac and skeletal actins has failed to reveal detectable differences in physico-chemical properties, amino acid composition, and number and reactivity of -SH groups (131). The present study has been concerned with a detailed physico-chemical study of the third of the more abundant cardiac myofibrillar proteins, tropomyosin, and comparisons have been made with its skeletal counterpart. Comparative studies on cardiac and skeletal muscle are subject to the criticism that a single species has not been utilized; most frequently the proteins isolated from dog hearts are compared with those of rabbit skeletal muscle. In order to explore possible species differences in molecular properties, comparative physico-chemical studies have been carried out on tropomyosin

homologues from beef and rabbit hearts.

The cardiac tropomyosins were isolated in homogeneous form by the ammonium sulfate fractionation procedure of Bailey (10), and were then subjected to detailed physico-chemical studies (sedimentation, viscosity, light scattering, diffusion and optical rotation). Essentially no significant differences in molecular properties were observed in the two cardiac tropomyosins; however, distinct differences between the cardiac and skeletal tropomyosin systems were clearly established. Molecular weights of beef and rabbit cardiac tropomyosin, evaluated both by the Archibald method and from integration of sedimentation-diffusion data via the Svedberg equation, resulted in a weight-average molecular weight of $\sim 100,000$, compared to 55,000 reported by other workers for skeletal tropomyosin. In addition, the molecular weight of beef cardiac tropomyosin was examined by means of the complete angular light scattering plot of Zimm and found to be similar to that found from hydrodynamics. The possibility that cardiac tropomyosin represented a dimeric form of the skeletal molecule was discounted on the grounds that exposure of this system to solvents known to dissociate proteins into subunits, such as 8M urea, did not reduce the molecular weight.

Differences in other parameters such as the diffusion constant and the weight intrinsic viscosity were also noted for the two systems. At the same time, however, similarities in other quantities such as the sedimentation coefficient and the degree of α -helix in the two molecules, as reflected by both optical rotatory dispersion and infra-red deuterium-

exchange studies, were established. The amino acid composition of cardiac tropomyosin resembled the skeletal pattern very closely in terms of high content of polar amino acids; however, the cardiac molecule possessed no measurable half-cystine residues.

The Scheraga-Mandelkern prolate ellipsoid model was satisfactorily invoked to interpret the hydrodynamic data for both cardiac tropomyosins, and to assess the extent of folding, or otherwise, of the polypeptide chains in the molecule. It was found that a composite two-three chain particle, 510 \AA long and 36 \AA wide, would satisfy the hydrodynamic data. A check of the length of the beef cardiac tropomyosin molecule, by means of the radius of gyration value from light scattering, resulted in a figure of 557 \AA , which agrees within experimental error with that assessed hydrodynamically for the major axis of the prolate ellipsoidal form.

In view of earlier light scattering studies carried out on rabbit skeletal tropomyosin which suggested that extensive aggregation of this molecule occurred in the absence of salt (35), a second aspect of this work has been concerned with a systematic study of the polymerization process of beef cardiac tropomyosin with decreasing ionic strength, using both ultracentrifugal and viscometric techniques.

Treatments of Steiner (112) and Rao and Kegeles (113) for reversibly interacting systems were applied in order to assess the compositional make-up and energetics of the

polymerization process at the different ionic strengths.

That the association of tropomyosin particles is dependent both on the protein concentration and ionic strength of the medium was established by the Archibald method for molecular weight determination, and the change in weight intrinsic viscosity. At any one protein concentration, as the ionic strength was decreased from 0.6, the appearance of n-mer species increased. The composition of the system with ionic strength was established as follows: at ionic strength 0.4 and 0.3, monomers and dimers coexist; at ionic strength 0.2, monomers and dimers are evident at low concentration and monomers and trimers predominate at higher concentration levels; and at ionic strength 0.1, monomers and trimers are present except at high concentration levels where the appearance of higher n-mer species is indicated.

The energetics of dissociation of dimer (concentration, 1 g/liter) at ionic strengths 0.3 and 0.2 resulted in free energy changes of -1812 and -1642 cal/mole dimer, respectively, and suggests that the dissociation process is a spontaneous one. On the other hand, trimer dissociation occurs with free energy changes of -102 and +27 cal/mole trimer at ionic strengths 0.2 and 0.3, respectively.

No significant change in any optical rotatory parameter accompanied the association process suggesting little alteration in secondary and tertiary structure attendant the phenomenon. On the basis of these observations, it was suggested that the association was largely electrostatic in nature and that the process was predominantly end-to-end.

Dedication

To my wife, Shirley, whose trust, encouragement
and patience has provided a foundation for this work.

ACKNOWLEDGMENTS

I wish to express my sincere appreciation, first of all, to my thesis supervisor, Dr. C. M. Kay, for his generous help and for giving so unstintingly of his time throughout the course of this work. I would also like to thank Dr. J. S. Colter and members of the Biochemistry Department who have all, from time to time, given me help and advice. In particular, I wish to thank Drs. W. A. Green and J. A. Verpoorte for numerous discussions and help during the assembly of the thesis, and Dr. L. B. Smillie for consultations on the amino acid analyses.

Special thanks are due to Mr. J. Durgo, Mr. T. Keri, and Mr. K. Oikawa for their skillful technical assistance. Mr. Edward Paradowski kindly ran the amino acid analyses reported herein, and Mr. Bob Swindlehurst of the Department of Chemistry carried out the infra-red determinations.

A special thanks is due Mrs. Laura Randall for her organizational help in the thesis assembly as well as its final typing.

Financial assistance in the form of a Dissertation Fellowship from the University of Alberta is gratefully acknowledged.

TABLE OF CONTENTS

	<u>Page</u>
Abstract	iii
Acknowledgments	viii
List of Illustrations.	xii
List of Tables	xvi
List of Abbreviations.	xviii
I. INTRODUCTION	1
Classification of Muscle Proteins and Myofibril Morphology.	1
Phylogenetic Differences in Proteins.	4
Purpose of Present Study.	6
II. METHODS AND MATERIALS.	8
Isolation of Tropomyosin.	8
Determination of Concentration.	8
Partial Specific Volume	10
Sedimentation Velocity.	11
Archibald Approach to Equilibrium	13
Amino Acid Analysis	16
Viscometry.	17
Diffusion Measurements.	18
Optical Rotatory Dispersion	22
Deuterium Hydrogen Exchange Technique	24
Light Scattering.	26
Background	
Specific Refractive Increment	
III. RESULTS	
Part A. Hydrodynamic Treatment of the Cardiac Tropomyosins	36
1. Homogeneity Studies and Preliminary Investigation of the Monomeric State	36

	<u>Page</u>
2. Molecular Properties of Monomeric Cardiac Tropomyosin.	39
(a) Sedimentation Velocity	39
(b) Partial Specific Volume.	40
(c) Diffusion Coefficient.	41
(d) Intrinsic Viscosity.	42
(e) Molecular Weight	43
(i) Archibald Method and the Svedberg Equation	43
(ii) Light Scattering.	46
(f) Optical Rotatory Dispersion Measurements (ORD)	48
(g) Deuterium-Hydrogen Exchange.	49
(h) Amino Acid Composition	51
3. Model Forms for Cardiac Tropomyosin Based on the Hydrodynamic and Thermodynamic Measurements	51
(a) Representation of Cardiac Tropomyosin in Terms of a Prolate Ellipsoid Model	51
(b) Effective Volume and Axial Ratio of the Prolate Model Form.	54
(c) Extension of the Cardiac Tropomyosin Molecule and Polypeptide Chain Arrangement.	57
Part B. Association Reactions of Beef Cardiac Tropomyosin in Low Ionic Strength Media	59
1. Introduction	59
2. Influence of Ionic Strength on the Molecular Weight, Viscosity and Diffusion Properties of Beef Cardiac Tropomyosin.	62
3. Reversibility of the Polymerization Process and Formulation of Expressions for the Nature of the Equilibrium State.	65

4.	Extent of Polymerization of Beef Cardiac Tropomyosin over the Ionic Strength Range 0.1-0.4 all at pH 7.0	67
5.	Determination of Equilibrium Constants for the Polymerization System at Ionic Strengths 0.2 and 0.3 . .	70
6.	Optical Rotatory Dispersion Measurements on the Polymerization Process	73
7.	Nature of the Polymerization Process	75
IV.	CONCLUSIONS.	77
1.	Hydrodynamic and Thermodynamic Parameters of Cardiac Tropomyosin.	77
2.	Size and Shape of Cardiac Tropomyosin . . .	79
3.	Phylogenetic Relationships.	81
4.	Association Reactions	82
5.	Suggestions for Further Investigation . . .	84
V.	BIBLIOGRAPHY	86
VI.	APPENDICES	95

LIST OF ILLUSTRATIONS

<u>Figure</u>	<u>Page*</u>
1. Diagram showing the behavior of the filaments in the I and A bands during changes in length of the myofibril according to the Huxley-Hanson sliding filament model.	2
2. Maximum ordinate plot for the determination of the apparent diffusion coefficient.	20
3. A schematic diagram of Rayleigh interference patterns produced in a diffusion experiment, and the determination of the number of fringes.	20
4. Typical Zimm plot for extrapolation of light scattering data	28
5. Absorption spectrum of rabbit cardiac (preparation M) and beef cardiac (preparation O) tropomyosin in 0.5M KCl, 0.067M phosphate buffer, pH 7.0	37
6. Reduced specific viscosity of beef cardiac tropomyosin	38
7. Concentration dependence of the sedimentation coefficient ($S_{20,w}$) of beef and rabbit cardiac tropomyosin	39
8. Kraemer plots of partial specific volume	40
9. A plot of apparent diffusion constant of beef cardiac and rabbit cardiac tropomyosin in 0.067M phosphate buffer, pH 7.0, with 0.5M KCl against protein concentration in g/ml	41
10. Shear rate of beef cardiac tropomyosin (c=.48%) using the multi-bulb calibrated Cannon viscometer	42
11. Reduced specific viscosity of beef cardiac and rabbit cardiac tropomyosin in 0.5M KCl, 0.067M phosphate buffer at pH 7.0 as a function of protein concentration	42
12. Concentration dependence of the apparent molecular weight of beef cardiac tropomyosin by means of the Archibald method	44
13. Concentration dependence of the apparent molecular weight of rabbit cardiac tropomyosin by means of the Archibald method	44

14.	Plot of the apparent molecular weight of beef cardiac tropomyosin versus protein concentration as derived by means of the Svedberg equation	44
15.	Plot of the apparent molecular weight of rabbit cardiac tropomyosin versus protein concentration as derived by means of the Svedberg equation. .	44
16.	Zimm plot for beef cardiac tropomyosin in 0.5M KCl, 0.067M phosphate buffer, pH 7.0.	46
17.	A Moffitt plot of the optical rotatory dispersion of beef cardiac tropomyosin in 0.5M KCl, 0.067M phosphate buffer, pH 7.0	48
18.	Optical rotatory dispersion of beef cardiac tropomyosin in 0.5M KCl, 0.067M phosphate buffer, pH 7.0 in the ultraviolet region.	48
19.	A Moffitt plot of the rotatory dispersion of rabbit cardiac tropomyosin in 0.5M KCl, 0.067M phosphate buffer, pH 7.0	49
20.	Optical rotatory dispersion of rabbit cardiac tropomyosin in the ultraviolet region	49
21.	Infra-red spectrum of beef cardiac tropomyosin in D ₂ O	49
22.	Infra-red spectrum of rabbit cardiac tropomyosin in D ₂ O	49
23.	Optical rotatory dispersion data on rabbit cardiac and beef cardiac tropomyosin in 8M urea, 0.5M KCl, 0.067M phosphate buffer, pH 7.0 . . .	50
24.	Experimental weight-average molecular weight (Archibald ultracentrifugation) versus tropomyosin (beef cardiac) concentration in 0.1 ionic strength medium, pH 7.0	62
25.	Weight-average molecular weight (Archibald ultracentrifugation) of beef cardiac tropomyosin versus protein concentration in 0.2 ionic strength medium, pH 7.0.	62
26.	Weight-average molecular weight (Archibald ultracentrifugation) of beef cardiac tropomyosin versus protein concentration in 0.3 ionic strength medium, pH 7.0	62

27.	Weight-average molecular weight (Archibald ultracentrifugation) of beef cardiac tropomyosin versus protein concentration in 0.4 ionic strength medium, pH 7.0	62
28.	Analysis of boundary spreading for beef cardiac tropomyosin (4.4 g/liter) in terms of the increase of the corrected second moment, m_2^0 ($1-\omega_{st}^2$), in 0.1 ionic strength buffer system .	64
29.	Diffusion coefficient of beef cardiac tropomyosin in 0.1 ionic strength buffer system (pH 7.0)	64
30.	Plot of $(M_w - M_l) / (2M_l - M_w)^2$ against beef cardiac tropomyosin concentration in 0.1 ionic strength medium	67
31.	Plot of $(M_w - M_l) / (2M_l - M_w)^2$ against beef cardiac tropomyosin concentration in 0.2 ionic strength medium	67
32.	Plot of $(M_w - M_l) / (2M_l - M_w)^2$ against beef cardiac tropomyosin concentration in 0.3 ionic strength medium	68
33.	Plot of $(M_w - M_l) / (2M_l - M_w)^2$ against beef cardiac tropomyosin concentration in 0.4 ionic strength medium	68
34.	Plot of $(M_w - M_l) / (3M_l - M_w)^3$ against beef cardiac tropomyosin concentration (c^2) for 0.1 ionic strength medium	68
35.	Plot of $(M_w - M_l) / (3M_l - M_w)^3$ against beef cardiac tropomyosin concentration (c^2) for 0.2 ionic strength medium	68
36.	Plot of $(M_w - M_l) / (3M_l - M_w)^3$ against beef cardiac tropomyosin concentration (c^2) for 0.3 ionic strength medium	68
37.	Plot of $(M_w - M_l) / (3M_l - M_w)^3$ against beef cardiac tropomyosin concentration (c^2) for 0.4 ionic strength medium	68
38.	Plot of $\frac{(1/2 AM_l r) dc/dr - c}{c_a e^{2\phi_l}}$	70

versus $e^{2\phi_l}$ for beef cardiac tropomyosin in 0.2 ionic strength medium (pH 7.0)

39.	Percent composition of beef cardiac tropomyosin in the form of monomers, dimers and trimers in 0.2 ionic strength medium (pH 7.0)	70
40.	Percent composition of beef cardiac tropomyosin in the form of monomers and dimers in 0.3 ionic strength medium (pH 7.0)	70
41.	Plot of $(M_w/XM_1-1)/XC$ versus XC of beef cardiac tropomyosin in 0.2 ionic strength medium, pH 7.0	72
42.	Plot of $(M_w/XM_1-1)/XC$ versus XC of beef cardiac tropomyosin in 0.3 ionic strength medium, pH 7.0	72
43.	Plot of maximum ordinate-area method for determination of beef cardiac tropomyosin diffusion coefficient	96
44.	Comparison of a normal distribution curve with the experimental diffusion curve obtained from measurements on 0.47% beef cardiac tropomyosin at pH 7.0	97
45.	Δd versus concentration of KCl at $\lambda = 435.8 \text{ m}\mu$	100

Plate

A.	Electron micrograph of longitudinal section of rabbit psoas muscle	2
B.	Ultracentrifugal pattern of purified beef cardiac tropomyosin at a concentration of 0.31 in 0.067M phosphate buffer, pH 7.0 containing 0.5M KCl and at 59,780 r.p.m.	36
C.	Ultracentrifuge schlieren pattern during the approach to sedimentation equilibrium (Archibald) of rabbit cardiac tropomyosin	59
D.	1. Rabbit cardiac tropomyosin ($c=0.467\%$) in 0.5M KCl - 0.067M phosphate buffer, pH 7.0, bar angle 75°	59
	2. Beef cardiac tropomyosin ($c=0.71\%$) in 0.067M phosphate buffer, pH 7.0, ionic strength 0.1, bar angle 75°	59
E.	Diffusion and Rayleigh interference patterns for beef cardiac tropomyosin in 0.5M KCl - 0.067M phosphate buffer, pH 7.0, and bar angle 50° ..	59

*Illustrations precede the pages indicated.

LIST OF TABLES

<u>Table</u>	<u>Page*</u>
I. Amino Acid Composition of Skeletal and Cardiac Tropomyosin	37
II. The Molecular Weight of Tropomyosin in 0.5M KCl - 0.067M Phosphate Buffer, pH 7.0 with Time of Centrifugation (Archibald Procedure) .	37
III. A. Partial Specific Volume of Beef Cardiac Tropomyosin as Determined from Amino Acid Composition	40
B. Partial Specific Volume of Rabbit Cardiac Tropomyosin as Determined from Amino Acid Composition	40
IV. The Intrinsic Molecular Weights of Cardiac Tropomyosin as Determined by the Archibald Method and the Svedberg Equation	44
V. Particle Weight of Beef and Rabbit Cardiac Tropomyosins from Archibald Measurements . . .	45
VI. Molecular Properties of the Monomeric Tropomyosins	50
VII. Calculated Values for the β -function, the Viscosity Increment, ν , the Frictional Ratio, f/f_0 , and the Axial Ratio, a/b , as Determined from the Scheraga-Mandelkern Equation for Beef and Rabbit Cardiac Tropomyosin	53
VIII. Frictional Ratios, f/f_0 , and Corresponding Axial Ratios, a/b , for Rabbit Cardiac and Beef Cardiac Tropomyosins at Infinite Dilution. . .	56
IX. Dimensions of the Equivalent Ellipsoid of Revolution Model for the Cardiac Tropomyosins.	56
X. Estimation of the Length of the Equivalent Prolate Ellipsoid Model for Beef Cardiac and Rabbit Cardiac Tropomyosins.	57
XI. Molecular Weight of Beef Cardiac Tropomyosin (Archibald Method) from Top Portion of the Cell at a Concentration of: (a) 3.5 g/liter, (b) 4.4 g/liter (both at ionic strength 0.1, pH 7.0) .	65
XII. Free Energy Expressions for Dimer and Trimer Forms	72

<u>Table</u>	<u>Page*</u>
XIII. Optical Rotatory Parameters for Beef Cardiac Tropomyosin at Different Ionic Strength Conditions	74
XIV. Molecular Weight and C-terminal Data for Some Tropomyosins	81
XV. Composition of n-mer Species of Beef Cardiac Tropomyosin at Various Ionic Strength Conditions	82

*Tables precede the pages indicated.

LIST OF ABBREVIATIONS

		<u>Units</u>
$S_{20,w}$	Sedimentation coefficient in water at 20°C.	Svedbergs (S)
$S_{20,w}^0$	Intrinsic sedimentation coefficient	"
$D_{20,w}$	Diffusion coefficient in water at 20°C.	Fick (cm ² sec ⁻¹)
$D_{20,w}^0$	Intrinsic diffusion coefficient in water at 20°C.	"
η_{red}	Reduced viscosity	dl/g
η_{sp}	Specific viscosity	"
$[\eta]$	Intrinsic viscosity	"
ν	Viscosity increment	-
a/b	Axial ratio	-
p	Axial ratio of ellipsoidal particle	-
V_e	Effective volume of ellipsoidal particle	\AA
f/f_0	Frictional ratio	-
β	Scheraga-Mandelkern function	-
M	Molecular weight of anhydrous particle	g/mole
M_{app}	Apparent molecular weight of anhydrous particle	"
M^0	Intrinsic molecular weight of anhydrous particle	"
\overline{M}_w	Weight-average molecular weight of anhydrous particle	"
M_1	Monomeric molecule weight of anhydrous particle	"
B	Second virial coefficient	moles-ml/g ²
C_0	Total concentration of macromolecule in arbitrary units (Archibald)	cm ²
dc/dx	Concentration gradient (Archibald)	cm
\overline{v}	Partial specific volume of anhydrous particle	ml/g
$[\alpha]_\lambda$	Specific rotation at wavelength	degrees
λ_c	Critical wavelength Yang/Doty plot	mμ
$[m']_\lambda$	Reduced residue rotation at wavelength	degrees
λ_0	Dispersion parameter Moffitt plot	mμ
a_0	Ordinate intercept Moffitt plot	degrees
b_0	Slope Moffitt plot	"
HEAH	Hard-to-exchange amide hydrogen	-
$E_{1\%}^{1cm}$	Extinction coefficient of protein	-
ORD	Optical rotatory dispersion	-
N	Avogadro's number	mole ⁻¹

I. INTRODUCTION

Movement, in its various forms, is considered one of the most typical vital phenomena. Existing at all levels of the evolutionary scale, from the movements of all living cells during cell division to the locomotion of some bacteria by flagella, it reaches its highest specialization and perfection in muscular contraction.

Progress made in understanding those forces responsible for biological mobility has centered mainly on muscle contraction. In recent years, examination of the fine structure of the muscle fiber, made possible by the electron microscope, has shed new light on the morphology and principal energy yielding reactions that physiologists and biochemists have been investigating for nearly a century. It must be admitted that knowledge of this process is far from complete. However, it may soon be possible to describe the fine structure of a functional unit within the muscle cell in terms of the molecules of which it is composed.

The majority of investigations have been carried out on skeletal muscles, especially in the determination of the contractile system and its protein constituents. Several recent reviews have been published which treat this subject thoroughly (1-4).

Classification of Muscle Proteins and Myofibril Morphology

Muscle proteins may be classified into several distinct



Electron micrograph of longitudinal section of
rabbit psoas muscle (by H. E. Huxley, see [2]).

Plate A

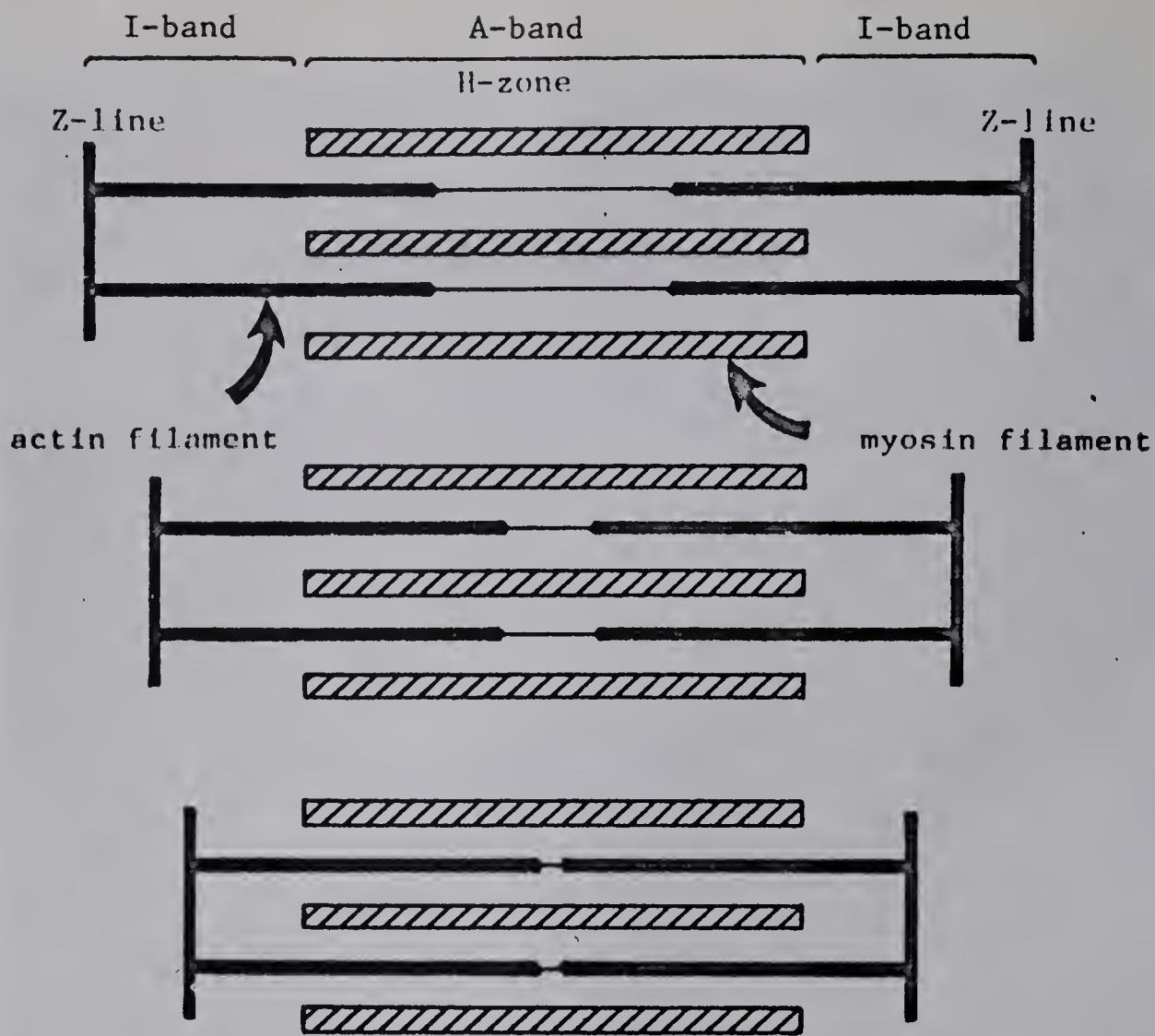


Figure 1

Diagram showing the behavior of the filaments in the I and A bands during changes in length of the myofibril according to the Huxley-Hanson sliding filament model (from H. E. Huxley cited in S. V. Perry [2]).

categories (5). The sarcoplasmic proteins are sometimes referred to as "soluble proteins" due to their ease of extraction. Included in this category are myoglobin, enzymes of the glycolytic system, and phosphokinase. These proteins do not contribute to the filamentous organization of muscle, but are mainly concerned with metabolic functions. Secondly, there are the proteins of the granules, which include the nuclear proteins, proteins associated with the sarcosomes, "relaxing factor" and enzymes of the oxidative cycle, that is, those associated with mitochondria. The proteins of the myofibrils constitute the third major classification. The myofibril consists mainly of the proteins myosin, actin, and tropomyosin in the proportions of approximately 50-55% myosin, 20-25% actin, and 10-15% tropomyosin (6).

The functional unit of muscle action is the myofibril: the contraction of a muscle fiber is made possible by the collective and coordinated shortening of the many myofibrils which comprise the fiber (see Plate A). Perhaps the greatest advance in this field recently has been in describing the different morphological features of striated (skeletal) muscle in terms of its component proteins, and in associating these features with the various stages of muscle contraction. The end result of these studies led Huxley and Hanson to propose the sliding filament model (7). Their findings were based on the observation that during stretch and contraction the I-band does all the changing in length, while the A-band does not change at all (7,8) (see Figure 1).

Section electron microscopy of the outer part of the

A-band under normal conditions reveals a double array of fibers consisting of both thin and thick filaments. Huxley suggests that the thin filaments are actin and the thicker ones myosin, and that the process of muscle action is a sliding of the one into the other, with the subsequent formation of cross-bridges between actin and myosin. Chemical energy in the form of ATP is utilized for this process. The current view is that myosin is localized in the A-band since extraction of the A-substance brings into solution approximately 95-100% of the myosin ATPase (9).

Tropomyosin, first discovered in rabbit skeletal muscle by Bailey (10), is a quantitatively significant component of the myofibril, but it has not been precisely localized cytologically nor is its role understood. It has been suggested by some workers (11,12) that tropomyosin crystals viewed in the electron microscope bear a close resemblance to the Z-band of the myofibril and thus may be a constituent of the Z-band. However, Perry and Corsi (13) have reported that selective extraction of myofibrils at low ionic strength removes the I-band and yields a solution free of myosin, but containing tropomyosin and inactive actin, suggesting that tropomyosin associates with actin in the myofibril (14,15).

In light of the above findings, it has been proposed by Marechal and Mommaerts that tropomyosin might act to retard the interaction between actin and myosin (16). Lowey and Cohen (17) have suggested that it may serve as a "backbone" upon which the myosin is deposited.

It is interesting to note that a protein similar in

many respects to vertebrate tropomyosin, termed paramyosin, has been implicated in the so-called "catch" mechanism in molluscan muscles. These muscles are characterized by their ability to resist stretch and to remain contracted over very long periods with little expenditure of chemical energy (18). Studies with model systems suggest that the great resistance to stretch in tonically contracted muscles is not entirely due to the active state of the contractile units themselves, but predominantly to the "set" of the fibrils containing paramyosin (19). Whether the role of tropomyosin is similar in function to paramyosin is not clear at the present time.

Phylogenetic Differences in Proteins

From the standpoint of function, it has been observed by many workers that certain portions of a biologically active protein molecule are more dispensible than others (20). This implies that a given protein molecule is fundamentally subject to variation and selection, as is the organism. Thus one might expect molecular differences to occur for a given protein depending on the species and tissue of origin. For example, alkaline phosphatase from swine kidney has a molecular weight of 37,000 compared to 60,000 for that found in the intestinal mucosa (20); α -amylase from barley malt is 59,000 while that from Bacillus stearothermophilus is 15,500 (21); and phosphorylase from dog liver is 250,000 (22) compared to 495,000 when found in rabbit muscle (23).

Investigations by Kaplan and his colleagues using immunological techniques have demonstrated that as embryonic skeletal muscle develops, the isoenzyme patterns change from

a cardiac type to the adult skeletal distribution (24). ATPase activity of myosin from skeletal muscle varies according to species, as reported by Bailey (25); and Brahms and Kay have found that in a given species, cardiac myosin has a lower ATPase activity than its skeletal counterpart (26). In addition, Dorothy Needham has observed a still lower ATPase activity for uterine myosin (27).

The state of development of the animal also appears to be significant in defining enzymatic properties. For example, investigations by Perry and Hartshorne (28) have shown that myosin isolated from skeletal muscle of the rabbit foetus has a lower ATPase activity than the protein from the corresponding adult tissue, and that the activity increases progressively with muscle development. These differences cited for the myosin component may reflect subtle or major differences in the structural characteristics of the protein (for example, in the primary, secondary, and/or tertiary structures). On the other hand, they might also reflect the presence of smaller molecules in any one myosin preparation, and these may be functioning as activators or inhibitors of enzymatic activity.

Distinct differences in primary structure for cardiac and skeletal myosin have been observed by Stracher (29) at the level of the -SH group involved in the ATPase active site. In addition, Kay and Brahms (30) have noted differences in molecular properties between the two myosin homologues, as well as differences in the susceptibility of the two molecules toward trypsin, the cardiac enzyme being much more resistant. It may well be that the observed physiological differences

between cardiac and skeletal muscle, that is, the lower tension per unit area developed by cardiac muscle and the relative slowness of onset of the active state (i.e., response of the contractile material to a stimulus) of cardiac muscle when compared to its skeletal counterpart (31,32), are intimately related to these molecular and enzymic differences. Comparative studies of homologous proteins, such as those outlined for cardiac and skeletal myosin, should provide information as to the minimum structure necessary for biological function as well as furnish additional criteria for establishing phylogenetic relationships.

Purpose of Present Study.

Tsao et al. (33), utilizing osmotic pressure measurements, have reported that tropomyosins from different species and different muscle types possess a wide range of molecular weights. The values reported for duck gizzard and pig cardiac muscle were 150,000 and 89,000 respectively, while prawn striated and sepia mantle smooth muscle had molecular weights of 77,000 and 68,000. However, investigations by Katz and Converse (34) have failed to demonstrate any difference between rabbit cardiac and skeletal tropomyosin. Comparative studies on cardiac and skeletal muscles are subject to the criticism that a single species has not been used; most frequently the protein isolated from dog heart has been compared with that from rabbit skeletal muscle.

The purpose of this project has been to investigate systematically physico-chemical and chemical parameters of cardiac tropomyosin isolated from two distinct species - beef and rabbit - as well as to compare these values with those reported for rabbit skeletal tropomyosin. By so doing, it was hoped to estab-

lish whether there are any species and/or organ differences in this fibrous protein.

Tropomyosin was considered an ideal model for these studies because it can be prepared in large yields with a high degree of purity. Also, some of its interesting molecular characteristics such as (a) formation of highly polymerized solutions at neutral pH in the absence of salt, (b) reversible depolymerization by salt, (c) resistance toward denaturing organic solvents and acid pH, and (d) high α -helical content, have made this protein a useful model for many protein investigations.

In view of the light scattering studies of Kay and Bailey (35) which suggest that rabbit tropomyosin undergoes extensive aggregation in the absence of salt, a second aspect of this work has been concerned with a systematic study of the polymerization process by means of ultracentrifugal and viscometric techniques. These studies have been integrated and examined in the light of recently developed treatments for reversibly interacting systems (36) in order to interpret the nature of the polymerization process in terms of kinetics and model forms.

II. METHODS AND MATERIALS

Isolation of Tropomyosins.

Cardiac tropomyosins were prepared according to the original Bailey procedure (10). In this method the muscle was minced, homogenized in a Waring blender and extracted with 50% ethanol followed by two changes of 95% ethanol, and finally two changes of ether in order to remove the soluble proteins and lipid material. The dried powder was extracted with M-KCl overnight at room temperature. The viscous solution was then precipitated at the isoelectric point (pH 4.5), the precipitate collected by centrifugation and dissolved in water. The tropomyosin was precipitated from this solution by addition of 41-70% saturated ammonium sulfate. This cycle of precipitation and salt fractionation was repeated twice, with the exception that the protein was collected in the 47-70% saturated ammonium sulfate range.

The tropomyosin was solubilized and dialyzed exhaustively against several changes of deionized water in order to remove traces of salt, prior to freeze drying. The lyophilized powder was stored in a vacuum desiccator over P_2O_5 and refrigerated until needed. The amount of tropomyosin obtained varied according to tissue and species, but was usually in the neighbourhood of 3 to 5%, based on dry tissue weight.

Determination of Concentration.

Concentrations were measured routinely by ultraviolet absorption at a wavelength of 278 mμ in a DU Beckman spectrophotometer. The concentration of protein may be calculated

on the basis of the extinction coefficient according to the following relationship:

$$\text{Optical Density} = E_{1\text{cm}}^{1\%} \times \text{Concentration of protein (g/100 ml)} \quad (1)$$

The basis for the extinction coefficient was the preparation of a solution of protein from a dried sample, the moisture content of which had been accurately determined. Samples used for the determination of moisture content were taken from a lyophilized preparation which had been exhaustively dialyzed against water to remove traces of salt. Part of this preparation was also used to make up a solution on a weight basis. Moisture content was determined by drying known weights of the freeze-dried preparation in vacuo at 105° for approximately 18-24 hours. At the end of this period, the weighing bottles and contents were transferred to a desiccator equipped with phosphorus pentoxide and allowed to cool to room temperature before re-weighing. A correction based on the percentage moisture content in the samples was applied to the amounts of protein weighed for optical density measurements.

By using equation (1), the corresponding $E_{1\text{cm}}^{1\%}$ was determined for the tropomyosin preparations. These values were 3.45 and 3.50 for beef cardiac and rabbit cardiac tropomyosin respectively, all in 0.5M KCl and 0.067M phosphate buffer at pH 7.0. Additional verifications of protein concentration were made using a modified form of the Folin-Biuret (39) procedure with bovine serum albumin*

*Armour Pharmaceutical Co., Kankakee, Ill.

as a standard, and micro-Kjeldahl nitrogen analysis (40), using ammonium sulfate as a standard.

Partial Specific Volume.

The experimental use of ultracentrifuge data from either Archibald approach to equilibrium or sedimentation velocity studies requires the evaluation of the term $(1 - \bar{v}\rho)$. Accurate values of partial specific volume, \bar{v} , are necessary since for most proteins the value is between 0.70 and 0.76 ml/g, and ρ , the density of solvent, is near unity. Thus an error of 1% in the determination of \bar{v} results in an error of $\sim 3\%$ in the calculation of molecular weights.

Measurements of \bar{v} involved the determination of the mass of a fixed volume of protein in a pycnometer for a series of known concentrations of protein. The procedure consisted in placing a protein solution in a 10 ml capped pycnometer of known volume to such a level that, after equilibration in a constant-temperature water bath, the insertion of the ground glass stopper caused air to be displaced with some overflow of protein solution. The capillary side arm was capped, the vessel completely wiped dry and immediately weighed in a semimicro Sartorius balance. In this way the pycnometer was filled routinely with a reproducible volume for the series of protein solutions measured.

The mass of the protein was calculated from the known protein concentration and the volume of the pycnometer. The weight fraction, w_1 , of the solute was determined by dividing the mass of protein by the mass of solution, which was readily available. The partial specific volume was deduced from the equation of Kraemer (41):

$$(1 - \bar{v}\rho) = \frac{1 - w_1}{m} \cdot \frac{dm}{dw_1} \quad (2)$$

by plotting mass content of pycnometer, m , against weight fraction of solute, w_1 . The slope of the plot, $\frac{dm}{dw_1}$, was then evaluated from the linear relationship obtained. The ordinate intercept (solvent point) yielded the mass content of the pycnometer filled only with solvent, and thus provided a check of the plot.

Another method used for determining the partial specific volume of the tropomyosins involved summation of the molar volumes of the constituent amino acids, as determined from their amino acid composition, in accordance with the procedure recommended by Cohn and Edsall (42).

Sedimentation Velocity.

Ultracentrifugal studies of the sedimentation properties of the tropomyosins were obtained using a Model E Spinco ultracentrifuge equipped with an RTIC (Rotor Temperature Indicator and Control) unit. A rotor speed of 59,780 rpm (250,000 x g), and a standard 12 mm single sector Kel-F center piece were used. The temperature of the rotor was maintained at $20 \pm 2^\circ\text{C}$ for most runs. Photographs were taken on Kodak metallographic plates at eight-minute intervals over a period ranging from 48 to 64 minutes. The plates were placed on a Gaertner two-dimensional comparator and aligned so that the meniscus was perpendicular to the cross motion of the comparator. Distances from the maximum ordinate to the reference hole were measured in each photograph and converted to true distance in the cell by dividing by the magnification factor of the schlieren optical system (2.138).

The distance from the axis of rotation to the reference hole is 5.70 cm, with an additional 0.02 cm introduced to allow for the expansion of the rotor at 59,780 rpm in accordance with the observations of Waugh and Yphantis (43). This value of 5.72 cm was added to the distance in the cell to give the total distance of the maximum ordinate from the axis of rotation, in centimeters.

The sedimentation coefficient is expressed as the velocity of the sedimenting molecules per unit field, and is given by the relation (44,45):

$$s = \frac{d(\ln x)}{\omega^2 dt} \quad (3)$$

or

$$s = \frac{1}{\omega^2 x} \frac{dx}{dt}$$

where x is the distance of the maximum ordinate in cm from the axis of rotation,

t is the time in seconds,

ω is the angular velocity in radians per second.

Integrating the above equation yields the following expression:

$$s = \frac{2.303}{\omega^2 (t_0 - t_1)} \left[\log x_0 - \log x_1 \right] \quad (4)$$

S was then obtained by plotting graphically the logarithm of the maximum ordinate ($\log x$) against (t) from which the slope of this line $\left(\frac{\log x_0 - \log x_1}{t_0 - t_1} \right)$ was calculated. This value

was multiplied by $2.303/\omega^2$ to give the sedimentation coefficient under the experimental conditions. However, sedimentation coefficients are usually reported as $S_{20,w}$, the value the protein would have in a solvent with the characteristics of water at 20° C. To obtain these standard conditions, the following equation was utilized (46):

$$S_{20,w} = S \left(\frac{\eta_T}{\eta_{20}} \right) \left(\frac{\eta}{\eta_o} \right)_T \left(\frac{1-\bar{v}}{1-\bar{v}_T} \rho_{20,w} \right) \quad (5)$$

where $\left(\frac{\eta_T}{\eta_{20}} \right)$ is the ratio of the viscosity of water at temperature T of the experiment relative to that at 20°C,

$\left(\eta/\eta_o \right)_T$ is the relative viscosity of the solvent to that of water at temperature T,

$\rho_{20,w}$ is the density of water at 20°C,

ρ_T is the density of the solvent at T°.

The partial specific volume, \bar{v} , was assumed to remain unaltered by temperature and solvent composition. This may not be completely true, as noted by Kay (47), but assuming that a large degree of selective binding does not exist, these differences would be small (48). Density and viscosity values were obtained from International Critical Tables or determined experimentally.

Archibald Approach to Equilibrium

One means of computing the molecular weight of proteins in the ultracentrifuge is the sedimentation equilibrium method. Considerable time may be required for the attainment of complete sedimentation equilibrium; however, molecular weights may be calculated from data obtained during the early part of a sedi-

mentation equilibrium run by use of the theoretical developments of Archibald (49). It has been pointed out by Archibald that from the moment of commencement of rotation, the sedimentation equilibrium equation holds true at the top and bottom of a liquid column in a centrifuge cell containing a solution of sedimentable solute. In other words, the conditions for equilibrium (transport of protein by sedimentation equals transport by back-diffusion) are fulfilled at these two positions in the cell at all times during a run. In the usual type of sedimentation equilibrium approach, the plateau region remains throughout the run so that measurements of the concentration distribution at the meniscus and the bottom of the cell will yield the molecular weight of the protein.

Evaluation of the concentration distribution was accomplished by performing two distinct runs on the protein in the ultracentrifuge. The first involved the determination of an area which was proportional to the total concentration of the protein in the solution (C_0). The value of C_0 was provided by an ultracentrifuge run using a synthetic boundary cell (50). An alternative procedure for estimating C_0 involved area measurements of the schlieren peak obtained in a sedimentation velocity run on the protein in question, carried out in a standard Kel-F cell. A second run was made at a much lower speed, usually in the range of 9,000 to 14,000 rpm, chosen so as to give a satisfactory gradient curve at the cell meniscus and cell bottom positions. Throughout both runs, the bar angle was maintained at 75° , since this angle position yielded the sharpest outlines of the plateau regions for the tropomyosins. The introduction of silicone

fluid onto the cell bottom facilitated the measurement of the gradient curve at this position; however, difficulty was encountered in the extrapolation of the ordinate intercept for the tropomyosin systems, and this was usually omitted.

Photographs of the sedimentation patterns were taken at 16-minute intervals over a period of 96 to 128 minutes. These were subsequently enlarged ten times and traced directly onto 1mm graph paper using the procedure of Erlander and Babcock (51). The concentration at the meniscus (C_M) was determined by the equation of Klainer and Kegeles (52):

$$C_M = C_O - \frac{0.1\text{cm}}{F \cdot x_m^2} \sum_{n=0}^{n_x} x_n^2 \frac{dc}{dx} \quad (6)$$

where C_O is the original protein concentration,
 0.1cm is the value of the interval between tabulated readings along the X-axis,
 F is the enlargement factor,
 X_m is the distance of the meniscus from the axis of rotation,
 X_n is the distance of the n^{th} interval from the axis of rotation,
 n_x is the number of intervals required to bring the ordinate (dc/dx) to zero,
 $n=0$ is the meniscus interval.

The molecular weight was obtained from the Archibald equation which is:

$$M_n = \frac{RT}{\omega^2 (1 - \bar{v}\rho)} \frac{(dc/dx)_m}{X_m C_m} \quad (7)$$

where M is the anhydrous molecular weight of the protein,
 \bar{v} is the partial specific volume,
 R is the gas constant (8.314×10^7 ergs/mole/degree),
 T is the absolute temperature,
 ρ is the density of the solution,
 ω is the angular velocity of the rotor in radians per second,
 C_m is the concentration at the position X_m ,
 $(dc/dx)_m$ is the concentration gradient at the position X_m .

The corresponding equation with the subscript b refers to the bottom of the cell. This method and its application are described in greater detail by Schachman (45).

Amino Acid Analysis.

The amino acid analyses were performed after protein hydrolysis in 6N HCl for 22, 30 and 72 hours at 110° . The hydrolyses were carried out in Pyrex tubes (25mm x 65mm) sealed off under vacuum. The hydrolysates were then evaporated to dryness in a rotory evaporator, and dissolved in a suitable amount of deionized water. One ml aliquots (proportional to about 1mg of protein) were then analyzed in a Spinco Model 120 B amino acid analyzer according to the method of Moore et al. (53,54). The values of the residues were calculated on the basis of number of moles per 100,000 g of protein. The yields of serine, threonine, amide nitrogen, methionine and tyrosine were extrapolated to zero time to correct for hydrolytic destruction.

Viscometry.

These measurements were made in Ostwald-type viscometers of 6.5ml capacity, having flow times of ~ 250 seconds for water. The usual procedure was to prepare a stock solution of about 1.5% protein and dialyze it overnight against the appropriate buffer. The buffer was then passed through a millipore filter of pore size 0.45 microns to remove any dust particles. It was found that if clarification of protein was achieved by means of the millipore filter, the resulting solution exhibited anomalies in both specific viscosity and molecular weight values, due to fibril formation. As a result, in order to effect clarification, the protein was subjected to centrifugation in a Model L Spinco preparative ultracentrifuge at 20,000 rpm for 20 minutes.

Prior to use, the viscometer was washed several times with a dilute solution of Ninol* detergent, followed by rinses with tap water, deionized water and several treatments with acetone. An aspirator pump equipped with a trap was used to pull the liquid through the capillary. Air was pulled through by the same pump in order to insure complete dryness of the interior surface.

Serial dilutions were made on the stock protein solution, and the resulting concentrations were determined spectrophotometrically. The flow time of each solution was determined in addition to that of the solvent, and seldom deviated for a given solution by more than 0.3 seconds. The solvent flow

* Beckman Instruments Corporation

time for a particular viscometer did not vary by more than 0.4 seconds in any of the experiments.

The density difference between solution and solvent due to the contribution of protein was ignored. Temperature was accurately maintained at 20°C by placing the viscometer in a thermostatic bath* coupled with a refrigeration unit. Specific viscosities (η_{sp}) were calculated from the flow times of solution and solvent without considering the kinetic energy correction.

The specific viscosity, η_{sp} , is expressed as $\eta_{sp} = \eta - \eta_0 / \eta_0$ where η is the viscosity of the solution, and η_0 is the solvent viscosity. Knowing the concentration and specific viscosity of the solution, the reduced viscosity (η_{sp}/C) may be obtained.

The weight intrinsic viscosity $[\eta]$ was determined by plotting reduced viscosity versus concentration and extrapolating the curve obtained to zero concentration. The intercept of the reduced viscosity axis was taken as the weight intrinsic viscosity $[\eta]$ (55).

Diffusion Measurements.

Measurements were made at 1.5°C in a Spinco Model H electrophoresis-diffusion apparatus equipped with the Rayleigh interference optical system. The protein solution was dialyzed against a large volume of buffer solution for 18 hours and then clarified by centrifugation. Prior to use, the diffusion cell and rack were placed in the thermostatically controlled water-

* Scientific Development Company, State College, Pa.

ethylene glycol bath to pre-cool the cell. This was done to diminish the likelihood of air bubbles forming when the cold protein solution was placed in a warm cell. Following introduction of the protein solution into the cell, the buffer was carefully layered on top and the boundary sharpened by the siphoning procedure of Kahn and Polson (56) which is described fully by Schachman (45). The protein concentrations used were from 0.20 to 0.90%. Total duration of the experiment was 64 to 96 hours with photographs being taken on Kodak Ortho film at approximately eight-hour intervals.

A majority of the diffusion coefficients were calculated by means of the maximum ordinate-area method. Use of the Rayleigh fringe and second moment methods provided a means of double-checking the values obtained. In the maximum ordinate-area method (57,58) the following relationship is used:

$$\frac{A^2}{Y_{\max}^2} = 4 k^2 \pi D (t - t_0) \quad (8)$$

where A is the area between the gradient curve and the base line at time t , measured from the instant when the synthetic boundary was created (t_0).

Y_{\max} is the maximum height of the gradient curve (maximum ordinate),

k is the magnification factor of the apparatus,

D is the diffusion coefficient.

The total area beneath the gradient curve was measured from photographs which were placed in a photographic enlarger and traced directly onto 1mm graph paper. These values were averaged to give an area proportional to the concentration.

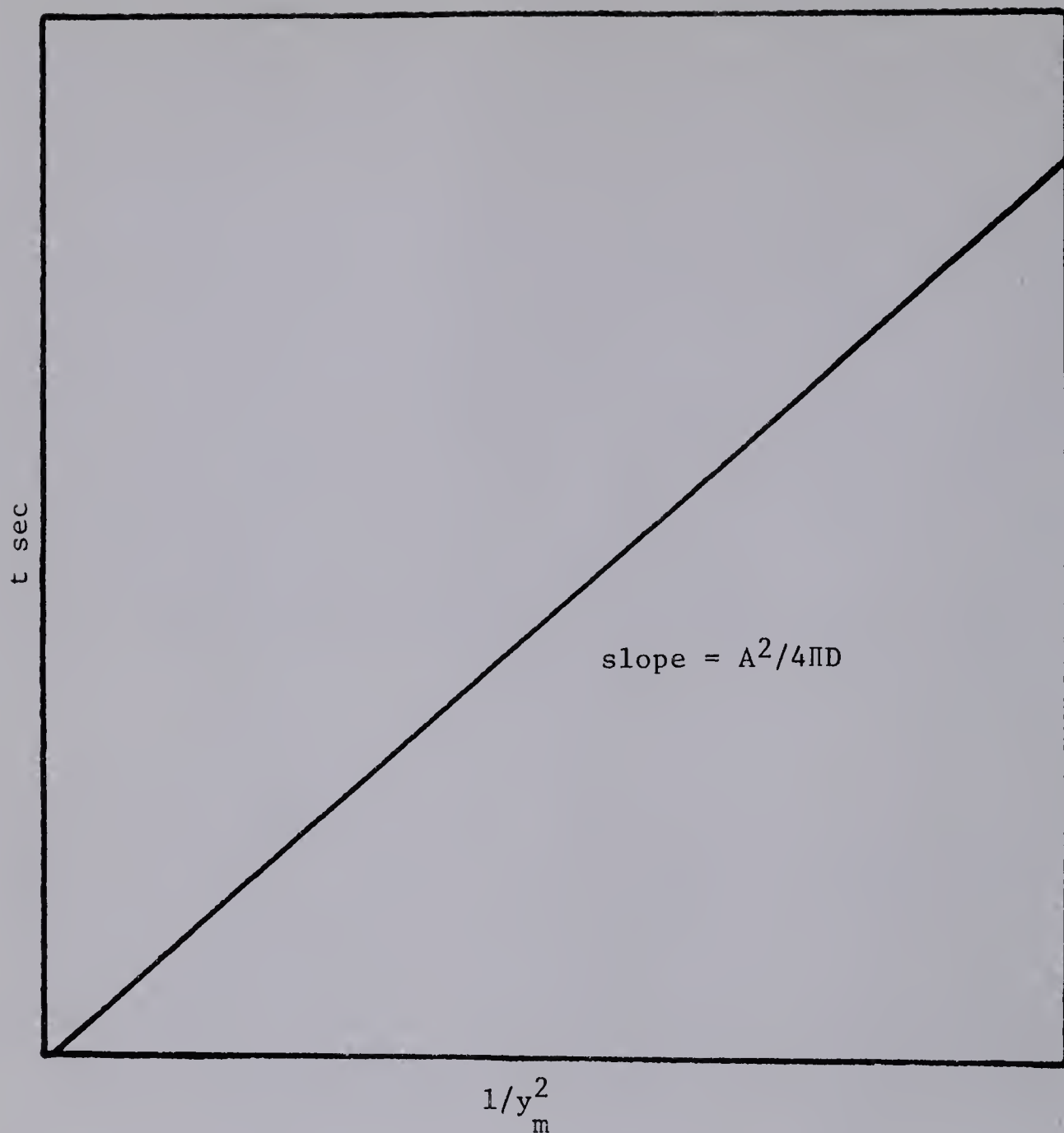
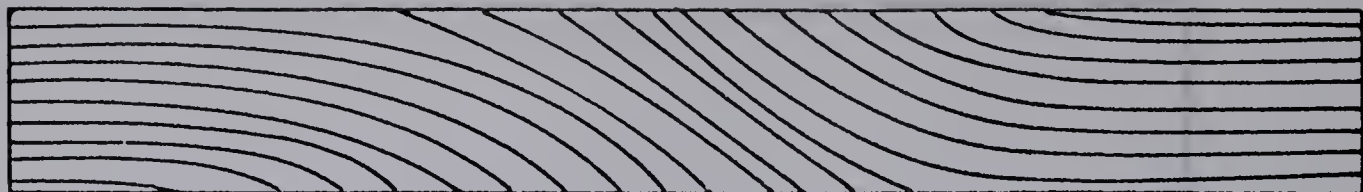


Figure 2

Maximum ordinate plot for the determination of the apparent diffusion coefficient.



solution

solvent

$J = 13.3$ fringes

Figure 3

A schematic diagram of Rayleigh interference patterns produced in a diffusion experiment, and the determination of the number of fringes.

The maximum ordinate for each photograph was measured in centimeters in a two-dimensional comparator. The maximum ordinates (Y_{\max} values) were squared and the reciprocals of the squares ($1/Y_{\max}^2$) were plotted versus the recorded time in seconds. From such a plot, the slope, $A^2/4\pi D$, was obtained (see Figure 2). The apparent diffusion coefficient, D , may then be calculated based on knowledge of the area, A .

The second moment method as outlined by Neurath (59) and Greenberg (60) was applied as an alternative means of determining diffusion constants. Experimentally, the diffusion curve was treated statistically in order to obtain the standard deviation, \sim . This deviation is related to the second moment, μ_2^0 , of the diffusion curve about the central axis* according to the expression $\sim^2 = \mu_2^0$ which in turn is related to the diffusion constant as follows:

$$D = \frac{\sim^2}{2t} \quad (9)$$

Thus, the quantity \sim in this expression is the distance through which a molecule has migrated in a given time from the original boundary.

The Rayleigh fringe method was the third technique used to calculate diffusion constants. Rayleigh interference patterns (fringes) (see Fig. 3) are composed essentially of a section of a plot of refractive index against cell distance. Since the refractive index of a protein varies linearly with respect to solute concentration, this method provides a plot of solute

* Also called the centroidal ordinate, in which the first moment is equal to zero.

concentration against cell distance. A plot of the fringe number as a function of fringe position would be similar to the integral of the curve obtained by the schlieren method. As diffusion takes place in the cell, refractive index gradients will be set up in the solution resulting in a shift of the fringe patterns. The refractive index gradients are directly proportional to the changes in concentration in the cell, and therefore, the fringe shift is directly proportional to concentration changes. In order to calculate the diffusion constant, the total number of fringes, J , must be evaluated as well as the distance between a pair of fringes (one on each side of a boundary), X_1 and X_2 . Calculations involving these parameters were made as outlined in detail by Longworth (61) and illustrated by Schachman (45).

The apparent diffusion constant derived by any of the above methods must be corrected to the value for water at 20° through the use of the following expression:

$$D_{20,w} = D_{app} \left(\frac{293}{273 + t} \right) \left(\frac{\eta_{solv}}{\eta_w} \right) \left(\frac{\eta_{t,w}}{\eta_{20,w}} \right) \quad (10)$$

where t is the temperature of the diffusion experiment in degrees centigrade,

$\frac{\eta_{solv}}{\eta_w}$ is the relative viscosity of the solvent to that of water,

$\frac{\eta_{t,w}}{\eta_{20,w}}$ is the viscosity of water at the temperature of the experiment and at 20° respectively.

The value of $D_{20,w}^0$ was obtained by plotting $D_{20,w}$ as a function of concentration and extrapolating to infinite dilution.

Optical Rotatory Dispersion.

The secondary structure of proteins is frequently expressed in terms of the content of right-handed α -helix in the polypeptide chain, the assumption being made that the only other conformational form present in the molecule is the random chain. This, of course, is not strictly true since there might well also be present β -structure or sections of the polypeptide chain coiled into left-handed α -helices. Unfortunately, present optical rotation theory as applied to proteins does not allow estimates of the amounts of all four conformational forms in any one molecule.

Two widely used methods, involving optical rotatory dispersion measurements, have been employed for estimating the amount of right-handed α -helical content in synthetic polypeptides and proteins. One of these, the Moffit type plot (62), expresses partial helical content in the visible region (340-600 $m\mu$); and the other relates helical content to the amplitude of the negative conformational Cotton effect at 233 $m\mu$ in the ultraviolet region (63). A complete review on this subject has been reported by Urnes and Doty (64).

In this study a Rudolph Model MSP-4 manual spectropolarimeter * and a Cary Model 60 automatic recording spectropolarimeter** were used to measure the optical rotation

* Rudolph Instruments, Little Falls, New Jersey

** Applied Physics Corporation, Monrovia, California

of the protein solutions as a function of wavelength. The wavelength ranges covered were 320-600mμ, 280-320mμ and 220-280mμ for which the cell path lengths employed were 0.5, 0.1 and 0.01 dm respectively. Generally, a tropomyosin solution of 0.3% was used in the visible region, whereas the ultraviolet region required only 0.03% due to the large rotation in this region.

The Moffitt equation (62) is represented as follows:

$$[m'] = \frac{a_0 \lambda_0^2}{\lambda^2 - \lambda_0^2} + \frac{b_0 \lambda_0^4}{(\lambda^2 - \lambda_0^2)^2} \quad (11)$$

where $[m'] = \frac{3}{n^2 + 2} \cdot \frac{m}{100} [\alpha]$ is equal to the effective residue rotation,

$[\alpha]$ is the specific rotation in c.c. deg./gm dm,

λ is the wavelength at which the rotation is measured,

M is the average residue weight,

n is the refractive index of the solvent.

The Moffitt equation was plotted as $[m'] \frac{\lambda^2 - \lambda_0^2}{\lambda_0^2}$ versus $\lambda_0^2 / \lambda^2 - \lambda_0^2$ from which the slope corresponded to b_0 and the intercept to a_0 . The value of λ_0 was taken to be 2120 Å in accordance with that found for polyglutamic acid in terms of linearizing the Moffitt plots (64). The percentage helical content was calculated from the b_0 (helix constant) value on the assumption that a figure of -640 degrees characterizes a fully coiled, right-handed α-helix (62).

Confirmation of helical contents deduced from Moffitt plots was achieved by calculating the depth of the rotation trough in

terms of percent helix at 233m μ (63). As a reference, the mean residue rotation values, $[m']_{233}$, of a completely helical and random coil polypeptide at 233m μ were used. According to McCabe and Yang (65) these corresponded to 16,600° and -2000° for the α -helix and random coil conformations respectively.

Deuterium Hydrogen Exchange Technique.

Exchange of the hydrogen atoms of a protein with the deuterium atoms of the surrounding medium has provided biochemists with valuable information on the secondary structure of proteins. The pioneer investigations of Linderstrøm-Lang (66,67) have shown that hydrogen exchange in protein solutions of measurable helical content is generally characterized by a much reduced rate of exchange compared with that of randomly coiled polypeptides. Subsequent investigations have led toward the study of the deuterium exchange of proteins and polypeptides - the objective being to correlate the number and rates of hydrogen exchange to the overall conformation of the molecules. Those hydrogens in the molecule which are involved in an ordered structure such as an α -helix will exchange more slowly with the hydrogens of the medium in which the protein is dissolved, than will the hydrogens of side chain groups or of CONH bonds outside the ordered region. It is precisely this relative stability which the technique of deuterium exchange can measure.

The gradient-density technique of Linderstrøm-Lang has been the most widely used procedure for hydrogen exchange measurements. However, another procedure for measuring hydrogen exchange (and the one used here) is the study of infrared spectra. In the early work of Ambrose and Elliot (68) it was noted that

the infrared spectra of polypeptides depended upon their chain conformations. Further, the amide I band (C=O stretch) and the amide II band (NH deformation) could be used to gain information about the polypeptide conformation.

Blout and his colleagues utilized an infrared spectroscopic method which measured the rate of hydrogen to deuterium exchange in proteins and polypeptides (69). The method takes advantage of the fact that the absorption peak of the amide II band, at a frequency of 1550cm^{-1} in the infrared, shifts to a frequency of about 1450cm^{-1} when the hydrogen is replaced by a deuterium atom, whereas the amide I band remains constant (70-2).

In order to calibrate this exchange, polyglutamic acid was examined both in the helical and random configurations, from which a relationship between the optical densities of the amide I and amide II bands was determined (69). This calibration curve was found to hold true for proteins as well. It was observed by these workers that the random conformation exchanges within ten minutes, while the helical conformation requires several hours in order to achieve complete exchange. Thus the term "hard-to-exchange amide hydrogen" (HEAH) refers to the amount of non-exchangeable hydrogen remaining after ten minutes. By determining the optical density of the amide I band of a protein solution, it was possible to obtain from the calibration curve the corresponding optical density of the amide II band, labelled (b), for a completely helical protein. The actual value of the amide II band (b') was determined experimentally from the infrared spectrum. These values are expressed as:

$$\% \text{ HEAH} = b'/b \times 100 \quad (12)$$

In practice, the protein was dissolved in D_2O and the infrared spectra determined after 20 minutes, care being taken to avoid undue exposure to atmospheric water vapor. Spectra between 1700 and 1200cm^{-1} were taken in a Perkin-Elmer Model 21 double beam spectrophotometer. An identical sample was heated, usually for two hours at 65°C depending on the nature of the protein. The heating resulted in the complete disappearance of the amide II band, and the resulting spectrum was used to provide a base line for estimation of the change in optical density of the amide II band. The difference between the base line and peak corresponds to b' in the equation for HEAH.

Light Scattering.

Background. The method of light scattering has become a standard technique for studying the size, shape and degree of aggregation of proteins and polypeptides. Only a general treatment concerning some of its basic aspects will be presented in this section. There are several excellent reviews on the theory of light scattering (73,74), as well as its application to biological problems (75), which were consulted prior to using this method for the study of tropomyosin.

The method originates from the observations of Lord Rayleigh (76) that small isotropic particles scatter light according to the following expression:

$$\frac{I_\theta}{I_0} = \frac{8\pi^4 \sqrt{a^2}}{\lambda^4 r^2} (1 + \cos^2 \theta) \quad (13)$$

where i_{θ} is the excess intensity of light scattered (over that of solvent) at angle θ compared to the incident light intensity, I_0 ,

r is the distance from the scattered particle to the observer,

a is the polarizability of the scattered point,

λ is the wavelength of light in vacuo,

ν is the number of scattered particles in a unit volume.

When a beam of incident light is passed through a turbid medium, a reduction in light intensity occurs which is related to the quantity known as the turbidity, \mathcal{T} . The expression for the turbidity is analogous to the extinction coefficient in the Beer-Lambert equation viz.:

$$I = I_0 e^{-\mathcal{T}l} \quad (14)$$

where l is the optical path length through the solution. Integration of equation (14) leads to the following expression relating turbidity and reduced intensity:

$$\mathcal{T} = \frac{16\pi}{3} R_{\theta} \quad (15)$$

The reduced intensity is related to the molecular weight of the particle, from the following expression (77,78):

$$\frac{Kc}{R_{\theta}} = \frac{1}{M} + 2Bc \quad (16)$$

where B is the second virial coefficient (the interaction term) and K is a constant characteristic of a given solution under a definite set of experimental conditions.

Experimentally, it is possible to measure either the turbidity (\mathcal{T}) or the reduced intensity (R_{θ}) of the solution;

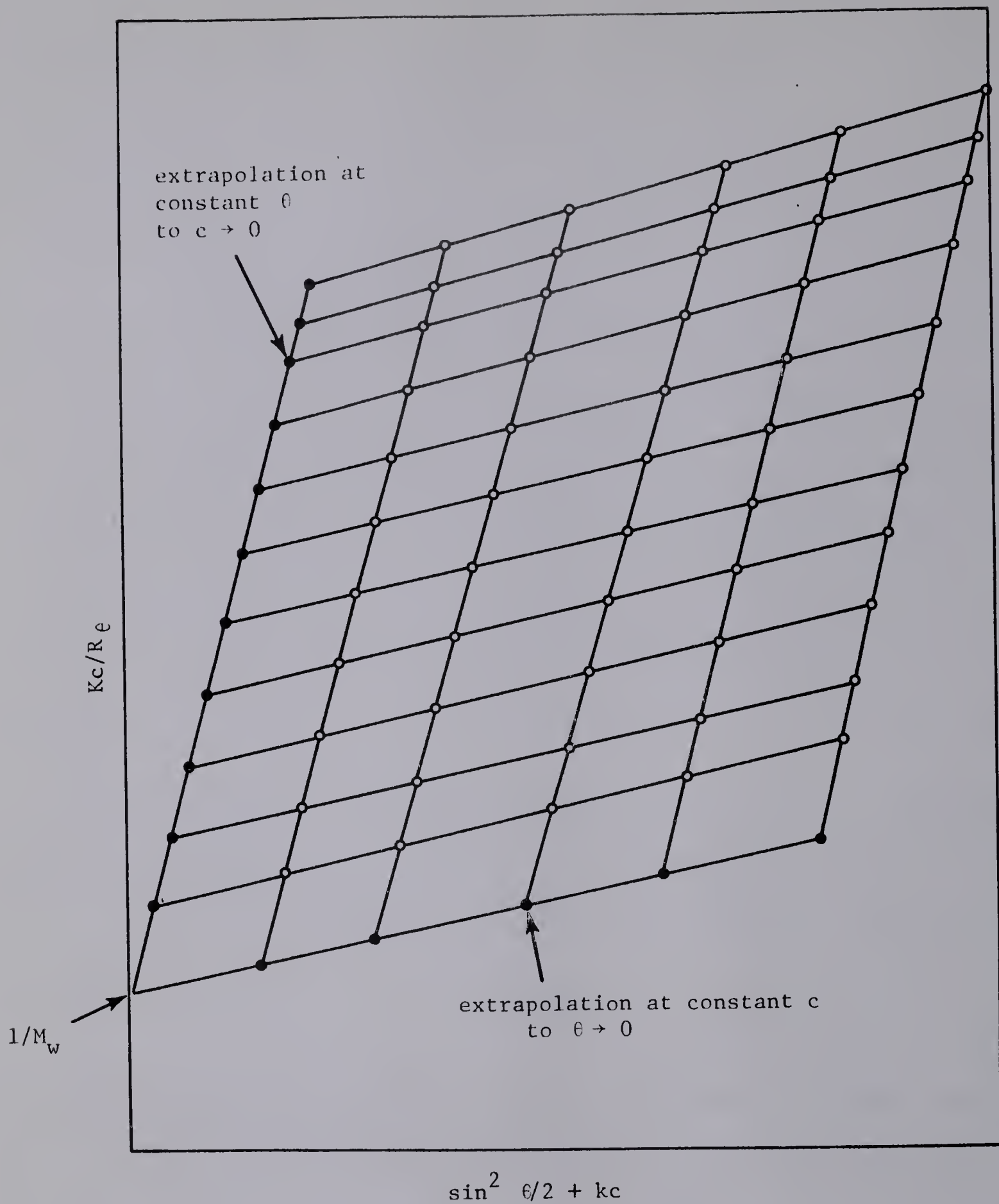


Figure 4

Typical Zimm plot for extrapolation of light scattering data.

however, it is more practical to measure the amount of scattered light directly, i.e. R_θ , because of the high sensitivity of the photomultiplier tube. Generally, the diminution in the intensity of the incident beam (\mathcal{I}) is too small to be accurately measured.

The above treatment assumes that the scattering particles have a dimension of only $1/20$ that of the wavelength of light. In the case of larger particles, internal interference of the scattered light occurs which causes a reduction of scattered intensity with increasing scattering angle θ . In such a case R is no longer a constant but depends on θ . At angles of θ greater than 0 degrees the light scattered by large particles is reduced by a particle scattering factor designated as $P(\theta)$. It was necessary to use this particle scattering factor to correct for the observed R_θ values.

The evaluation of $P(\theta)$ was effected using the well-known Zimm plot method (79). This technique involved plotting the values of Kc/R for different values of c and θ as ordinate, against values of $\sin^2 \frac{\theta}{2} + kc$ as abscissa. Here k is an arbitrary constant chosen to space the points conveniently and to facilitate the extrapolation to zero angle and concentration. Lines were drawn through each point at constant angle and constant concentration and then extrapolated to their zero values. These zero points were joined by two lines which met at the common intercept on the Kc/R_θ axis (Figure 4), from which the weight-average molecular weight was evaluated. The second virial coefficient, B , was obtained from the slope of the zero

angle line, and the radius of gyration of the particle was deduced from the ratio of the slope of the zero concentration line to the intercept value, i.e.,

$$\frac{\text{limiting slope}}{\text{intercept}} = \left(\frac{16\pi^2}{3\lambda^2} \right) R_g^2 \quad (17)$$

where R_g is the radius of gyration.

The particles of the various configurational types such as rods, spheres and coils have different radii of gyration. Therefore, the dimension of the scattering particle may be evaluated from the radius of gyration according to the following relationships:

If the particle is a sphere of radius r , then:

$$R_g^2 = \frac{3}{5} r^2 \quad (18)$$

For a long straight rod of length L , the expression is:

$$R_g^2 = \frac{L^2}{12} \quad (19)$$

while for random coils of end to end distance, r , the radius of gyration corresponds to:

$$R_g^2 = \frac{r^2}{6} \quad (20)$$

and

$$R_g^2 = \frac{R^2}{20} \quad (21)$$

for prolate ellipsoids where R is the length of the major axis (80).

The absolute calibration of the Brice-Phoenix Photometer* was determined for the standard square cell and wide

* Phoenix Precision Instrument Company, 3803-05 North 5th Street, Philadelphia 40, Pa.

slit system according to the procedure outlined by Yang (81) and the manufacturer's operational manual.

Since all measurements on the protein and buffer solution were carried out in cylindrical cells*, it was necessary to determine a cell constant. This constant correlates the light scattering of the cylindrical cell reaching the phototube at 90° in the narrow slit system to that of the standard square cell and wide slit system. The procedure followed in measuring this constant is described by Yang (81).

Dust-free water was added to the square cell and the ratio of scattered light at 0 and 90° was recorded. This water was then pipetted into the cylindrical cell to be calibrated, and the ratio of light scattering at 0 and 90° was again measured. This procedure was repeated for both the square and cylindrical cells, using a dilute dust-free Ludox solution instead of water. The use of Ludox, a colloidal silica, has been suggested by Alexander and Stacey (82), as well as Oster (83), as an ideal particle scatterer since it does not exhibit any selective absorption of dissymmetry. The Ludox solution was prepared to provide a scattering intensity approximately equal to that expected for the protein solution which is about 10 to 20 times more than water.

Light intensity measurements on the cylindrical cell were always made with the narrow slit system, while the wide slit system was used in the square cell measurements.

The cell calibration constant, a , was determined from

* Cells used were made of a Pyrex cylinder with a height of 12 cm and a diameter of 4.5 cm. Faces were ground flat at the exit and the entrance positions of the incident light beam.

the following expression:

$$a = \frac{F G_{90}/G_0 \text{ Ludox, square cell}}{F G_{90}/G_0 \text{ Ludox, cylindrical cell}} - \frac{F G_{90}/G_0 \text{ water, square cell}}{F G_{90}/G_0 \text{ water, cylindrical cell}} \quad (22)$$

where F = filter factor used,

G_{90} = recorder reading at 90° ,

G_0 = recorder reading at 0° .

In order to check the symmetry of the cylindrical cell, it was necessary to determine the angular dependence of the light scattered from a fluorescein solution. This was accomplished by using dust-free water and measuring the scattering of the cell over a range of 30° to 135° to the incident beam. Next, a dust-free solution of sodium fluorescein was added to the cell and the fluorescence was measured over the angular range given above. Calculations for each angle measured were determined from the following equation:

$$K = \left[(F G_\theta/G_0)_{\text{fluorescein solution}} - (F G_\theta/G_0)_{\text{water}} \sin \theta \right] \quad (23)$$

The value of K should not vary more than 1% at the different angles measured.

One of the factors involved in the absolute calibration of the Brice-Phoenix photometer was the consideration of proper corrections for reflection effects (84,85). Calibrations were usually performed at $\theta = 90^\circ$ using square cells. Reflection effects may not be the same for cells of different shapes or at angles other than 90° . Therefore, measurements

made under these conditions must be corrected so that application of the instrument constant determined during the square cell calibration will provide the proper R_{θ} values.

In the case of angular measurements in cylindrical cells, the effect of the frosted inside face of the cell (0° to $+180^{\circ}$) on reflection from the air-glass interface was determined by Tominatsu and Palmer (86,87). The Tominatsu-Palmer (T-P) reflection correction was applied for all the angles measured in the cylindrical cell.

In preparing solutions for light scattering, preliminary clarification procedures similar to those used for viscosity were adopted. Stock solutions of the protein, used directly in light scattering measurements and for making up more dilute solutions, were centrifuged for at least 45 minutes in the Spinco Model L ultracentrifuge at 20,000 rpm. Prior to measuring the protein, the cell was filled with buffer solution and the scattering intensity measured at 0, 35, 45, 60, 75, 90, 105, 120 and 135 degrees. Measurements were repeated until constant reproducible values were obtained at each angle position. Next, the clarified solution was pipetted into the cell and the scattering intensity measured in the same manner. The actual scattering intensity was obtained by subtracting the solvent scattering from the protein sample values.

The Rayleigh ratio was calculated at each angle θ from the following expression:

$$R_{\theta} = \text{cell constant} \times a \times \text{Brice constant} \times \underset{\text{correction}}{\text{back reflection}} \times J_{\theta} \quad (24)$$

where $J_{\theta} = \left[\left(\frac{F G_{\theta}}{G_0} \right)_{\text{solution}} - \left(\frac{F G_{\theta}}{G_0} \right)_{\text{solvent}} \right] \frac{\sin \theta}{1 + \cos^2 \theta}$

F = attenuation factor of neutral filters which are placed in the incident light beam when G_{θ} is determined,

G_{θ} = recorder reading at angle θ ,

G_0 = recorder reading at angle 0,

a = instrument constant.

The Brice constant is represented by the quantity,

$$\left[\frac{\eta_o TD}{1.045 \pi h} \quad \frac{R\omega}{Rc} \right]$$

where η_o = refractive index of solvent,

TD = diffuse transmittance of opal glass diffusor times the diffusor correction,

h = width of primary beam in cm,

$R\omega/Rc$ = correction for incomplete compensation of refraction effects which depend on the solvent system and wavelength used,

1.045 = correction factor for increased irradiance in the solution due to reflection of incident light at the face of the cell at the glass/air interface.

The Brice and instrument constants were determined previously, and are recorded in the operations manual.

Specific Refractive Increment. The difference in refractive index between a dilute solution and its solvent must also be known for the determination of molecular weights by the light scattering method. The change in refractive index with concentration of solute (dn/dc) must be determined with

accuracy since this term appears as a square term in the Debye equation (see equation 16). Thus an error in the value of dn/dc would cause at least twice the error in the molecular weight determination.

Specific refractive increment was measured in a Brice-Phoenix Differential Refractometer using the same wavelength employed for the light scattering measurements, which was 436 $m\mu$. The refractive index difference was obtained from the following expression:

$$\Delta n = K \Delta d \quad (25)$$

where the total displacement, Δd , corrected for solvent zero reading, is linearly related to the difference of refractive indices, Δn , of the solution in both sides of the refractometer cell, and k is the instrument constant. The value of k must be determined experimentally or by calibration.

The calibration of the instrument was determined by using reagent grade KCl solutions over the approximate range of Δn values expected for the protein solutions. The KCl crystals were dried in an oven at 100-105°C for 15 hours, cooled, weighed accurately on a Sartorius balance and dissolved in deionized water. The deviation (Δd) between the KCl solution and the deionized water was measured at 436 $m\mu$. The following equation was used for calculating Δd :

$$\Delta d = (d_0 - d_{180}) - (d'_0 - d'_{180}) \quad (26)$$

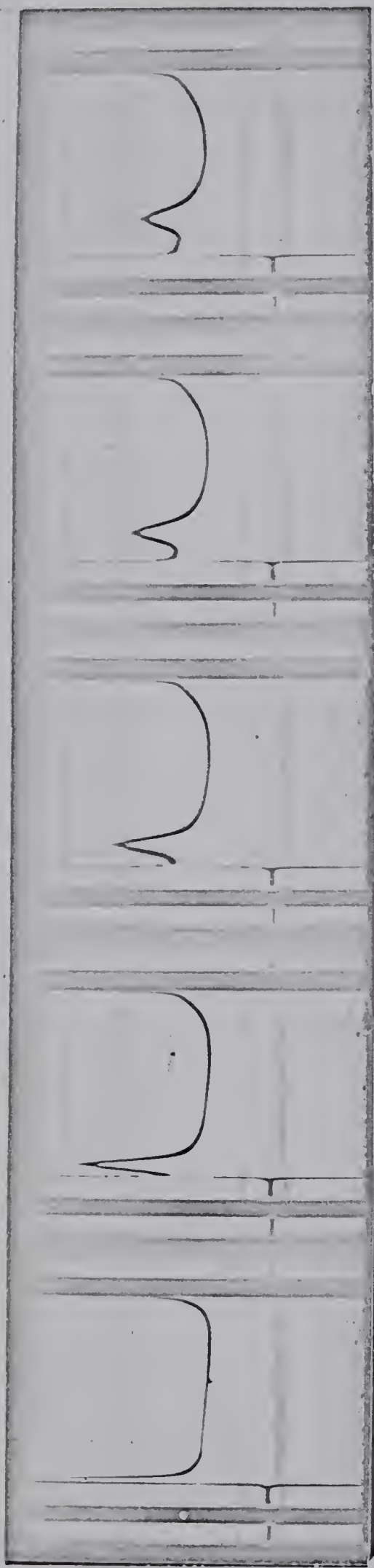
where d_0 corresponds to the solution and d_{180} to the solvent side of the cell. The d'_0 and d'_{180} both contain solvent in

each side of the cell, and provide the zero reading of the solvent.

From the data of Kruis (88), values of $(\Delta n/c)_{KCl}$ are given from which the instrument constant, k , may be calculated by rearranging equation (25) to give:

$$k = \frac{\Delta n}{\Delta d} = \frac{\Delta n/c}{\Delta d/c} \quad (27)$$

Clarification of protein solutions was achieved by ultracentrifugation at 20,000 rpm in a Spinco Model L ultracentrifuge for 30 minutes, while buffer solutions were passed through an HA millipore filter of pore size 0.45 microns. Concentration of protein solution was determined by absorbancy. Cells were cleaned with Ninol detergent and then rinsed with tap water, followed by several rinses with deionized water. The interior of the cell was dried using a blotter type paper or lens tissue. Both solution and solvent were placed in the refractometer cell which was held at constant temperature by circulation of water from a thermostatic bath coupled with a refrigeration unit. After 15 minutes equilibration, the readings for the total displacement (Δd) were made as outlined in the operations manual.



Ultracentrifugal patterns of purified beef cardiac tropomyosin at a concentration of 0.31% in 0.067M phosphate buffer, pH 7.0 containing 0.5M KCl and at 59,780 r.p.m. Photographs were taken at a phase plate angle of 50° at 16, 32, 48, 64, 80, 96, 112, and 128 minutes after top speed was reached. The direction of sedimentation is toward the right.

Plate B

III. RESULTS

Part A. Hydrodynamic Treatment of Cardiac Tropomyosin

1. Homogeneity Studies and Preliminary Investigation of the Monomeric State.

The tropomyosin used in these studies was obtained from several sources. Beef hearts were procured from a local meat packing plant (Swift and Co., Ltd., Edmonton, Alberta) for the beef cardiac preparation, while rabbit cardiac tropomyosin was obtained from frozen rabbit hearts which were available commercially (Pel-Freeze Biologicals, Inc., Rogers, Arkansas).

In order to determine the extent of homogeneity of the preparations, all solutions were first examined for evidence of impurities by means of velocity sedimentation in the ultracentrifuge. Only a single peak was evident at protein concentrations ranging from 2 to 15 mg per ml (Plate B). However, sedimentation patterns by themselves are not an absolute criterion for the homogeneity of tropomyosin. For example, in a medium of low ionic strength such as 0.1, the schlieren patterns revealed only a single component despite the presence in the system of aggregates in the form of dimers, trimers, and n-mers (see Results, Part B).

For this reason, several additional criteria of homogeneity were invoked. The principle contaminants in a tropomyosin preparation are invariably actin and myosin, both of which contain appreciable proline contents. Amino acid analysis carried out on the cardiac tropomyosin used in this

Table I

Amino Acid Composition of Skeletal and Cardiac Tropomyosin
(moles/100,000 g protein)

Amino Acid	Rabbit Skeletal		Beef Cardiac		Rabbit Cardiac	
	Bailey(132)	Kominz et al.(89)	Katz & Converse(34)	Kominz et al.(89)	Katz & Converse (34)	*
lysine (a)	110	107	114	104	103	102
histidine (a)	5.5	5.5	5.8	5.3	5.2	8
amide ammonia (b)	(64)	(64)	-	(62)	(66)	(67)
arginine (a)	42	42	42	41	41	41
aspartic acid (a)	89	89	85	88	88	89
threonine (b)	28	26	22	25	24	25
serine (b)	40	40	36	41	41	40
glutamic acid (a)	211	212	215	213	212	213
proline (a)	-	1.7	-	-	-	-
glycine (a)	12.5	12.5	11	9	9.5	9
alanine (a)	110	110	104	107	107	100
half-cystine (b)	6.5	6.5	-	-	-	-
valine (c)	38	27	26	27	27	27
methionine (b)	16	16	16	16	16	16
isoleucine (c)	29	30	31	30	30	31
leucine (a)	95	95	95	95	97	90
tyrosine (b)	15	15	17	15	15	15
phenylalanine (a)	3.5	3.3	3.6	3.7	3.75	3.5

(a) Average of 22-, 30- and 70 h hydrolysates.
 (b) Extrapolated to 0 time.
 (c) Average of 30- and 70- h hydrolysates.
 * This study.

Table II

The Molecular Weight of Tropomyosin in 0.5M KCl,
0.067M Phosphate Buffer, pH 7.0 with Time of
Centrifugation (Archibald Procedure)

Concentration %	Speed (rpm)	Time (min.)	Apparent Molecular Weight	
			Cell top	Cell bottom
rabbit cardiac				
0.26	12,590	16	103,510	100,180
		32	100,060	101,320
		48	100,560	100,395
		64	102,110	100,650
		Average		101,560
beef cardiac				
0.35	9,341	16	101,909	91,597
		32	104,740	100,493
		48	104,234	102,010
		64	100,232	102,819
		80	101,504	100,867
		96	103,729	101,606
		112	102,455	105,245
Average		102,650	102,174	

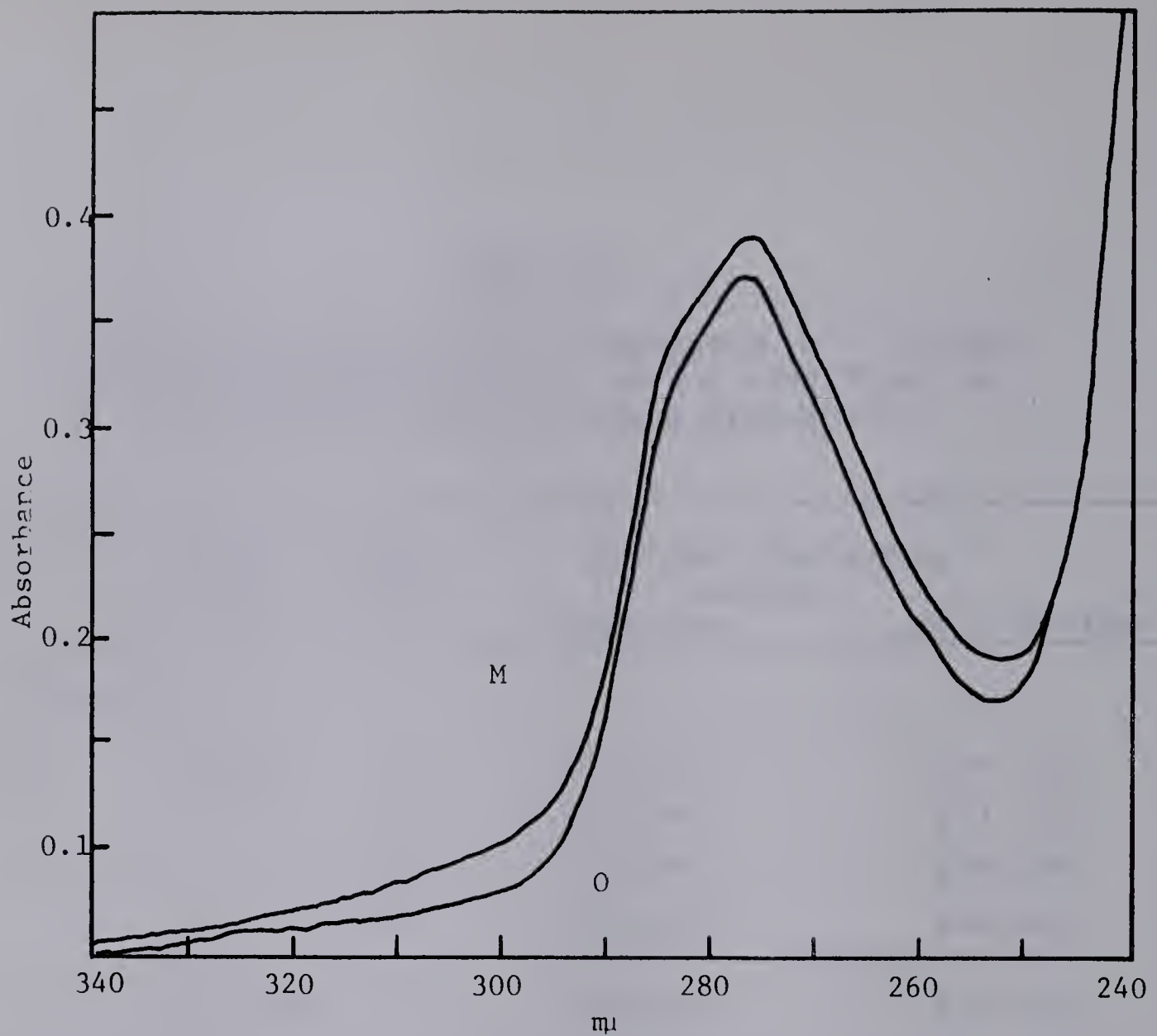


Figure 5

Absorption spectrum of rabbit cardiac (preparation M) and beef cardiac (preparation O) tropomyosin in 0.5M KCl, 0.067M phosphate buffer, pH 7.0. Spectra were recorded on a Cary 505 recording spectrophotometer over the wavelength range of 240 mμ to 340 mμ.

study (Table I), indicated the absence of any proline residues in these preparations, suggesting little contamination with actin and myosin.

Homogeneity was also established by observing the variation in molecular weight with time of centrifugation as deduced by the Archibald technique. Table II reveals that the weight-average molecular weights of beef and rabbit cardiac tropomyosin were constant at both the cell top and cell bottom positions during prolonged centrifugation. The presence of any high molecular weight component in these preparations would have caused the molecular weight at cell top to decrease with time, with a subsequent increase in molecular weight at the cell bottom.

In addition, the ultraviolet spectrum of the solution was examined at 280 and 260 $m\mu$ to detect the presence of any nucleic acid contamination. A typical spectrum is shown in Figure 5, indicating a maximum at 278 $m\mu$ and a minimum at 253 $m\mu$. The ratio of optical density at 260 $m\mu$ to that at 280 $m\mu$ was generally between 0.50 and 0.60 for both cardiac systems, in good agreement with the published value of 0.55 for mammalian tropomyosin (89), indicating the absence of any nucleic acid components.

A preliminary examination by means of viscometric measurements was carried out on cardiac tropomyosin in order to determine whether the molecule is sensitive to changes in the concentration composition of the buffer system at pH values close to neutrality.

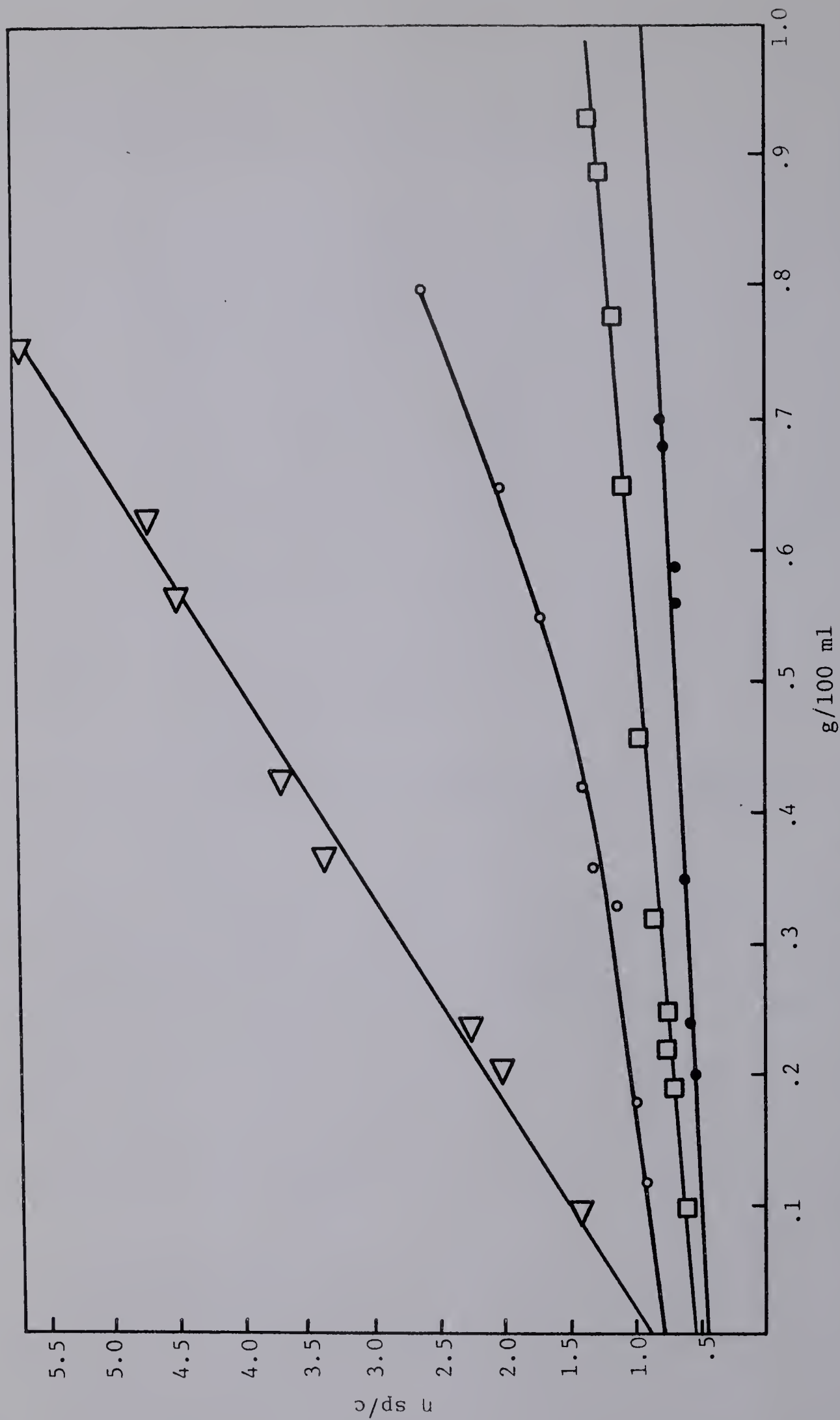


Figure 6

Reduced specific viscosity of beef cardiac tropomyosin in: (a) Δ 0.067M phosphate buffer, pH 7.0, (I=0.1); (b) \circ 0.1M KCl, 0.067M phosphate buffer, pH 7.0, (I=0.2); (c) \square 0.2M KCl, 0.067M phosphate buffer, pH 7.0, (I=0.3); (d) \bullet 0.5M KCl, 0.067M phosphate buffer, pH 7.0, (I=0.6).

Figure 6 illustrates a plot of reduced viscosity, (η_{sp}/c) versus protein concentration, in various ionic strength buffer systems, for beef cardiac tropomyosin. The increased slope of these plots at ionic strength values less than 0.6 is due to association of the tropomyosin molecule, as will be shown by molecular weight studies later on. The limiting ordinate intercept increases from a value of 0.46 dl/g at ionic strength 0.6 to 0.86 dl/g at ionic strength 0.1. At a higher ionic strength, 1.1, the ordinate intercept is essentially identical to that at ionic strength, 0.6 viz., 0.45 dl/g. Similar results were obtained by Tsao et al. for rabbit skeletal tropomyosin (90,91), where only at ionic strength 0.6 or greater was the monomeric hydrodynamic unit obtainable. It is interesting to note that the "monomeric" weight intrinsic viscosity value of 0.46 dl/g for beef cardiac tropomyosin is higher than the 0.39 dl/g figure for rabbit skeletal tropomyosin obtained by Noelken (92) indicating that, at least in this respect there are differences between these two tropomyosin systems. It would thus appear that an ionic strength of 0.6 is sufficient to achieve the monomeric state for cardiac tropomyosin.

This section gives an account of the physico-chemical characterization of the monomeric form of the cardiac tropomyosins carried out in a buffer solution of ionic strength 0.6 and pH 7.0. Molecular weights were measured directly by the use of the Archibald approach to equilibrium method as well as by light scattering measurements. In addition, the molecular weights were checked by treating the diffusion and sedimentation

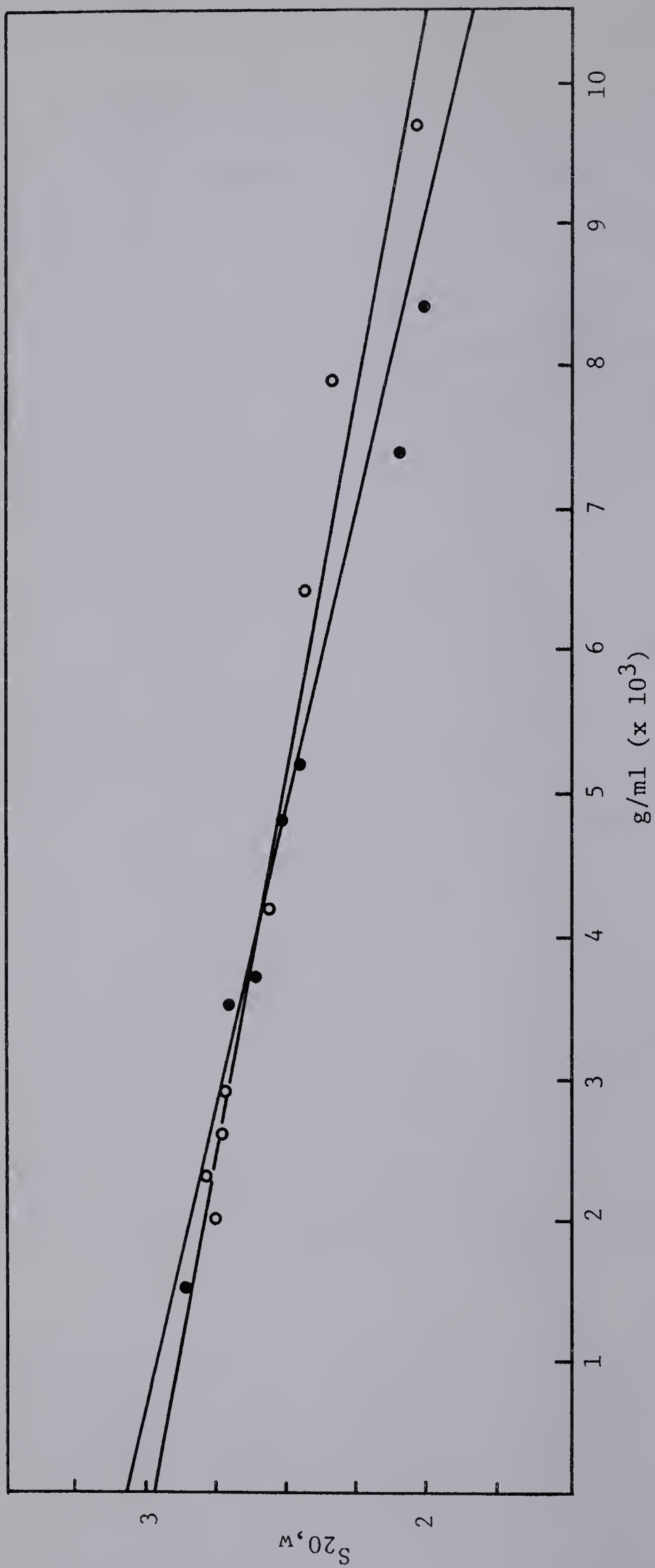


Figure 7

Concentration dependence of the sedimentation coefficient ($S_{20,w}$) of beef \bullet and rabbit \circ cardiac tropomyosin. Conditions: 0.067M potassium phosphate 0.5M KCl, pH 7.0.

data by means of the Svedberg equation. The optical rotatory dispersion was treated according to the Moffitt method, and additional information on secondary structure was derived from the extent of the Cotton effect at 233 mμ, as well as the extent of deuterium-hydrogen exchange.

The parameters obtained from sedimentation, viscosity, diffusion, and density measurements (\bar{v}), were incorporated into suitable equations from which the size and shape of the respective cardiac tropomyosins were evaluated, and expressed in terms of suitable models. In addition, these models were compared with those reported for the skeletal system.

2. Molecular Properties of Monomeric Cardiac Tropomyosin.

(a) Sedimentation Velocity. The sedimentation coefficients, $S_{20,w}$ values, were determined at several protein concentrations in the monomeric phosphate buffer system of 0.6 ionic strength, pH 7, and plotted as a function of the protein concentrations, as represented in Figure 7. The sedimentation data showed an appreciable variation with concentration for both rabbit and beef cardiac tropomyosins. The least square plot of the data gave an $S_{20,w}^0$ value of 2.97S for rabbit cardiac tropomyosin and the equation for the regression line was as follows:

$$S_{20,w} = 2.97 (\pm 0.046) - 0.87 (\pm 0.06)c \quad (28)$$

where c is expressed in g/100 ml. Similar treatment for beef cardiac tropomyosin resulted in an $S_{20,w}^0$ value of 3.08S and a slope term included in the equation:

$$S_{20,w} = 3.08 (\pm 0.054) - 1.21 (\pm 0.07)c \quad (29)$$

Table IIIA

Partial Specific Volume of Beef Cardiac Tropomyosin as
Determined from the Amino Acid Composition

Amino Acid	Total No. of Residues	Partial Weight (Wgt.)	Specific Volume (V ₁)	Weight Percent (w ₁)	V ₁ W ₁
lysine	103	15,038	.82	12.74	10.45
histidine	5	755	.67	.66	.44
arginine	41	7,134	.70	6.05	4.24
aspartic acid	88	11,704	.59	9.92	5.85
threonine	24	2,856	.70	2.42	1.69
serine	41	4,305	.63	3.65	2.30
glutamic acid	212	31,164	.67	26.41	17.69
proline	-	-	.76	-	-
glycine	10	750	.64	.64	.41
alanine	107	9,523	.74	8.07	5.97
half cystine	-	-	.63	-	-
valine	27	3,159	.86	2.67	2.30
methionine	16	2,384	.75	2.02	1.52
isoleucine	30	3,930	.90	3.33	2.99
leucine	97	12,707	.90	11.76	10.58
tyrosine	15	2,715	.71	2.30	1.63
phenylalanine	4	660	.77	.56	.43
asparagine	33	4,389	.60	3.72	2.23
glutamine	33	4,851	.67	4.11	2.75
Total				101.03	73.47

$$W_1 V_1 / W_1 = V_p = 73.47 / 101.03 = .727 \text{ cc/g.}$$

Table IIIB

Partial Specific Volume of Rabbit Cardiac Tropomyosin as
Determined from the Amino Acid Composition

Amino Acid	Total No. of Residues	Partial Weight (Wgt.)	Specific Volume (V ₁)	Weight Percent (W ₁)	V ₁ W ₁
lysine	102	14,892	.82	12.61	10.34
histidine	8	1,240	.67	1.05	.70
arginine	41	7,144	.70	6.04	4.23
aspartic acid	89	11,837	.59	10.03	5.92
threonine	25	2,975	.70	2.52	1.76
serine	40	4,200	.63	3.56	2.24
glutamic acid	213	31,311	.67	26.52	17.77
proline	-	-	.76	-	-
glycine	19	1,425	.64	1.20	.77
alanine	93	8,277	.74	7.01	5.19
half cysteine	-	-	.63	-	-
valine	27	3,159	.86	2.68	2.30
methionine	16	2,384	.75	2.02	1.51
isoleucine	31	4,061	.90	3.44	3.09
leucine	90	11,790	.90	9.99	8.99
tyrosine	15	2,715	.71	2.30	1.63
phenylalanine	6.4	1,056	.77	.89	.68
asparagine	34	4,522	.60	3.83	2.29
glutamine	34	4,998	.67	4.23	2.83
Total				99.92	72.25

$$W_1 V_1 / W_1 = V_p = 72.25 / 99.92 = .723 \text{ cc/g.}$$

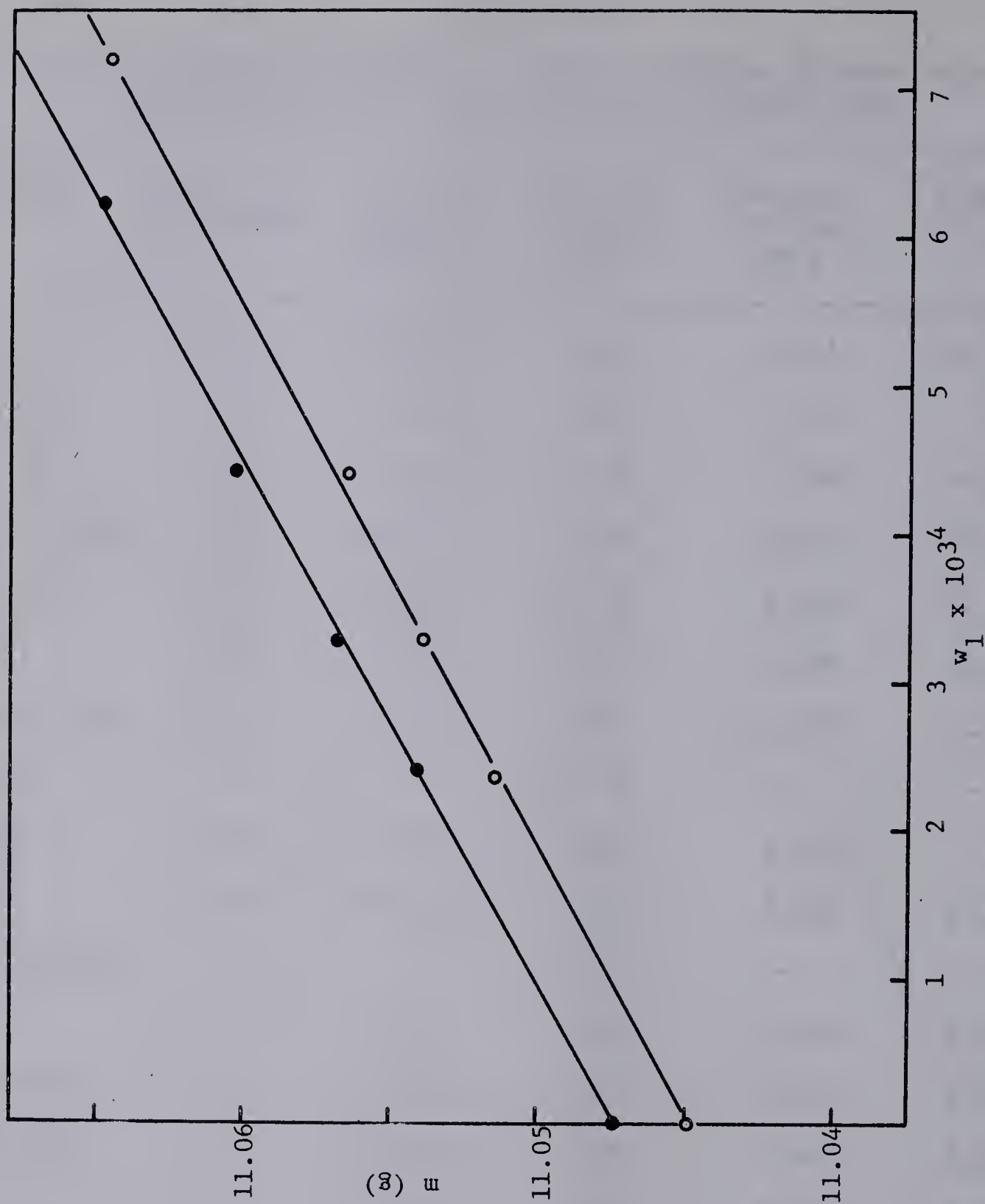
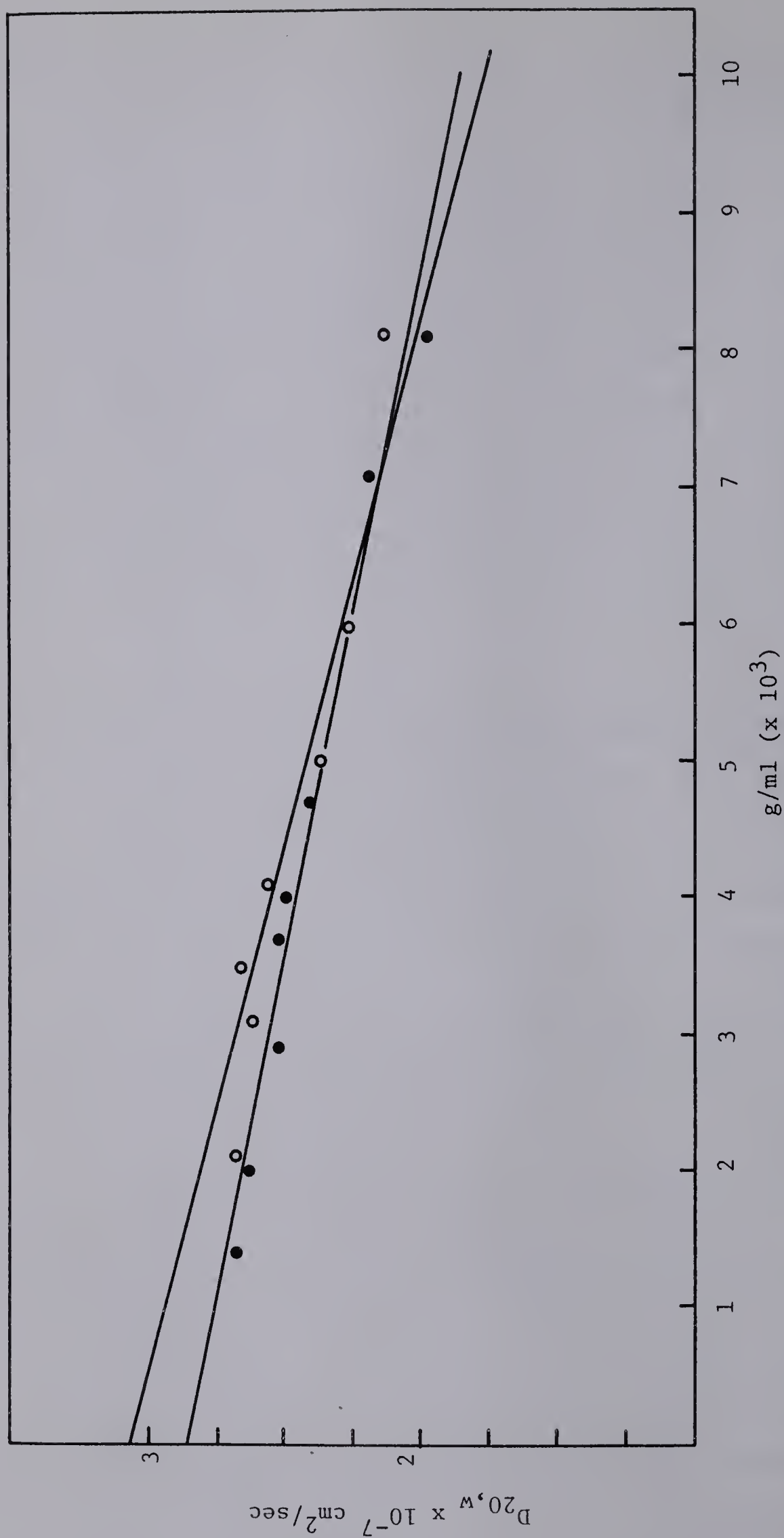


Figure 8

Kraemer plots of partial specific volume. Beef cardiac tropomyosin \circ and rabbit cardiac tropomyosin \bullet , 0.5M KCl, 0.067M phosphate buffer, pH 7.0. The quantity m refers to the mass contents of the pycnometer while w_1 is the weight fraction of protein.

where c is concentration in g/100 ml. These values were comparable to those obtained for the rabbit skeletal system, denoted by the straight line relationship, $S_{20,w} = 2.95 - 1.0c$ (89). Thus, it is apparent that only slight differences, if any, exist between the various tropomyosins insofar as sedimentation is concerned. This is not surprising in view of the fact that S , the sedimentation constant, is relatively insensitive to molecular weight for asymmetric molecules. This type of situation has been encountered by other workers when dealing with asymmetric molecules such as myosin (93) and the nucleic acids.

(b) Partial Specific Volume. The partial specific volumes of beef and rabbit cardiac tropomyosin were determined pycnometrically as outlined in the Methods and Materials section. Figure 8 illustrates a Kraemer type plot for beef and rabbit cardiac tropomyosin. The results for the two systems were essentially identical, averaging $0.728 (\pm 0.001)$ ml/g and $0.731 (\pm 0.002)$ ml/g for the beef and rabbit tropomyosins, respectively. Another method used for determining partial specific volume was based on a summation of the partial molal volume values of the amino acids present in the proteins as reflected by their amino acid composition (42). The results of this application for the two proteins are summarized in Tables IIIA and IIIB. It may be seen that there is close agreement between the experimental and the amino acid composition calculations.



A plot of apparent diffusion constant of beef cardiac ● and rabbit cardiac ○ tropomyosin in 0.067M phosphate buffer, pH 7.0, with 0.5M KCl against protein concentration in g/ml.

Figure 9

(c) Diffusion Coefficient. The diffusion coefficients for rabbit and beef cardiac tropomyosin were calculated either by the maximum ordinate-area method, the second moment method or the Rayleigh interference fringe method. Sample calculations involving each method are given in Appendix I.

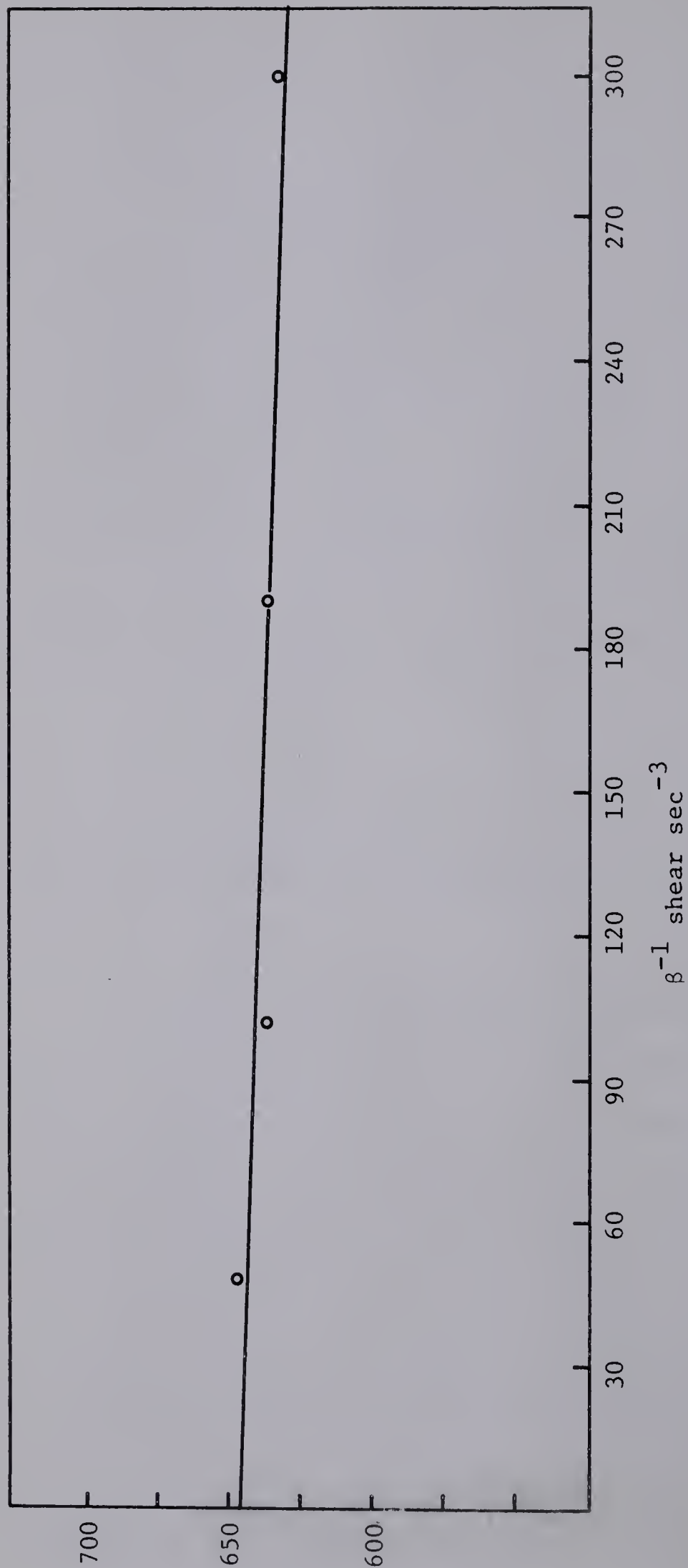
In order to determine the diffusion constant at zero protein concentration, $D_{20,w}^0$, diffusion constant values for each concentration of tropomyosin were plotted graphically, as in Figure 9. Some of the points in this figure are the resultant values obtained from application of the three methods of analysis. The variation of the diffusion constant with protein concentration for rabbit cardiac tropomyosin is represented by the equation:

$$\begin{aligned} D_{20,w} &= D_{20,w}^0 - kc \\ &= 3.02 (\pm 0.056) - 1.27 (\pm 0.11)c \text{ cm}^2/\text{sec} \end{aligned} \quad (30)$$

while a similar plot for beef cardiac tropomyosin yielded the following relationship:

$$D_{20,w} = 2.85 (\pm 0.069) - 1.01 (\pm 0.076)c \text{ cm}^2/\text{sec} \quad (31)$$

where k is the slope term and c is the concentration in g per 100 ml. The intrinsic values of 3.02 and 2.85 Fick units for the cardiac tropomyosins are to be compared with an approximate $D_{20,w}$ value of 4.5 for rabbit skeletal tropomyosin, determined by Kominz et al. (89). This larger D for rabbit skeletal tropomyosin is in fact what one would anticipate on the basis of the lower molecular weight (53,000) reported for this protein as compared with the cardiac system ($\sim 100,000$, this study) and the inverse relationship between M and D , as represented in the Svedberg equation.



Shear rate of beef cardiac tropomyosin ($c=.48\%$) using the multi-bulb calibrated Cannon viscometer (Cannon Instruments Co., State College, Pa., U.S.A.).

($\beta = 8V/3\pi \gamma^3 t$ where V is the volume of liquid flowing through the capillary of radius γ in time $t [90]$).

Figure 10

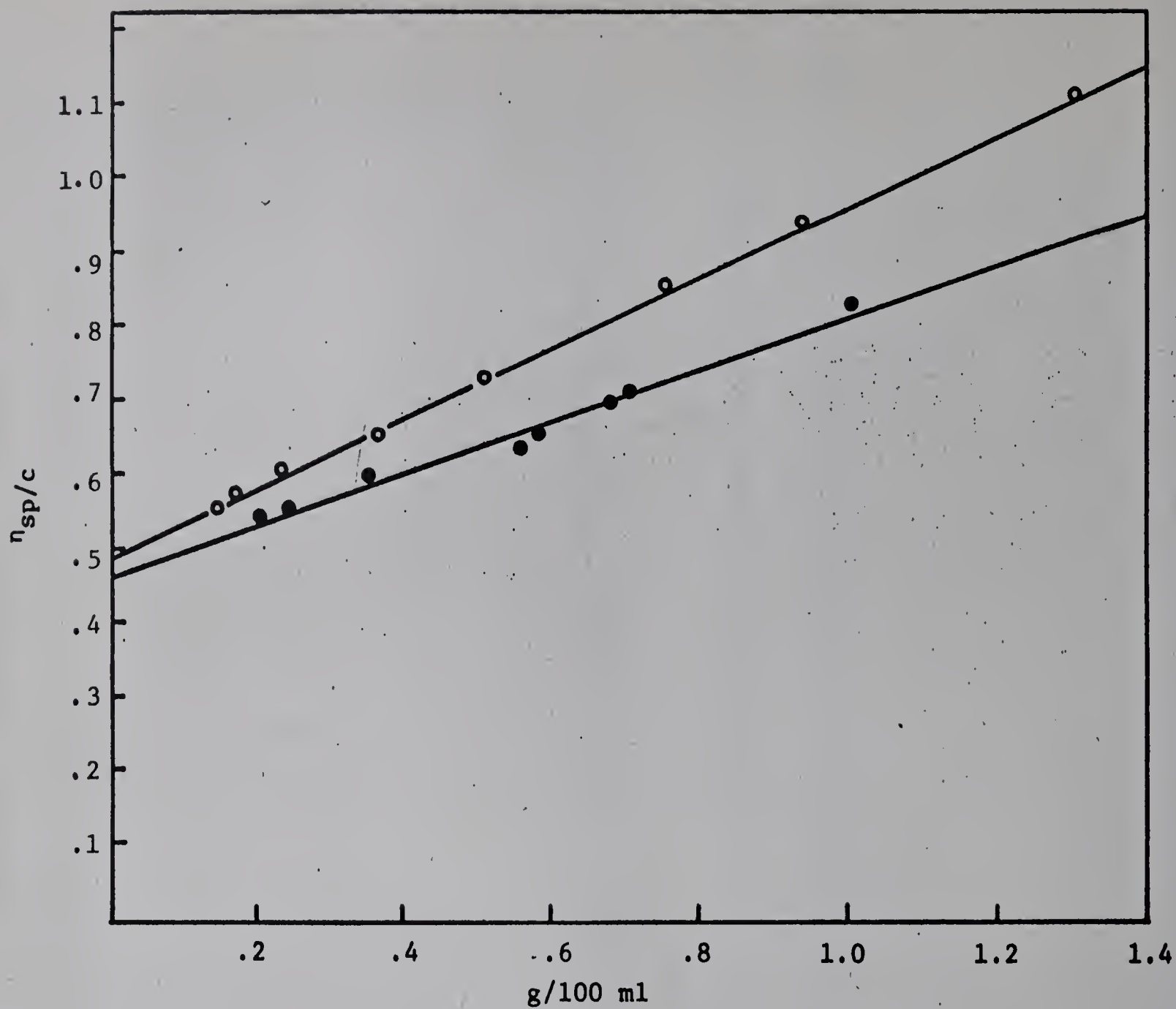


Figure 11

Reduced specific viscosity of beef cardiac ● and rabbit cardiac ○ tropomyosin in 0.5M KCl, 0.067M phosphate buffer at pH 7.0 as a function of protein concentration.

(d) Intrinsic Viscosity. As the viscosity of the tropomyosin solutions may be non-Newtonian (i.e. viscosity dependent on shear rate), it was felt essential to make measurements of viscosity at several shear gradients, using a multi-bulb capillary viscometer, to obtain a valid extrapolation to zero shear. A plot of the reduced viscosity against the rate of shear is illustrated in Figure 10. It is evident that there is no difference in the viscosity value for the beef cardiac system over a shear range of 30,000 to 300,000 reciprocal seconds. For this reason, all viscosity measurements were confined to the Ostwald-type capillary viscometer.

The intrinsic viscosity of tropomyosin was measured under the same solvent conditions as were used for sedimentation velocity. Figure 11 illustrates a plot of reduced viscosity (η_{sp}/c) versus protein concentration for the cardiac tropomyosins. The intrinsic viscosity values for the two protein systems are in close agreement with one another. The data may be represented by the following relationship:

$$(\eta_{sp}/c) = [\eta] + k' [\eta]^2 c \quad (32)$$

where $[\eta]$ is the weight intrinsic viscosity, c is in g/100 ml and k' is the Huggin's constant (94), and serves as a measure of the intermolecular attraction of polymer molecules. The weight intrinsic viscosity, $[\eta]$, and the corresponding k' values for the rabbit cardiac system are:

$$[\eta] = 0.48 (\pm 0.009) \text{ dl/g}; k' = 2.1 \quad (33)$$

and for beef cardiac tropomyosin:

$$[\eta] = 0.46 (\pm 0.017) \text{ dl/g}; k' = 1.6 \quad (34)$$

For comparison, Noelken (92) reported a reduced viscosity of 0.39 dl/g (solvent system, 1M KCl, 0.1M phosphate buffer, pH 7.4) for the rabbit skeletal system with a Huggin's constant of 3.54. The lower $[\eta]$ value for the skeletal protein suggests that the molecule is not as asymmetric as cardiac tropomyosin, and is also a reflection of the lower molecular mass, referred to previously.

There is also some variation in the concentration dependency term for the skeletal and cardiac systems as reflected in the k' values. Since intrinsic viscosity gives a measure of the effective hydrodynamic volume of the protein molecule in solution, the observed variation might indicate that the molecular conformations of rabbit skeletal and cardiac tropomyosins are not identical in this solvent system. The large Huggin's constant (3.54) for the rabbit skeletal system may also reflect aggregation at higher concentrations for this system (95).

(e) Molecular Weight.

(i) Archibald Method and the Svedberg Equation. The molecular weights of the tropomyosin were determined by the Archibald approach to equilibrium method (49) and from the integration of sedimentation and diffusion constant measurements by means of the Svedberg equation (45).

In view of previous observations that the apparent molecular weight of the myosin system is appreciably concentration dependent (26,96), molecular weights were determined for the tropomyosins at several concentrations and, in the final analysis, the data were plotted as the reciprocal of

Table IV

The Intrinsic Molecular Weights of Cardiac Tropomyosin
as Determined by the Archibald Method and Svedberg Equation

Protein	Method	Reciprocal of the Intrinsic Molecular Weight	The Second Virial Coefficient
		$1/M^0 \times 10^{-6}$	$B \times 10^{-5}$
Beef	Archibald	9.625 (\pm 0.14)	1.84 (\pm 0.35)
Rabbit	Archibald	9.791 (\pm 0.21)	1.27 (\pm 0.15)
Beef	Svedberg	9.699 (\pm 0.08)	2.39 (\pm 0.24)
Rabbit	Svedberg	9.822 (\pm 0.07)	1.81 (\pm 0.10)

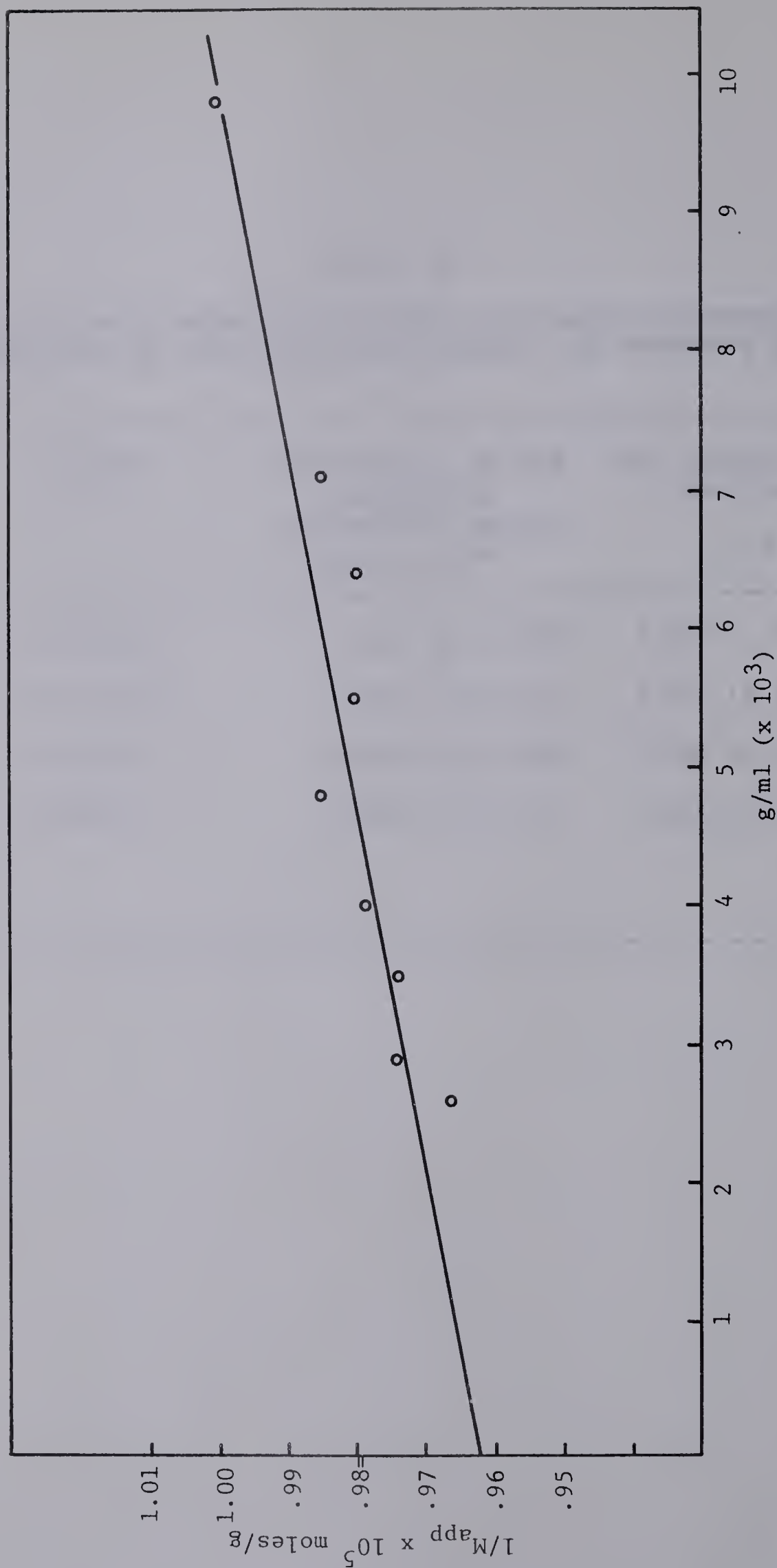


Figure 12

Concentration dependence of the apparent molecular weight of beef cardiac tropomyosin by means of the Archibald method. The solvent was 0.067M phosphate buffer, pH 7, with 0.5M KCl.

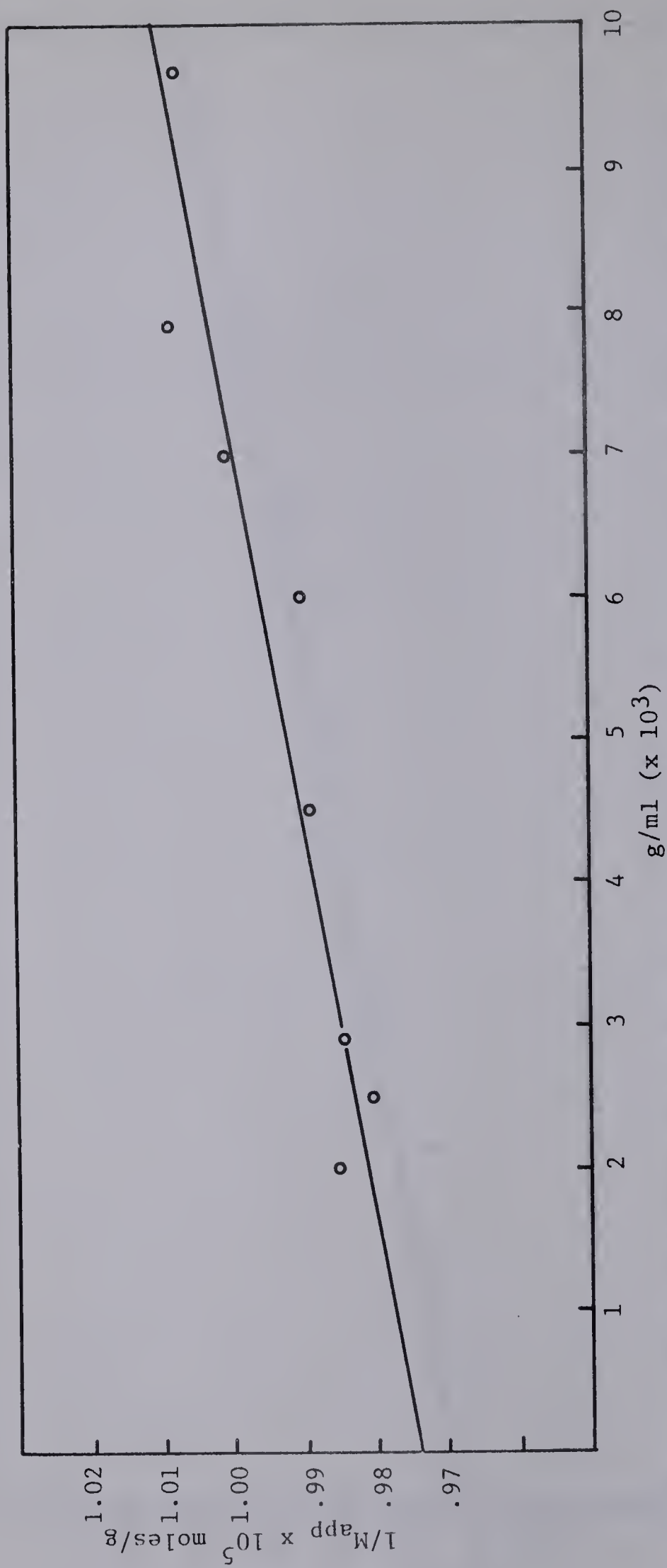


Figure 13

Concentration dependence of the apparent molecular weight of rabbit cardiac tropomyosin by means of the Archibald method. The solvent was 0.067M phosphate buffer, pH 7.0, with 0.5M KCl.

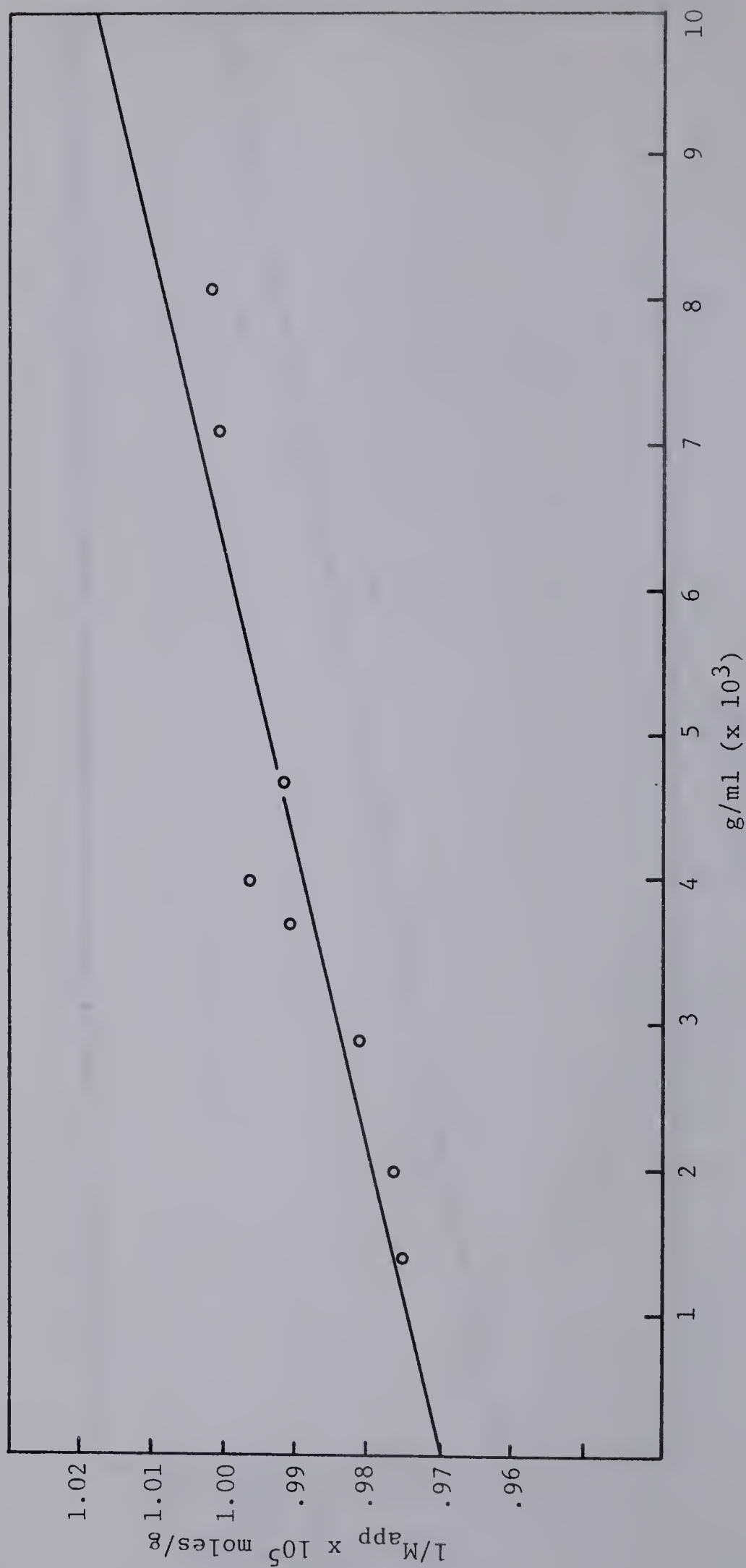


Figure 14

Plot of the apparent molecular weight of beef cardiac tropomyosin versus protein concentration as derived by means of the Svedberg equation. Conditions were similar to those used in the Archibald experiment.

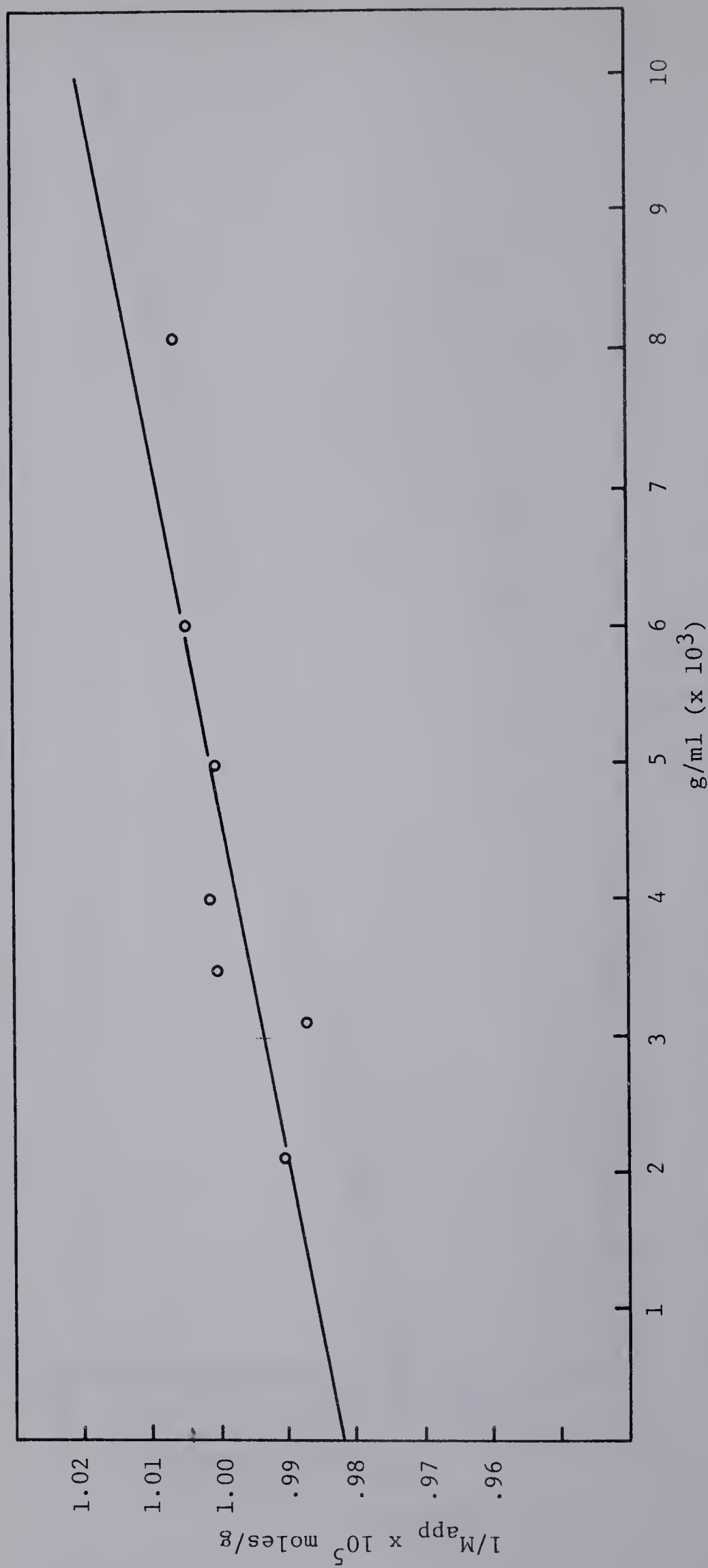


Figure 15

Plot of the apparent molecular weight of rabbit cardiac tropomyosin versus protein concentration as derived by means of the Svedberg equation. Conditions were similar to those used in the Archibald experiment.

the apparent molecular weight, $1/M_{app}$, versus c (g/ml) (Figures 12 and 13). The molecular weight was obtained from the limiting ordinate intercept. The concentration dependency of M for cardiac tropomyosin is represented by the general equation:

$$1/M_{app} = 1/M^0 + 2Bc \quad (35)$$

where M^0 is the intrinsic molecular weight and B is the second virial coefficient.

Table IV summarizes the intrinsic molecular weights and second virial coefficients for beef cardiac and rabbit cardiac tropomyosin deduced by both the Archibald method and the Svedberg equation. The Archibald technique yields an intrinsic molecular weight (M^0) of 103,800 g/mole and a second virial coefficient, B , of 1.84×10^{-5} moles-ml/g², for beef cardiac tropomyosin. For rabbit cardiac tropomyosin, the corresponding intrinsic molecular weight is 102,100 g/mole and a second virial coefficient (B) of 1.27×10^{-5} moles-ml/g², was calculated.

By integrating the values of $S_{20,w}$ and $D_{20,w}$ (Figures 7 and 9) in terms of the Svedberg equation, the apparent molecular weight of cardiac tropomyosin was obtained, and plotted graphically in Figures 14 and 15 as $1/M_{app}$ versus c (g/ml). The line, deduced from least square calculations, resulted in a molecular weight (M^0) of 102,000 g/mole for the rabbit cardiac system upon extrapolation of the plots to infinite dilution. A second virial coefficient (B) of 1.81×10^{-5} moles-ml/g² was obtained from this same plot. Similar results were found for the beef cardiac system, where values of 103,100

Table V

Particle Weight of Beef and Rabbit Cardiac Tropomyosin
from Archibald Measurements*

Solvent	Rabbit Cardiac	Beef Cardiac
5M guanidine . HCl .057M PO ₄ , pH 7.0	98,320 (c=.27%)	98,494 (c=.75%)
1M KCl .067M PO ₄ , pH 7.0	96,950 (c=.32%)	100,901 (c=.75%)
6.67M urea .01M PO ₄ , pH 7.0 .3M KCl	91,420 (c=.51%)	92,784 (c=.48%)
0.3M KCl 0.01M HCl, pH 2.0	107,600 (c=.57%)	99,134 (c=.47%)

*

The \bar{v} values in all these solvents were assumed to be identical with the aqueous value determined for these proteins in 0.6M KCl, phosphate buffer at pH 7.0. This may not be so, in view of Kay's observation that \bar{v} decreases by ~1% in denaturants such as 8M urea (47). This would result in an uncertainty of ~5% in molecular weight determinations.

g/mole and 2.39×10^{-5} moles-ml/g² were determined for M⁰ and B, respectively.

Since the molecular weight reported here for both beef and rabbit cardiac tropomyosin ($\sim 100,000$) is about double the 53,000 value reported for rabbit skeletal tropomyosin (89,90), it seemed worthwhile to establish whether the cardiac homologues were in fact dimeric aggregates of the skeletal monomer. Accordingly, both beef and rabbit cardiac tropomyosins were subjected to treatment with various denaturants such as 6.67M urea and 5M guanidine.HCl, which are known to dissociate proteins into subunits. Also the cardiac tropomyosins were dialyzed against two additional solvents, 0.3M KCl-0.01M HCl, pH 2.0, and 1M KCl-0.067M phosphate buffer, pH 7, in order to observe whether extreme acid or higher ionic strength could effect dissociation. The resulting solutions were then studied by Archibald ultracentrifugation and the results are summarized in Table V. It is apparent that the molecular weight of beef and rabbit cardiac tropomyosin remained rather constant at $\sim 100,000$ in all solvent media explored, suggesting that this value is in fact the fundamental molecular unit for cardiac tropomyosin.

Comparison with previous literature values indicates that there are certain discrepancies reported for the tropomyosins. In a comparative study of rabbit skeletal and cardiac tropomyosin, Katz and Converse (34) reported a molecular weight of 54,800 for both tropomyosin components based on the Scheraga-Mandelkern equation. In the light of the present investigation, the molecular weight of the cardiac system

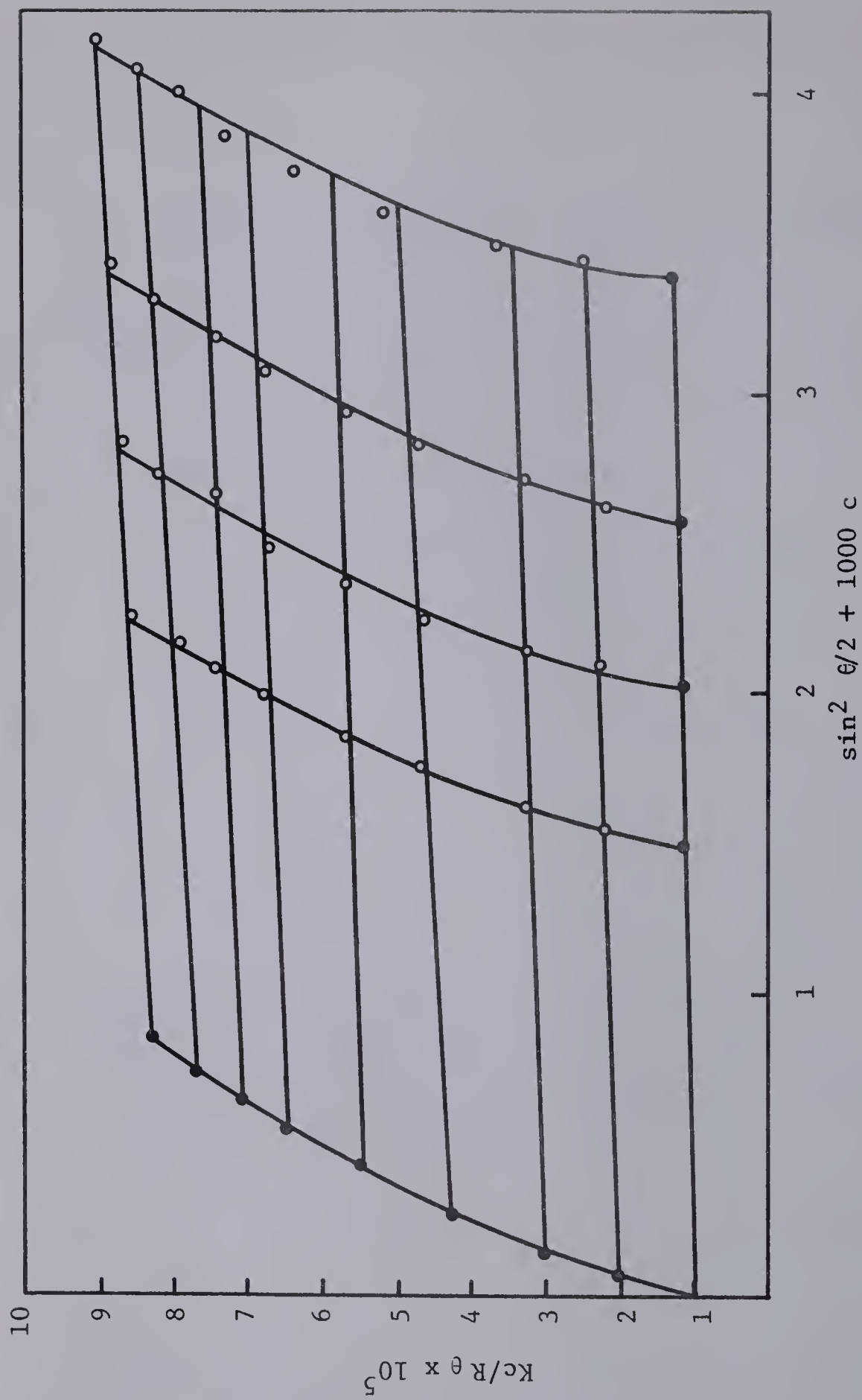


Figure 16

Zimm plot for beef cardiac tropomyosin in 0.5M KCl, 0.067M phosphate buffer, pH 7.0.

cited by these authors appears much too low. A possible explanation for this anomaly is that the latter authors calculated the parameter β (2.75) from the viscosity increment of the protein (58.9) using the tables of Scheraga and Mandelkern (97). Substitution of β along with the other measured hydrodynamic parameters (34) into the Scheraga-Mandelkern equation resulted in their calculated molecular weight of 54,800. While it is recognized that the significance of the β -function relates to unhydrated values, since in the derivation of the function the effective volume term has been eliminated by the use of f/f_0 , nevertheless the intrinsic viscosity depends both on the asymmetry of the particle and its effective volume (V_e). Since proteins in solution are for the most part hydrated entities, one cannot use the $[\eta]$ as a means of calculating the viscosity increment, ν , with the anhydrous partial specific volume value, \bar{v} . This is in effect what Katz and Converse have done which results in an abnormally high β and hence a low molecular weight. This would emphasize that as a general rule, it is far better and safer to estimate the molecular weight from direct experimental procedures such as Archibald and light scattering (see below), than by calculations from an assumed model which may or may not be valid.

(ii) Light Scattering. Light scattering data for beef cardiac tropomyosin solutions at high ionic strength were interpreted by the formulation of a Zimm plot (79). The amount of scattering was measured over a wide angular range, usually from 30° to 135° , and over several concentrations, as seen in Figure 16. Detailed sample calculations of these

results are included in Appendix 2. The reciprocal of the ordinate intercept gave a weight-average molecular weight of 99,000, in good agreement with the Archibald method and the Svedberg equation. The value of the second virial coefficient, B, obtained from the slope of the zero angle line was 2.5×10^{-5} mole-ml/g². This value is somewhat larger than that deduced from either the Archibald method or through the use of the Svedberg equation. However, the light scattering measurements were not treated statistically and thus the B value difference may not represent a significant deviation from those of Archibald and sedimentation-diffusion calculations.

The radius of gyration, R_g, for the tropomyosin particle was determined as 124.7 Å from the ratio of the slope of the zero concentration line to its intercept on the Kc/R_θ axis in the Zimm plot, in accordance with the equation:

$$R_g = \frac{3 \lambda'^2 (\text{slope})}{16 \pi^2 (\text{intercept})} \quad (36)$$

Here λ' refers to the wavelength of light in solution. The R_g value of 124.7 Å corresponds to 432 Å for the length, L, of a rod-model having high asymmetry ($L = \sqrt{12} R_g$). On the other hand, an end to end distance of 306 Å is calculated for a coil model ($L = \sqrt{6} R_g$). For a model with a non-uniform mass distribution, such as a prolate ellipsoid, the length of the major axis is $\sqrt{20} R_g$, and in this case is evaluated as 557 Å.

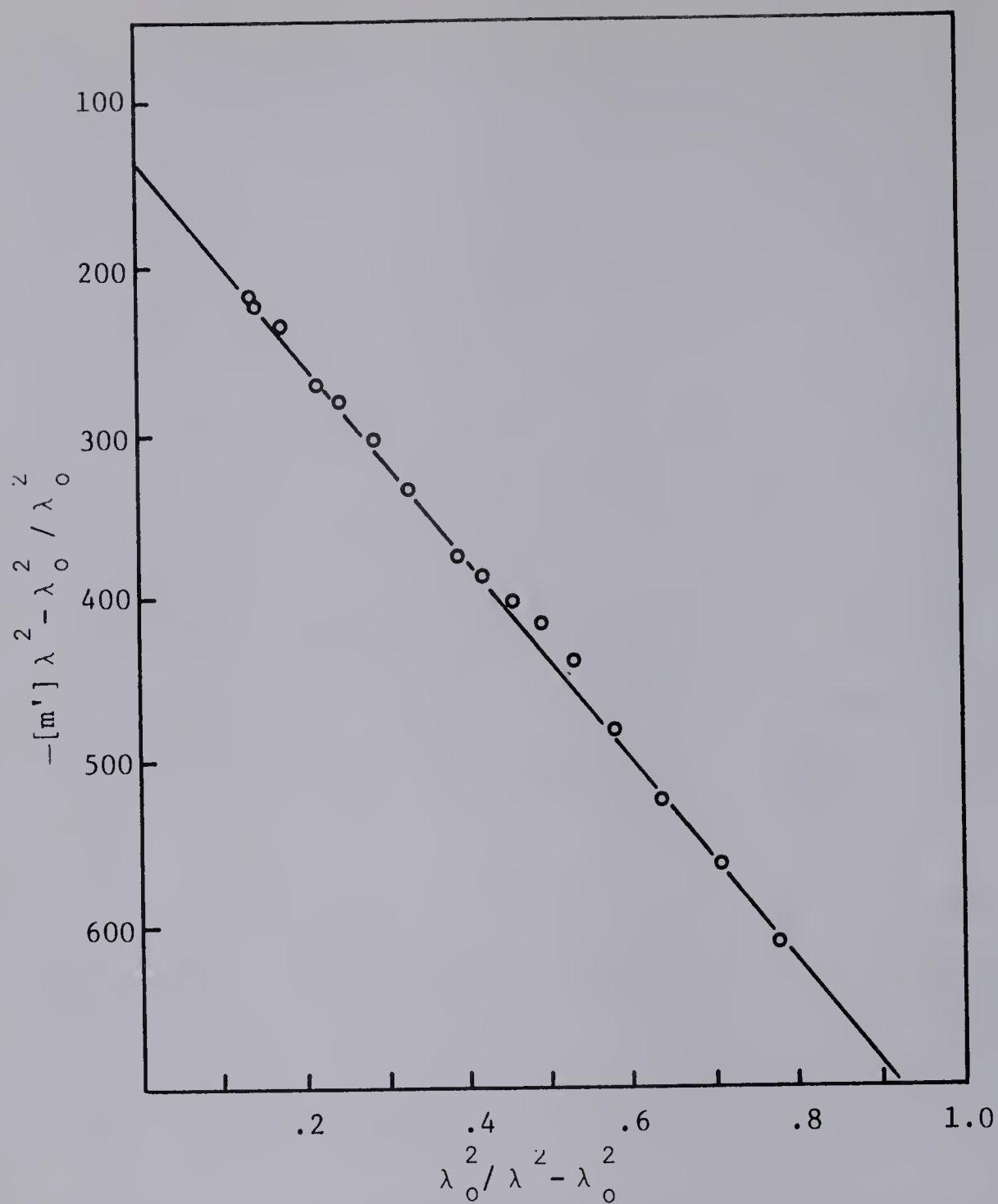
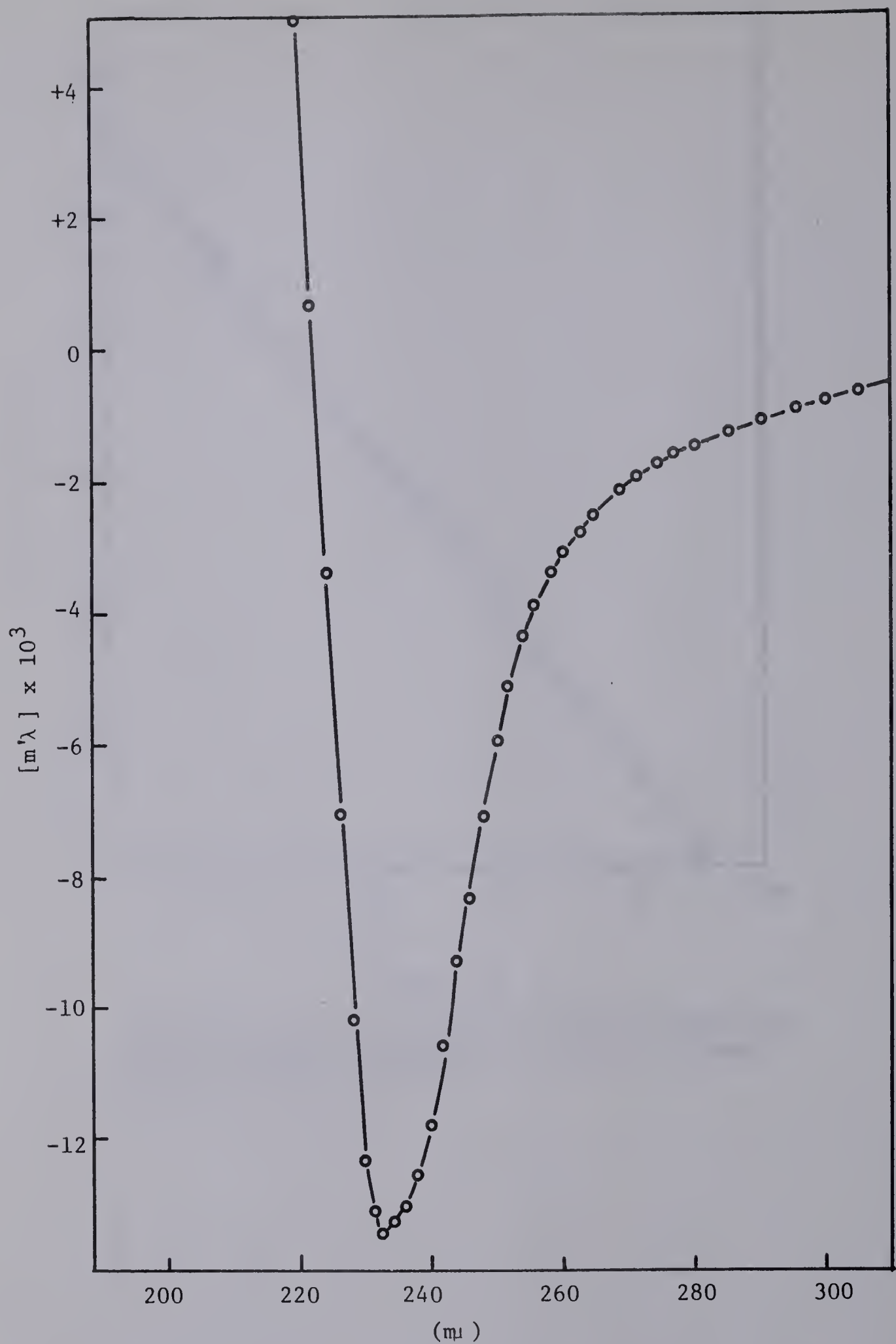


Figure 17

A Moffitt plot of the optical rotatory dispersion of beef cardiac tropomyosin in 0.5M KCl, 0.067M phosphate buffer, pH 7.0.



Optical rotatory dispersion of beef cardiac tropomyosin in 0.5M KCl, 0.067M phosphate buffer, pH 7.0 in the ultraviolet region.

Figure 18

(f) Optical Rotatory Dispersion Measurements (ORD).

The α -helical content of cardiac tropomyosin was measured by the method of optical rotatory dispersion. The helical content of rabbit skeletal tropomyosin has been previously reported to be in excess of 90% (98).

Two methods involving optical rotatory dispersion measurements were used in this study, for estimating the helical content of the cardiac tropomyosins. One of these was the Moffitt type plot which expresses partial helical content in the visible region (340-600 m μ), and the other relates helical content to the amplitude of the negative conformational Cotton effect at 233 m μ in the ultraviolet region.

Figure 17 shows a Moffitt plot of the ORD data obtained for beef cardiac tropomyosin. The percent helix was calculated from the b_0 (helix content) value obtained directly from the slope of this plot (-607°), and found to be 95%. This figure is based on the assumption that a value for b_0 of -640° characterizes a fully coiled, right-handed α -helix (62). Confirmation of this result was achieved by extending the optical rotatory dispersion analysis into the ultraviolet region and estimating percent helix on the basis of the amplitude of the negative Cotton effect at 233 m μ (63). Figure 18 represents a plot of the effective residue rotation m' , as a function of wavelength in the ultraviolet region for the beef cardiac system. On the basis of a $\Delta[m']_{233}$ value of $14,600^\circ$ between helix and random coil (65), the value of $-12,475^\circ$ noted here corresponds to a helicity of 86%, in good

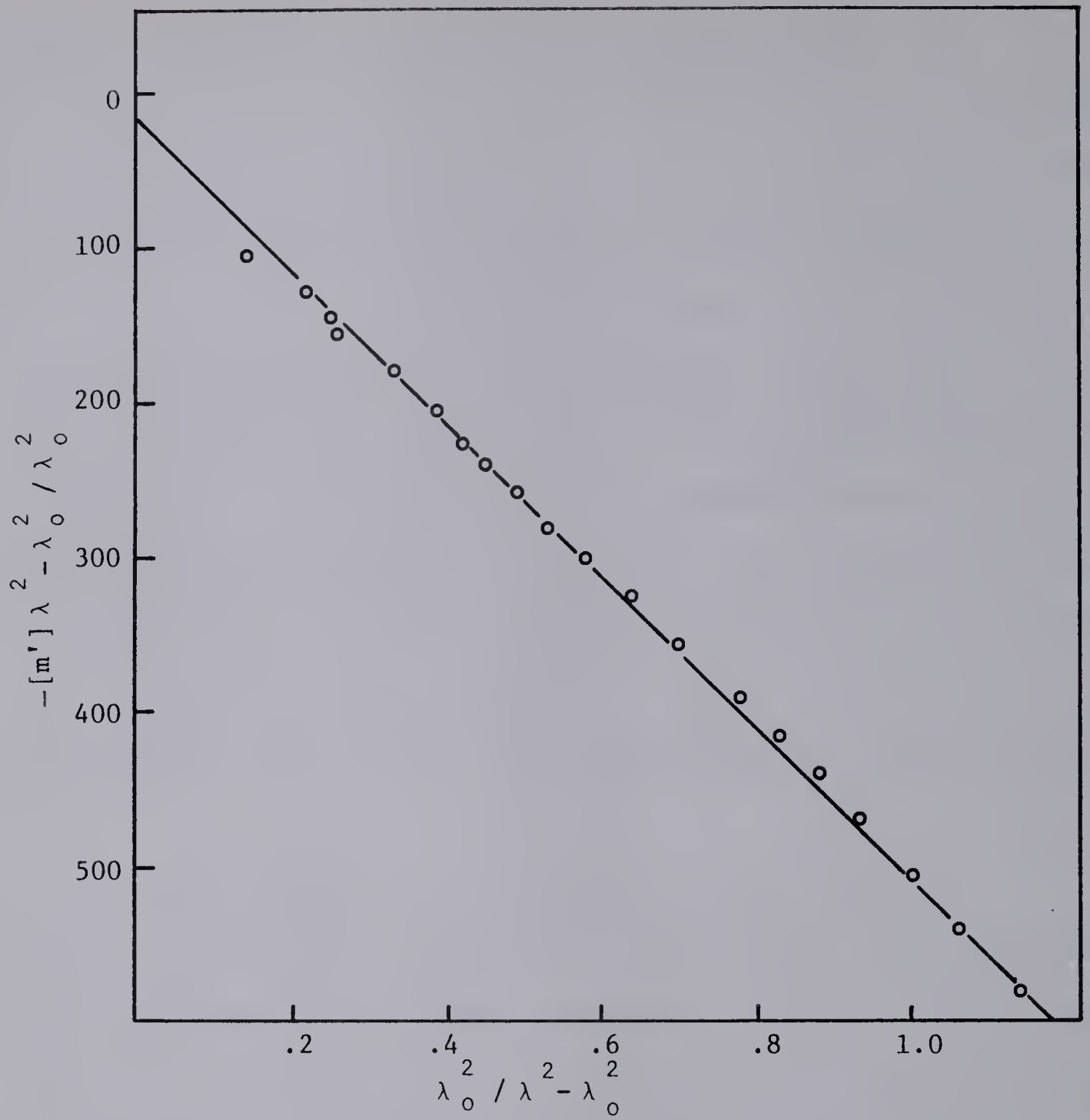


Figure 19

A Moffitt plot of the rotatory dispersion of rabbit cardiac tropomyosin in 0.5M KCl, 0.067M phosphate buffer, pH 7.0.

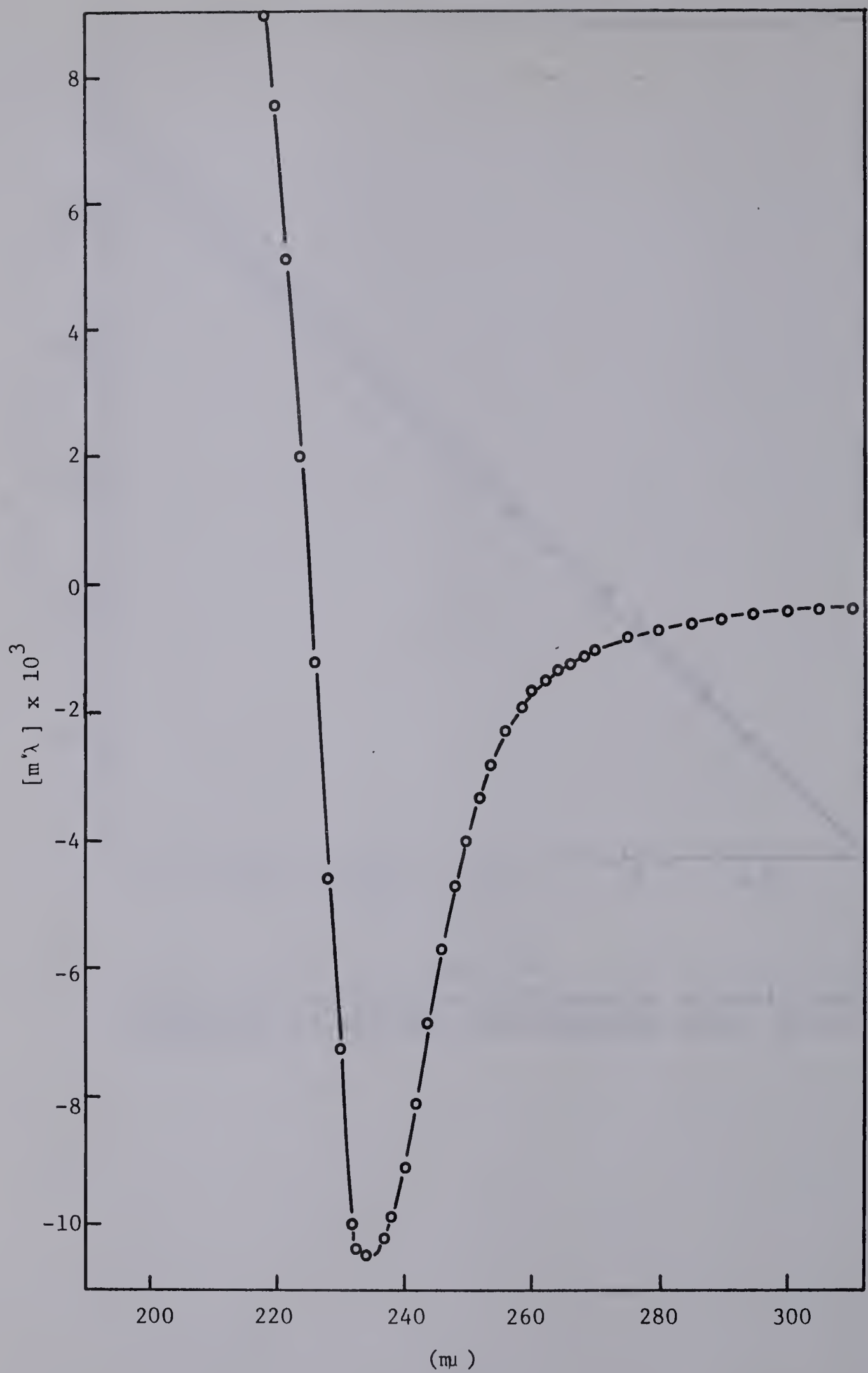


Figure 20

Optical rotatory dispersion of rabbit cardiac tropomyosin in the ultraviolet region. Conditions same as in Figure 14.

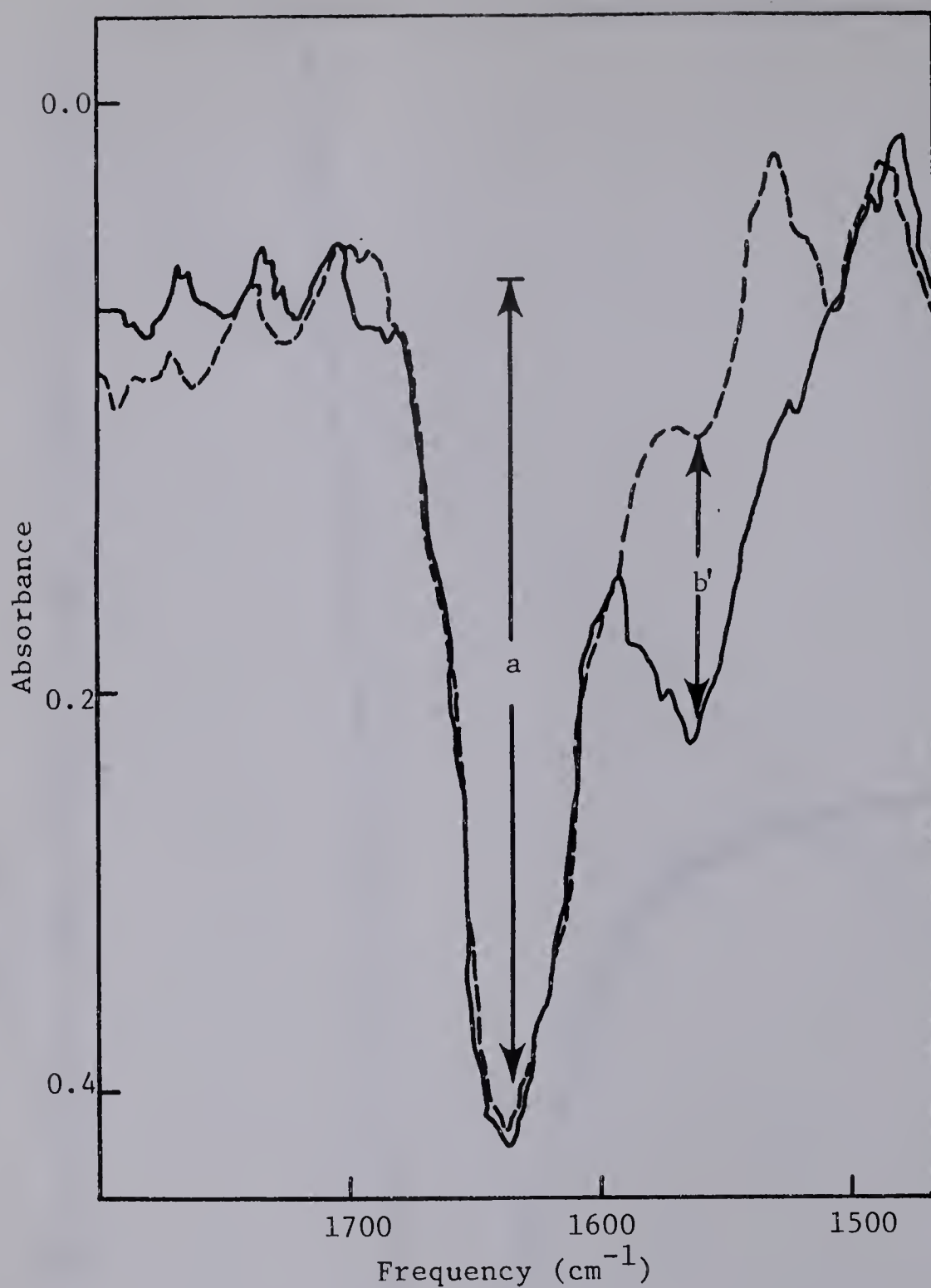


Figure 21

Infrared spectrum of beef cardiac tropomyosin in D₂O; (A) — spectra after 20 min. incubation in D₂O; (B) --- spectra of identical sample but heated 2 hrs. at 60°C.

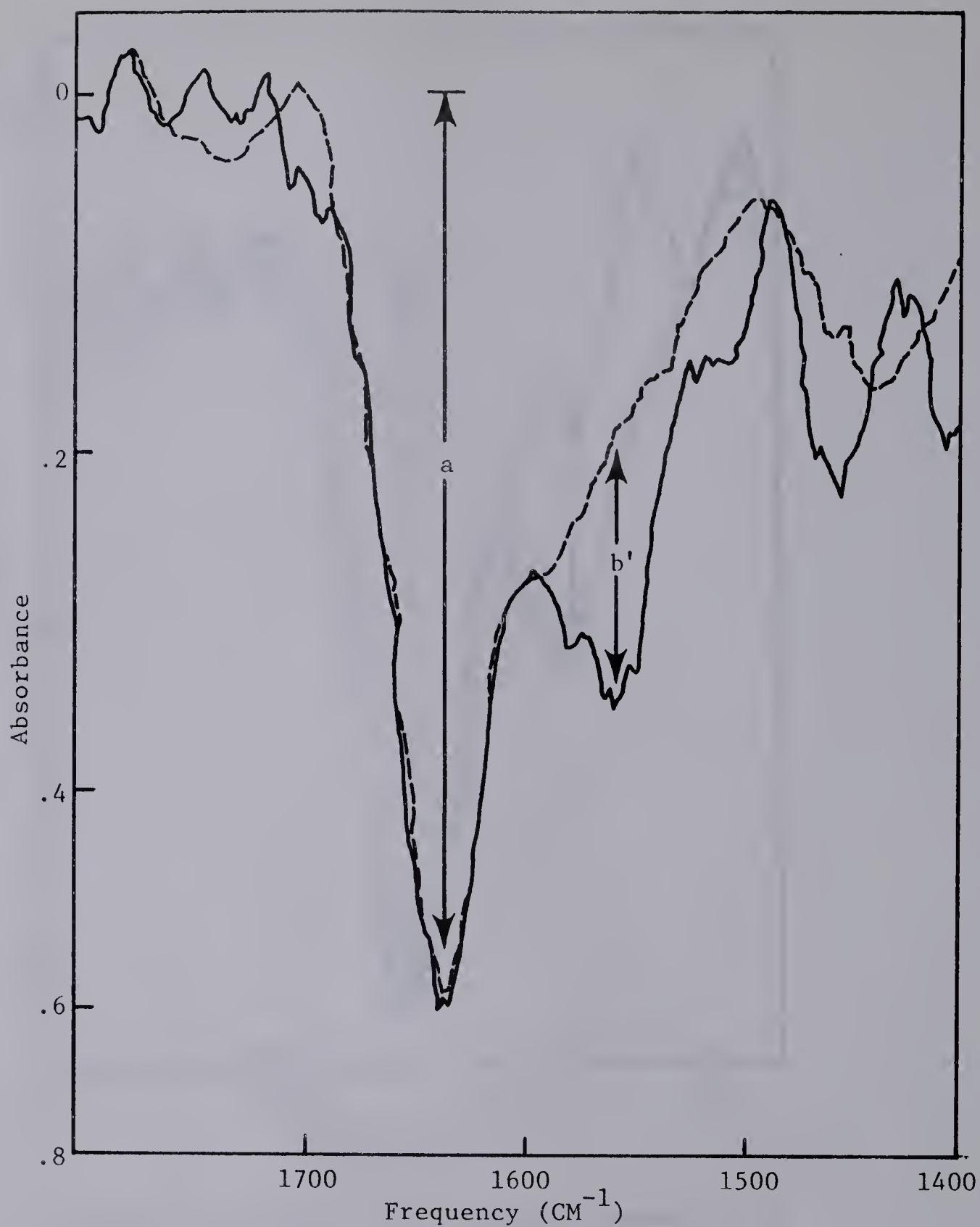


Figure 22

Infrared spectrum of rabbit cardiac tropomyosin in D₂O:
(A) — spectra after 20 min. incubation in D₂O; (B) ----
spectra of identical sample but heated 2 hours at 60°C.

agreement with the Moffitt plot. A definite difference in secondary structure is evident in the case of rabbit cardiac tropomyosin. The Moffitt evaluation yields a value of -495° for the b_0 parameter resulting in a helical content of only 77% (Figure 19) while a value of $-10,880^{\circ}$ for $(m')_{233}$ corresponds to a helix content of 75% (Figure 20).

(g) Deuterium-hydrogen Exchange. As a check on the values of helicity obtained by use of the Moffitt equation and the Cotton effect, the extent of deuterium exchange was determined for the beef and rabbit cardiac systems. Figure 21 shows the characteristic spectrum of the amide bands at 1550 cm^{-1} and 1660 cm^{-1} for beef cardiac tropomyosin, while Figure 22 shows a similar spectrum for the rabbit cardiac system. The amount of "hard-to-exchange-amide hydrogen" (HEAH) was calculated from the ratio of the amide II band at 1550 cm^{-1} (denoted as b') to the amide I band at 1660 cm^{-1} (denoted as a).

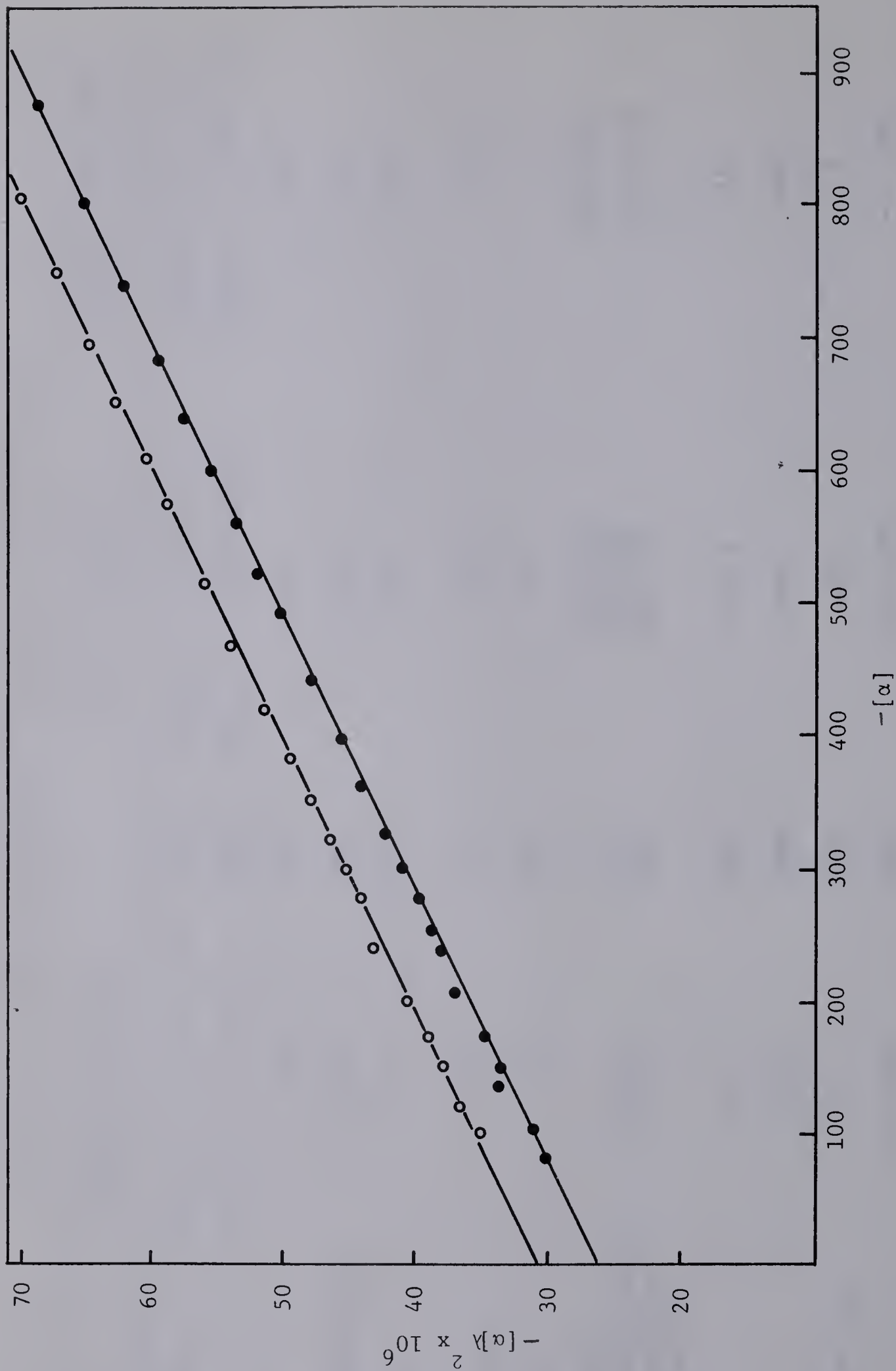
The "HEAH" values calculated for beef and rabbit tropomyosin are 86% and 88%, respectively. It may be seen that the results for beef cardiac tropomyosin are in good agreement with those obtained from ORD measurements, whereas, there exists a significant difference in the rabbit cardiac system - the ORD values being somewhat lower. A possible explanation for the divergence is that portions of the polypeptide chain may be in hydrophobic regions and thus are not available for deuterium exchange, leading to higher HEAH values.

Co-existence of right-handed α -helix and left-handed

Table VI
Molecular Properties of the Monomeric Tropomyosins

Property	Rabbit Skeletal		Beef Cardiac*	Rabbit Cardiac*
sedimentation	$S_{20,w} = 2.95-1.00c$	(89)**	$S_{20,w} = 3.08-1.21c$	$S_{20,w} = 2.97-.87c$
diffusion	$D_{20,w} = 4.5-4.1c$	(89)	$D_{20,w} = 2.85-1.01c$	$D_{20,w} = 3.02-1.27c$
$[\eta]$ (dl/g)	.039	(92)	0.46	0.48
Huggins' constant, k'	3.54	(92)	1.60	2.10
$E_{1cm}^{1\%}$ (278 m μ)	3.55	(107)	3.45	3.55
\bar{v} (ml/g) experimental	.736	(47)	.728	.731
theoretical	.730	(89)	.727	.723
M_w (Archibald) (light scattering)	- 54,000	(35)	103,800 99,000	102,000 -
(sedimentation- diffusion)	59,000	(89)	103,100	102,000
a_o degrees	-11.1	(98)	-13.4	-19
b_o degrees	-600	(98)	-607	-495
% helix (from b_o)	91	(98)	94	77
$[m']_{233}$	-12,100	(63)	-12,475	-10,880
% helix (from $[m']_{233}$)	83		86	75
% helix (IR)	-		86	88

*This study. **Figures in parentheses refer to references.



Optical rotatory dispersion data on rabbit cardiac o and beef cardiac • tropomyosin in 8M urea, 0.5M KCl, 0.067M phosphate buffer, pH 7.0.

Figure 23

α -helix has been postulated for certain proteins (e.g. insulin, (99)) which may also be a possibility for the rabbit cardiac system. Another possibility for the divergency noted is that the rabbit hearts were obtained in a frozen state from the commercial supplier, and this freezing may alter the secondary structure of the molecule, which is reflected in a lower helical content.

Treatment of rabbit and beef cardiac tropomyosin with 8M urea solutions resulted in loss of helicity as illustrated in Figure 23. The data were evaluated by the method of Yang and Doty (100) which consists in plotting $-\lambda^2 [\alpha]$ against $-\alpha$ to determine the dispersion constant, λ_c . A λ_c value of 2200 Å was obtained for both cardiac systems and this value is very characteristic of denatured proteins (101).

The optical rotatory parameters and other physical properties, thus far studied, for the cardiac system are summarized in Table VI, along with those reported for rabbit skeletal tropomyosin. This table illustrates the similarities and differences between the skeletal system on the one hand and the cardiac on the other. For example, some of the parameters such as sedimentation coefficient and helical content, are practically identical for both skeletal and cardiac tropomyosins, whereas distinct differences occur in others, such as in diffusion coefficients and molecular weights. The similarities and differences will be further elaborated upon in the model discussion of cardiac tropomyosin.

(h) Amino Acid Composition. The amino acid composition of beef and rabbit cardiac tropomyosins were determined with a Spinco Model 120B Amino Acid Analyzer on 22-, 30- and 72-hour acid hydrolysates. A composite summary of these results, as well as those reported by other workers for the rabbit skeletal system, is presented in Table I.

The major differences are that both beef and rabbit cardiac tropomyosin have no half-cystine residues, whereas rabbit skeletal tropomyosin has 6.5 moles/ 10^5 g of this residue. The amount of free -SH groups was not established in the current investigation, but it has recently been reported by Drabikowski and Novak (103) that rabbit skeletal tropomyosin contains up to 5.7 SH equivalents per 10^5 g of protein, so that it would appear that essentially all the half-cystine is present in the form of -SH groups. The significance of these groups in the polymerization of skeletal tropomyosin will be discussed in Part B of the experimental results.

Rabbit cardiac tropomyosin is distinguished from both the rabbit skeletal and beef cardiac homologues by a relatively larger amount of histidine and a lower amount of alanine. However, aside from these differences, the overall amino acid patterns are quite similar.

3. Model Forms for Cardiac Tropomyosin Based on the Hydrodynamic and Thermodynamic Measurements.

(a) Representation of Cardiac Tropomyosin in Terms of a Prolate Ellipsoid Model.

It is of interest to examine cardiac tropomyosin from the standpoint of reasonable equivalent models consistent

with the hydrodynamic measurements. There are, of course, certain limitations imposed when interpreting the hydrodynamic behavior of molecules in terms of various model forms. First, there is the uncertainty of the degree of hydration which no doubt will be reflected in the frictional coefficient and the overall dimensions of the unit. Secondly, the proposed model may not have any resemblance to the actual protein structure. These limitations should be kept in mind when comparing one protein model system with another.

One way to interpret the hydrodynamic properties of a molecule is in terms of the Scheraga-Mandelkern equation (97) viz:

$$\beta = \frac{N S_{20,w}^0 [\eta]^{1/3} \eta_0}{M^{2/3} (1-\bar{v} \rho)} \quad (37)$$

which may be rewritten in an alternative form:

$$\beta = \frac{D [\eta]^{1/3} \eta_0 [M]^{1/3}}{kT} \quad (38)$$

where N = Avogadro's number

$S_{20,w}^0$ = intrinsic sedimentation coefficient

$[\eta]$ = weight intrinsic viscosity

η_0 = solvent viscosity

\bar{v} = partial specific volume

ρ = solvent density

M = molecular weight

D = intrinsic diffusion coefficient

k = Boltzman constant

T = absolute temperature

Table VII

Calculated Values for the β -function, the Viscosity Increment, ν , the Frictional Ratio, f/f_0 and the Axial Ratio, a/b , as Determined from the Scheraga-Mandelkern Equation, for Beef and Rabbit Cardiac Tropomyosin. Values are expressed in terms of an equivalent ellipsoid of revolution model.

Equation:	$\beta = \frac{N S_{20,w}^{\circ} [\eta]^{1/3} \eta_0}{M^{2/3} (1-\bar{\nu} \rho)}$	*
Parameter	Rabbit Cardiac	Beef Cardiac
β	2.52 (\pm .12)	2.51 (\pm .10)
a/b	14 (\pm 6.0)	14 (\pm 4.0)
ν	22.77 (\pm 15.8)	22.77 (\pm 10.2)
f/f_0	1.74 (\pm .25)	1.74 (\pm .19)

Equation:	$\beta = \frac{D_{20,w}^{\circ} [\eta]^{1/3} \eta_0 [M]^{1/3}}{kT}$	*
Parameter	Rabbit Cardiac	Beef Cardiac
β	2.70 (\pm .09)	2.52 (\pm .11)
a/b	24 (\pm 6.0)	14 (\pm 5.5)
ν	51.10 (\pm 23.4)	22.77 (\pm 15.1)
f/f_0	2.14 (\pm .21)	1.74 (\pm .25)

*Symbols explained in text.

The experimentally measured intrinsic sedimentation coefficient, molecular weight, partial specific volume, and intrinsic viscosity may be defined in terms of a β function utilizing the above relationship. The parameter β interrelates the observed characterization of the protein particle to a hypothetical hydrodynamic equivalent ellipsoid of revolution. Values of β may be tabulated as a function of axial ratio (J) alone, and in the case of a prolate ellipsoid, β varies from 2.12×10^6 for $J = 1$ to 3.2×10^6 for $J = 100$.

Utilizing this approach and substituting the experimentally observed values into equation (37) results in β values of 2.52×10^6 and 2.51×10^6 for rabbit cardiac and beef cardiac tropomyosin, respectively. Use of the alternative equation (38) for β yields values of 2.70×10^6 for rabbit cardiac and 2.52×10^6 for beef cardiac tropomyosin. These results are summarized in Table VII along with the calculated axial ratios, viscosity increment values and frictional coefficients for the two cardiac systems. These latter values were deduced from the Scheraga-Mandelkern tables (97).

From the results presented, it is seen that within the limits of experimental error, the β -function values and their associated parameters, are essentially identical for the two cardiac systems. Furthermore, the virtual equivalence of β , for any one system, as estimated from two different calculation approaches, suggests an internal consistency in the measured experimental data. The large variation in the viscosity increment, V , for the two systems as determined from β , based on the diffusion constant (eq. 38) is a consequence

of the small variation in the $D_{20,w}^O$ values for the two systems (3.02 versus 2.85 Fick units for rabbit and beef cardiac tropomyosins, respectively). This is an excellent illustration of the extreme sensitivity of the β -function value to any one measured experimental parameter.

In contrast to the cardiac tropomyosins, a prolate ellipsoidal model is not regarded at present as a satisfactory one for defining the hydrodynamic parameters of rabbit skeletal tropomyosin. The reported values for sedimentation constant (2.95S), molecular weight (54,000), partial specific volume (0.736 dl/g), diffusion coefficient (4.5 F.U.) and weight intrinsic viscosity (0.39 dl/g) yield β values of 3.62×10^6 (eq. 37) and 3.03×10^6 (eq. 38) for this protein. On the basis of the above quantities for β , the calculated axial ratio is in excess of 300! One reason for the inadequacy of the model is that it may well be that one or other of the parameters reported for this molecule is incorrect. For example, the weight intrinsic viscosity for the rabbit skeletal system initially reported as 0.57 dl/g by Tsao et al. (90) was recently revised by Noelken to a value of 0.39 dl/g (92). It is conceivable that other molecular parameters for this system are also in error, and clearly deserve systematic re-investigation.

(b) Effective Volume and Axial Ratio of the Prolate Model Form.

The hydrodynamic properties of a molecule are to a large extent dependent on its overall structure, which is a reflection of size and shape. The size of the particle may

be evaluated by means of the effective volume (V_e) which is expressed (in ml/g) as:

$$V_e = \frac{[\eta] \cdot 100 \cdot M}{N \cdot \check{v}} \quad (39)$$

where $[\eta]$ is the weight intrinsic viscosity, M is the molecular weight, N is Avogadro's number, and \check{v} , the viscosity increment, is a function of the axial ratio only, and has been computed by Simha for the ellipsoidal model (104).

Calculations reveal that the effective volumes (V_e)* for rabbit and beef cardiac tropomyosin are 2.11 ml/g and 2.02 ml/g respectively, as compared to the anhydrous partial specific volume value of 0.73 ml/g. This indicates that the cardiac system is a voluminous particle with a large amount of water of hydration. As was pointed out earlier in this discussion, the degree of hydration for this system is not accurately known, and thus the contribution of water molecules to the effective volume remains uncertain.

The frictional coefficient, f , of a protein is dependent both on V_e and the axial ratio (a/b). However, if the frictional coefficient, f , is compared to that of a corresponding spherical particle, f_0 , whose volume is the same as that of the protein, then the value of the frictional ratio, f/f_0 , depends only on the axial ratio and is non-dependent on V_e , as suggested initially by Perrin (105).

In computing frictional ratios, the quantity f_0 was evaluated from the expression:

$$f_0 = 6 \pi \eta_0 \left(\frac{3V_e M}{4 \pi N} \right)^{1/3} \quad (40)$$

* In order to compare the effective volume with the partial specific volume (expressed in ml/g) it was necessary to divide V_e (in ml) by MN .

Table VIII

Frictional Ratios, f/f_0 , and Corresponding Axial Ratios, a/b , for Rabbit Cardiac and Beef Cardiac Tropomyosins at Infinite Dilution

Property	Rabbit Cardiac	Beef Cardiac
f/f_0	1.76	1.73
a/b	14.7	14.5

Table IX

Dimensions of the Equivalent Ellipsoid of Revolution
Model for the Cardiac Tropomyosins (Values are
based on V_e and frictional ratio deduced
from the Scheraga-Mandelkern equation)

	Rabbit Cardiac	Beef Cardiac
Axial ratio (a/b)	14	14
Axis of revolution (a)	511.6 Å ^o	506.9 Å ^o
Equatorial diameter (2b)	36.5 Å ^o	36.2 Å ^o

The quantity f was determined from the translational diffusion equation, viz.,

$$f = \frac{kT}{D} \quad (41)$$

In the above two equations, k represents the Boltzmann constant, T is equal to the absolute temperature, D the diffusion coefficient, and N is Avogadro's number. Table VIII summarizes the frictional ratios for both cardiac and skeletal tropomyosin systems. The numerical values of f/f_0 as a function of axial ratio are taken from Svedberg and Pedersen (106).

From the previously determined values of the effective volume and axial ratio of the ellipsoidal form of the tropomyosin molecule, the length of the axis of the ellipsoid may be calculated from the expression:

$$V_e = 4/3 \pi ab^2 \quad (42)$$

where a and b are the ellipsoidal semi-major and semi-minor axes, respectively. The results of this calculation for beef and rabbit cardiac tropomyosin are shown in Table IX.

As a further consideration, an estimation of the length of the equivalent ellipsoid for tropomyosin was obtained from the hydrodynamic expressions presented by Yang for a prolate ellipsoidal model (107):

$$L = 6.82 \times 10^{-8} ([\eta]M)^{1/3} (\rho^2/v)^{1/3} \quad (43)$$

$$L = 1.76 \times 10^{-25} (M(1-\bar{v}\rho)/N_0S) (Fp^{2/3}) \quad (44)$$

$$L = 1.46 \times 10^{-17} (T/N_0D) (Fp^{2/3}) \quad (45)$$

where

L = length of the major axis of the prolate ellipsoid

Table X

Estimation of the Length of the Equivalent Prolate Ellipsoid Model for Beef Cardiac and Rabbit Cardiac Tropomyosins

Expression	Rabbit Cardiac	Beef Cardiac
$L = 6.82 \times 10^{-8} ([\eta]M)^{1/3} (p^2/\nu)^{1/3}$	519 Å ^o	514 Å ^o
$L = 1.76 \times 10^{-25} [M(1-\bar{\nu}\rho)/N_oS] (F_p^{2/3})$	523 Å ^o	506 Å ^o
$L = 1.46 \times 10^{-17} (T/N_oD) (F_p^{2/3})$	479 Å ^o	504 Å ^o

p = axial ratio

ν = viscosity increment

F = frictional ratio

The values for $(p^2/\nu)^{1/3}$ and $(Fp^{2/3})$ are recorded as a function of axial ratio for a prolate ellipsoid model in the review by Yang (106) and are taken directly therefrom.

Equation 43 emphasizes the intrinsic viscosity and molecular weight whereas in equations 44 and 45 the molecular weight-sedimentation coefficient, and diffusion coefficient are highlighted. It may be seen that the dimensions (length) from these three equations (Table X) are consistent with those calculated on the basis of effective volume (Table IX). It is also to be noted that the molecular length deduced from hydrodynamics (average figure, 509 Å) is in reasonably good agreement with that established by light scattering (557 Å).

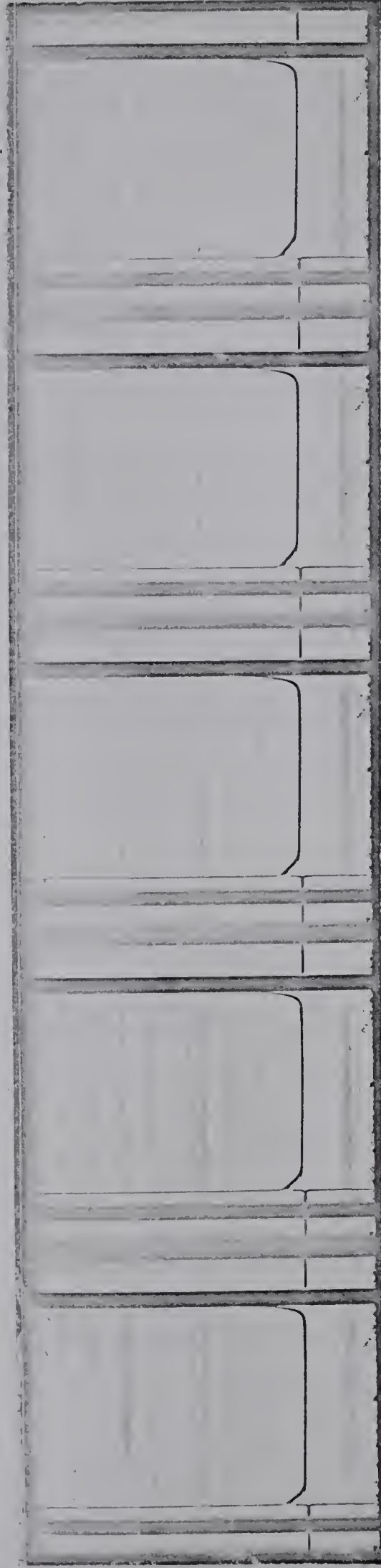
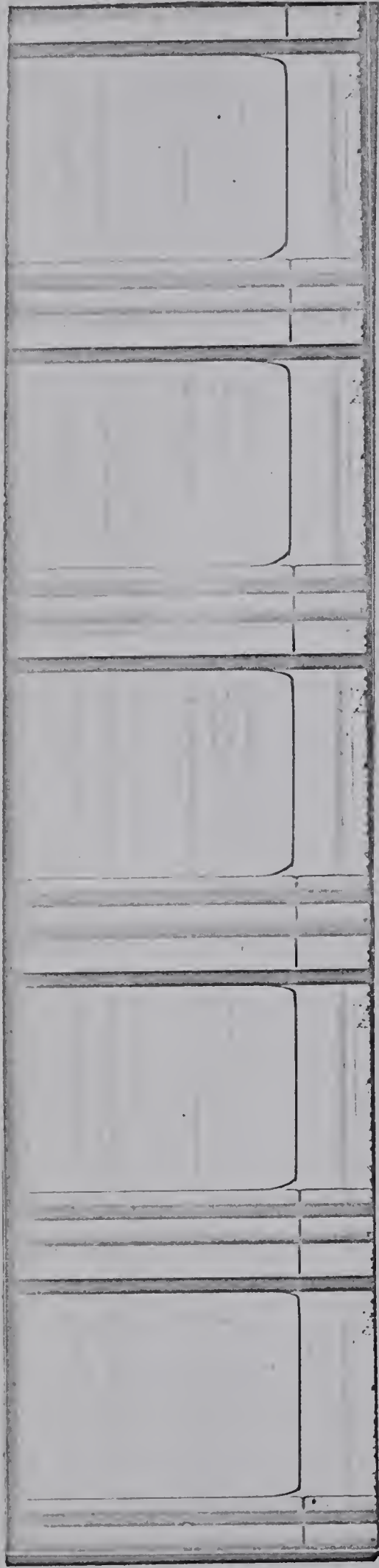
(c) Extension of the Cardiac Tropomyosin Molecule and Polypeptide Chain Arrangement.

The total extension of the cardiac tropomyosin molecule may be obtained from molecular weight, average amino acid residue weight and percent helicity. For example, the number of amino acids present in beef cardiac tropomyosin, based on a molecular weight of 103,000 and an average amino acid residue weight of 115, is 886. For a 100% α -helical rod, the length would be 1329 Å, that is, 886 times the α -helix residue extension of 1.5 Å. Based on a helicity of 90%, the total helical segment(s) would constitute a length of 1196 Å (that is, 90% of 1329 Å). The number of residues in the helical

segment(s) is $1196 \overset{\circ}{\text{\AA}} / 1.5 \overset{\circ}{\text{\AA}} = 797$ residues, which leaves 89 residues presumably without order. If $2.5 \overset{\circ}{\text{\AA}}$ is taken as the average random spacing (halfway between the α -helix amino acid extension of $1.5 \overset{\circ}{\text{\AA}}$ and the value of $3.5 \overset{\circ}{\text{\AA}}$ for a fully extended β structure), then the total extension of the random segment(s) is $2.5 \times 89 = 223 \overset{\circ}{\text{\AA}}$. The total extension of the particle is the sum of the helical and random segments which is $1419 \overset{\circ}{\text{\AA}}$.

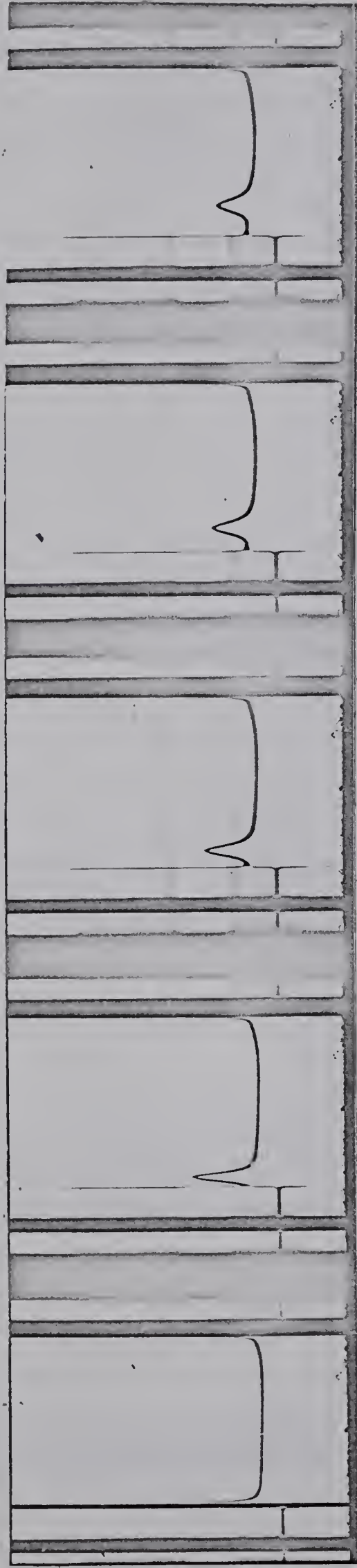
A direct measure of the molecular length of beef cardiac tropomyosin obtained from light scattering is $\sim 557 \overset{\circ}{\text{\AA}}$, assuming a prolate ellipsoid model (see Part A of Results). The number of polypeptide chains present in a single molecule may be calculated from the total extension of $1419 \overset{\circ}{\text{\AA}}$, and the light scattering length of $557 \overset{\circ}{\text{\AA}}$, which results in 2.55 chains (i.e. $1419/557$).

The length based on the prolate ellipsoid models (Table X) and the effective volume gives an extension, on the average, of $509 \overset{\circ}{\text{\AA}}$. Using this figure and the total extension length, a value of 2.79 chains is obtained for beef cardiac tropomyosin. The number of polypeptide chains present in a single cardiac tropomyosin molecule from the molecular lengths deduced from both light scattering and hydrodynamic measurements agree (7% variation) within experimental error. If we assign equal weight to both approaches, it would seem equally probable that both two-chain and three-chain regions are simultaneously present in the tropomyosin molecule. No doubt this structure is stabilized by hydrophobic bonding involving the neighboring helical chains, as well as by favorable interactions between

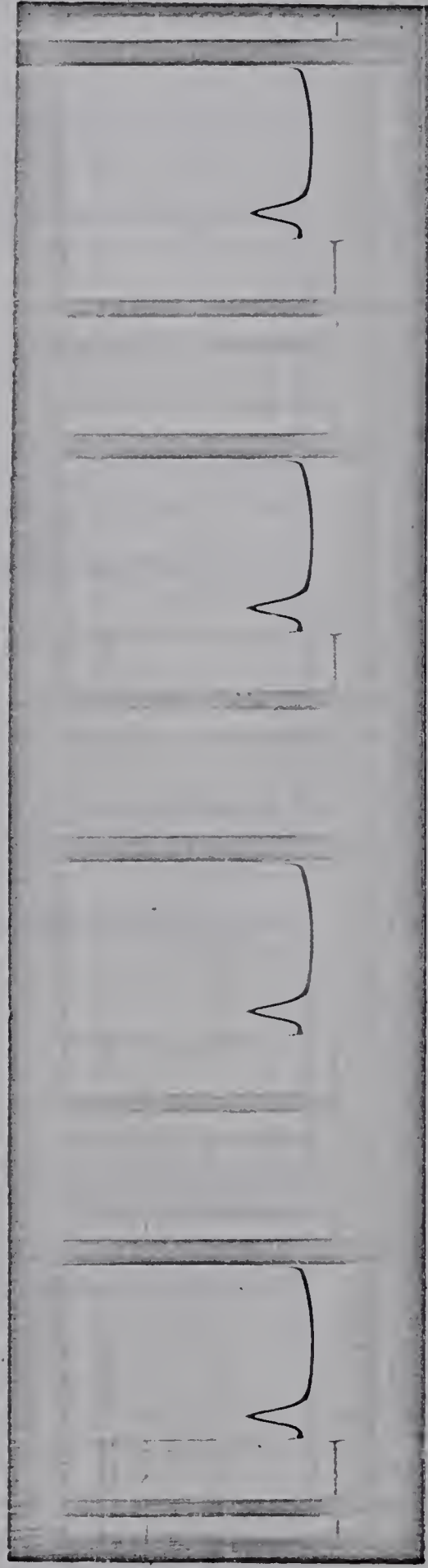


Ultracentrifuge schlieren pattern during the approach to sedimentation equilibrium (Archibald) of rabbit cardiac tropomyosin. The direction of sedimentation is from left to right at 12,590 r.p.m.; temperature, 9.5°; bar angle, 75°; protein concentration, 0.54% in 0.5M KCl - 0.067M phosphate buffer (pH 7.0). Pictures were taken at 16 minute intervals after maximum speed had been attained.

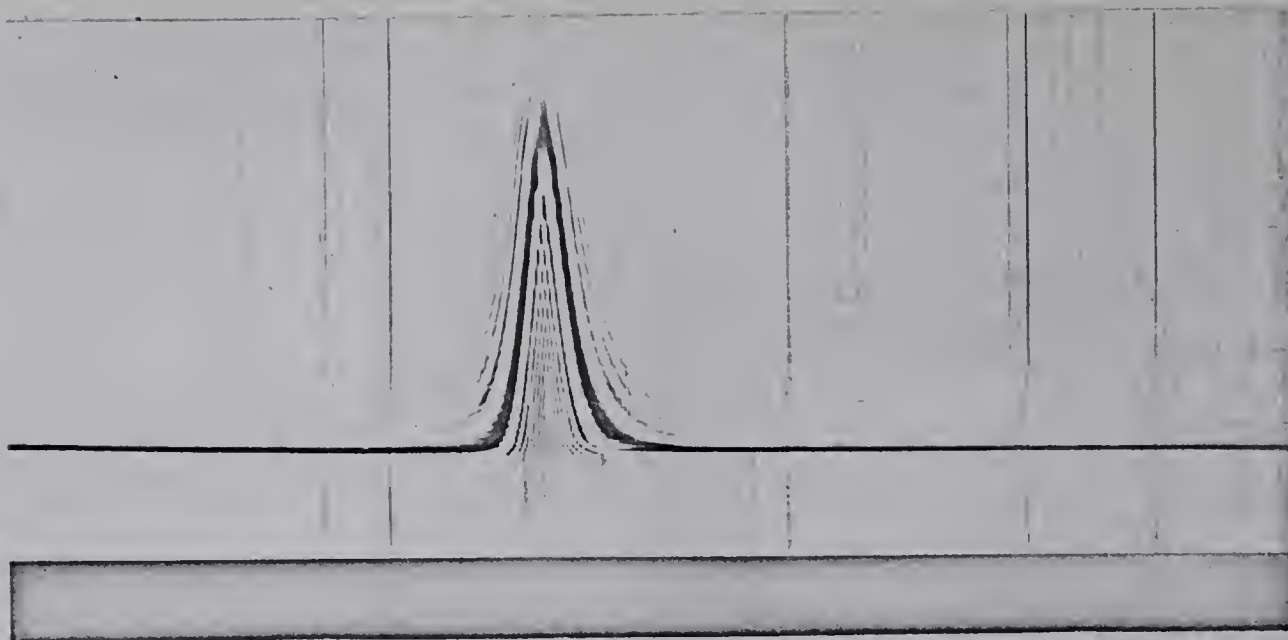
Plate C



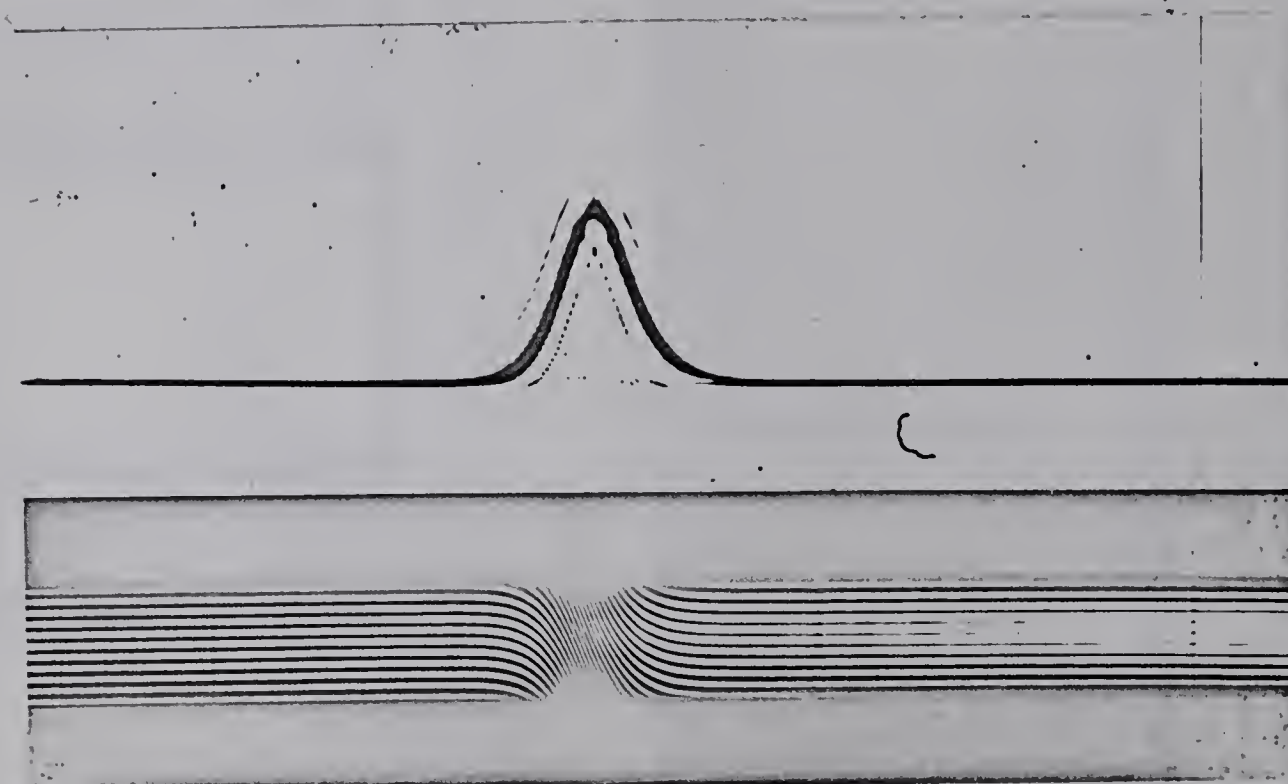
(1) Rabbit cardiac tropomyosin (c=0.467%) in 0.5M KCl - 0.067M phosphate buffer, pH 7.0, bar angle 75°. Picture intervals 16 mins., speed 59,780 r.p.m.



(2) Beef cardiac tropomyosin (c=0.71%) in 0.067M phosphate buffer, pH 7.0, ionic strength 0.1, bar angle 75°. Picture interval 8 mins., speed 59,780 r.p.m.



(1)



(2)

Diffusion and Rayleigh interference patterns for beef cardiac tropomyosin in 0.5M KCl - 0.067M phosphate buffer, pH 7.0, and bar angle 50° .

(1) Time after start 9.76 hrs.

(2) Time after start 33.90 hrs.

Plate E

water and the protein surface that remains exposed to it.

Similar calculations for the extension of rabbit cardiac tropomyosin result in a value of 1528 \AA . Based on model studies involving the use of the Scheraga-Mandelkern equation, it would appear that rabbit cardiac tropomyosin may also be interpreted as a composite of a two-chain, three-chain particle, similar to that of the beef cardiac system.

The arrangement of polypeptide chains in this fashion in muscle protein systems is not unique. At the present time, the current conception of the skeletal myosin molecule is that it is best represented as a particle of non-uniform mass distribution (108). The light meromyosin portion of the molecule is rod-like and possesses a diameter of $\sim 20 \text{ \AA}$ consistent with a two-chain model. The enzymatically active heavy meromyosin portion is ellipsoidal in shape with a larger average diameter ($\sim 28 \text{ \AA}$), consistent with a more complex arrangement of the polypeptide chains. Thus in some respects, cardiac tropomyosin resembles the myosin molecule (108,109).

Part B. Association Reactions of Beef Cardiac Tropomyosin in Low Ionic Strength Media.

1. Introduction.

The study of association-dissociation reactions between protein molecules of one type and those of another is of prime importance in the understanding of many biological processes. It is well-known that such systems as enzyme-substrate, antigen-antibody and protein-nucleic acid complexes involve the association of the active protein with other macromolecules.

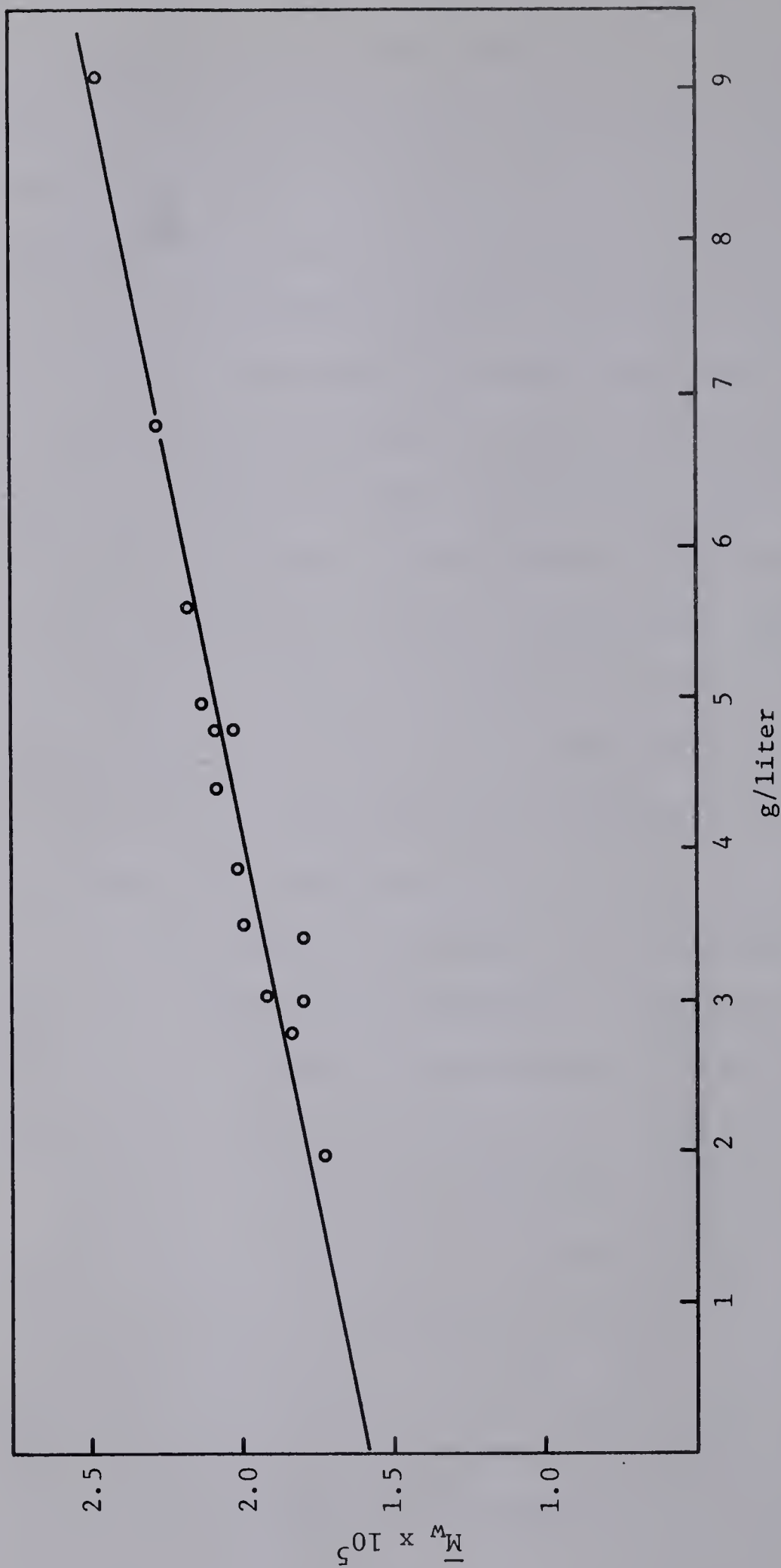
Furthermore, the degree of molecular association of these systems may greatly influence their biological properties.

Kinetic and thermodynamic parameters must be ascertained in order to form a basis for the evaluation of protein-macromolecular interactions. There are two basic approaches which may be used to study these molecular interactions. The first method consists in determining the velocity of the reaction under a prescribed set of environmental conditions. By interrupting the course of the reaction through a lowering of temperature, ionic strength or pH, or by the addition of inhibitors, the reaction rate may be evaluated. Latallo et al. (110) applied this method in a study of the influence of ionic strength and pH on fibrin polymerization, and Waugh et al. (111) used this technique on the kinetics of insulin fibril formation.

The second approach is to observe the polymerization reaction under equilibrium conditions, as was initially formulated by Steiner (112) for an ideal system and Rao and Kegeles (113) for the α -chymotrypsin system. The latter authors studied the polymerization of the protein at its isoelectric point by means of the Archibald approach to sedimentation technique from which the free energies of dissociation of the complex were evaluated. Of these two approaches, the Rao and Kegeles treatment is preferred since Waugh's method requires a means of stopping the polymerization process without disturbing the equilibrium of the system. It also must be established that the termination does not bring about any denaturation since such conditions

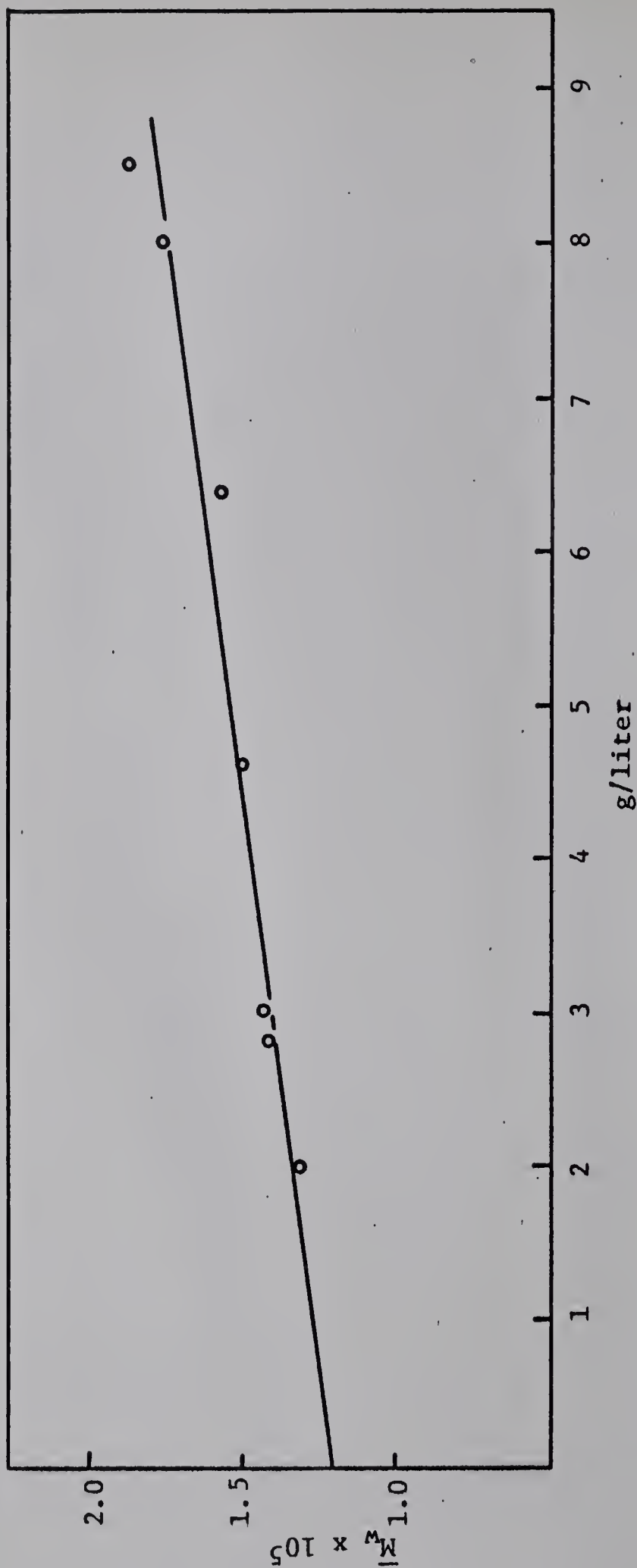
would upset the state of the system. The Rao and Kegeles approach involves determination of the weight-average molecular weight (\bar{M}_w) of the solute species from the total concentration (C) and concentration gradient (dc/dx) of the solute, provided the interaction obeys the law of mass action.

Tropomyosin solutions (skeletal) possess a high viscosity in neutral, salt-free media, which decreases rapidly as small amounts of salt are added. Physico-chemical investigations such as osmotic pressure (90), viscosity (90) and light scattering (35) have shown that the tropomyosin particles aggregate at low ionic strength into polymers, and that salt brings about the depolymerization of these polymers. Tsao et al. (33) have studied the polymerization of duck gizzard, pig heart, prawn and sepia tropomyosin by means of osmotic pressure measurements. They have shown that the polymerizability of pig heart tropomyosin is lower, and that of duck gizzard and prawn tropomyosin is higher than that of the rabbit skeletal system. In view of the above investigations which suggest that tropomyosin undergoes extensive aggregation at low ionic strength, it was of interest to extend these studies to cardiac tropomyosin, as well as to interpret the results by the techniques of ultracentrifugation and viscometry in terms of theories of reversibly interacting systems which have been developed largely in the past two years (36,113).



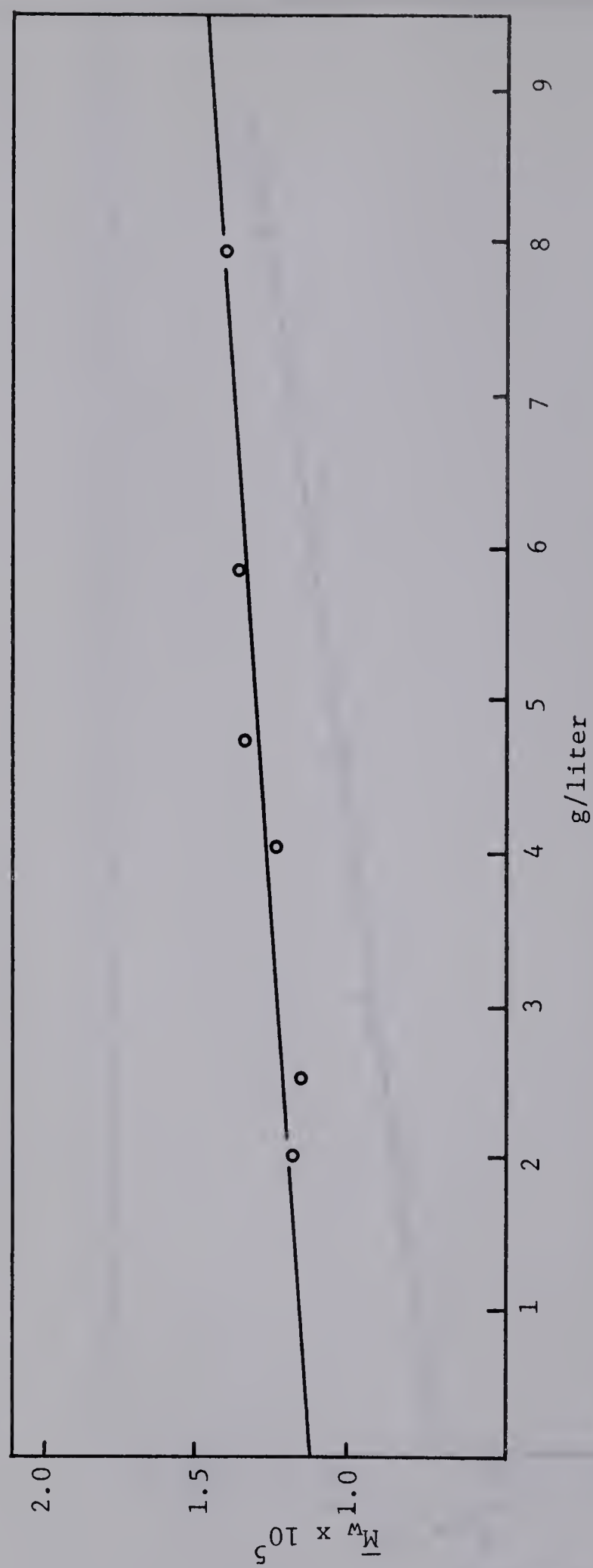
Experimental weight-average molecular weight (Archibald ultracentrifugation) versus tropomyosin (beef cardiac) concentration in 0.1 ionic strength media, pH 7.0.

Figure 24



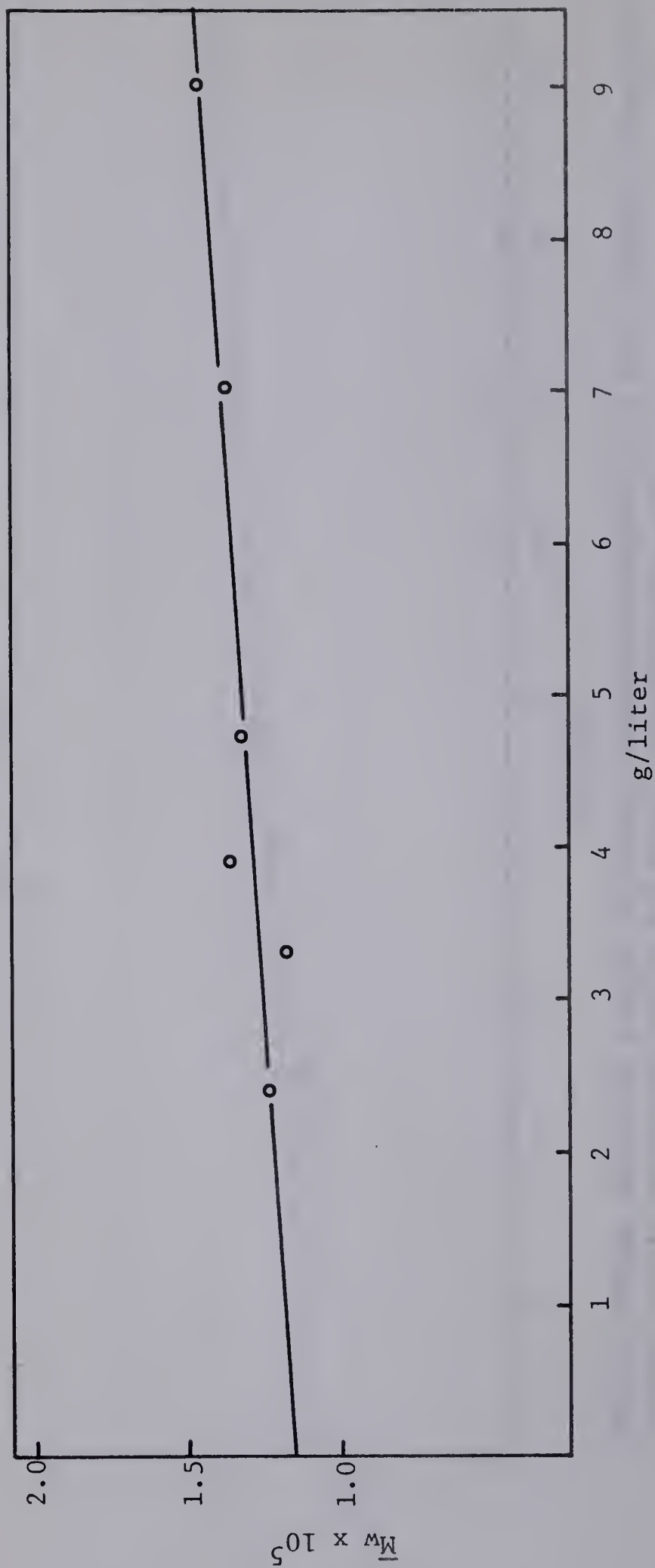
Weight-average molecular weight (Archibald ultracentrifugation) of beef cardiac tropomyosin versus protein concentration in 0.2 ionic strength media, pH 7.0.

Figure 25



Weight-average molecular weight (Archibald ultracentrifugation) of beef cardiac tropomyosin versus protein concentration in 0.3 ionic strength media, pH 7.0.

Figure 26



Weight-average molecular weight (Archibald ultracentrifugation) of beef cardiac tropomyosin versus protein concentration in 0.4 ionic strength media, pH 7.0.

Figure 27

2. Influence of Ionic Strength on the Molecular Weight, Viscosity and Diffusion Properties of Beef Cardiac Tropomyosin.

As mentioned earlier, association of tropomyosin may be conveniently studied by ultracentrifugation and viscosity. In this study, use was made of the Archibald technique, which provided a reliable estimate of the weight-average molecular weight. From molecular weight measurements, the degree of association was estimated either by assuming monomers and trimers only to be present in the system or by assuming the simultaneous presence of monomers, dimers and trimers. The validity of these assumptions was based on the following experimental observations. At ionic strength 0.6 and greater, a weight-average molecular weight of 100,000 was obtained which did not vary. Likewise, in the presence of denaturing solvents (urea, guanidine hydrochloride solutions), the molecular weight was determined to be approximately 100,000 (Table IV). This then is the "monomer" molecular weight. Figures 24-27 illustrate plots of the weight-average molecular weight of beef cardiac tropomyosin determined by Archibald ultracentrifugation at four different ionic strengths, 0.1, 0.2, 0.3 and 0.4 respectively, in buffer solution of pH 7.0. The reason for choosing this ionic strength range was that the molecular weights averaged from 115,000 to 145,000 for ionic strength 0.4, while at 0.1 the values varied from 170,000 to 250,000 over the concentration studied. These molecular weight values may be taken to indicate that the reaction system is composed of species no greater than the trimer.

The observed decrease in apparent molecular weight in

these systems with decreasing protein concentration at any one ionic strength was interpreted as due to the dissociation of tropomyosin particles with dilution. The dissociation with dilution of beef cardiac tropomyosin was also observed in the measurements of viscosity - the reduced viscosity decreased with decreasing protein concentration at low salt concentration. Higher ionic strength caused the lowering of the curve resulting in a lower $[\eta]$ value, and also a decrease in the concentration dependence as seen in Figure 6. Both these experimental observations suggest that the molecular unit is decreasing in asymmetry. That this phenomenon was not simply due to a shape change exclusively, but also to a decrease in mass was determined by Archibald measurements on the same system over an ionic strength range of 0.1 to 0.4. As the ionic strength was raised, the weight-average molecular weight decreased at any given concentration point (Figures 24-27).

As an additional test for the presence of n-mer species at ionic strength values less than 0.6, the sedimentation-velocity data at 0.1 ionic strength were analyzed for boundary spreading, following the treatment of Baldwin and Williams (114). Boundary spreading may be expressed in terms of the second moment (m_2^0) about the mean,* in accordance with the following expression:

$$m_2^0 = (p \omega^2 r t)^2 (1 + \frac{1}{2} \frac{D}{\omega^2 r t}) + 2 D t / 1 - \omega^2 s t \quad (46)$$

*

The second moment is equal to the square of the average deviation about the mean, σ^2 .

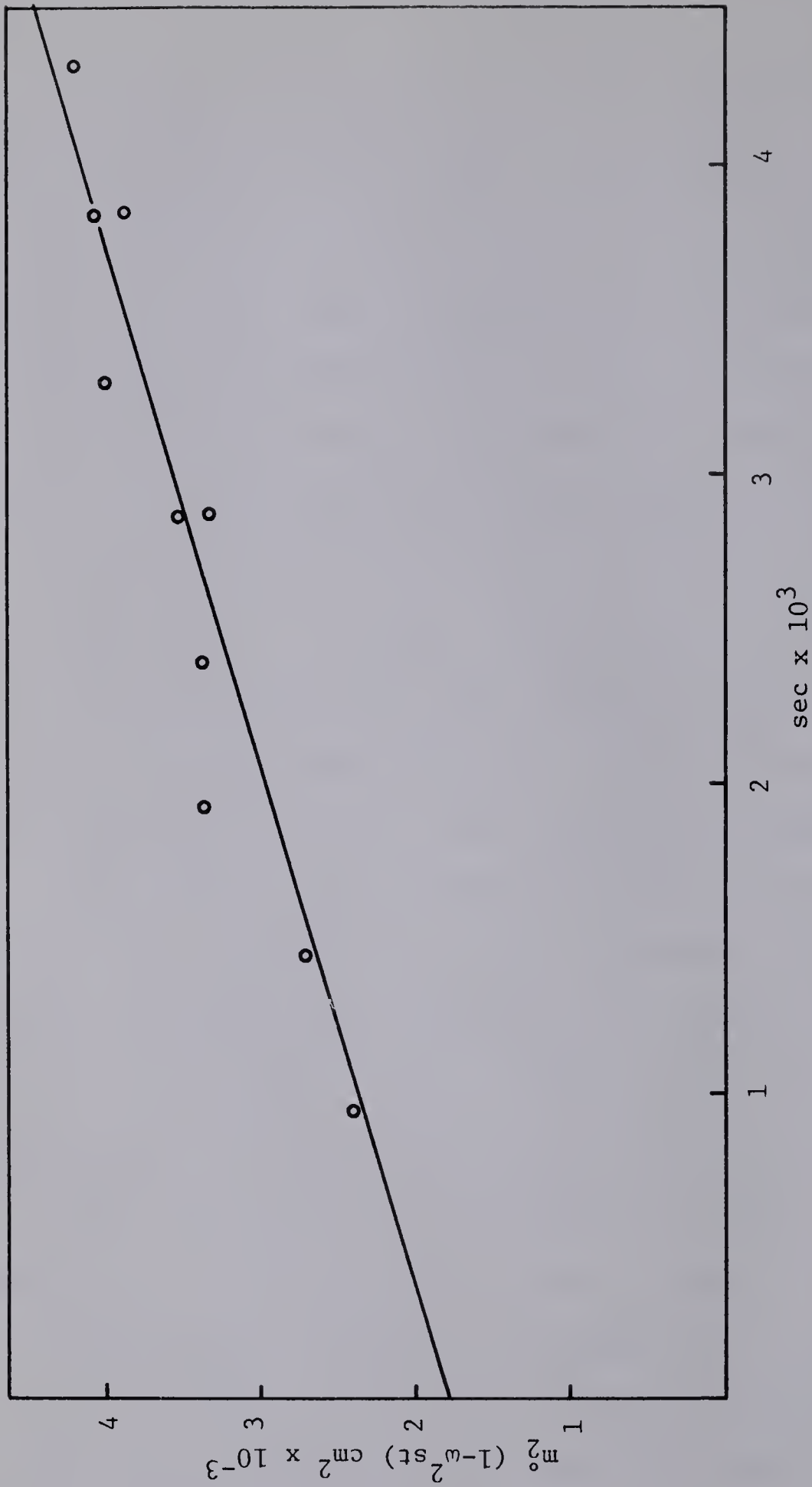


Figure 28

Analysis of boundary spreading for beef cardiac tropomyosin (4.4 g/liter) in terms of the increase of the corrected second moment, $m_2^0 (1-\omega^2_{st})$, in 0.1 ionic strength buffer system. Rotational speed was 59,780 rpm at bar angle 75° .

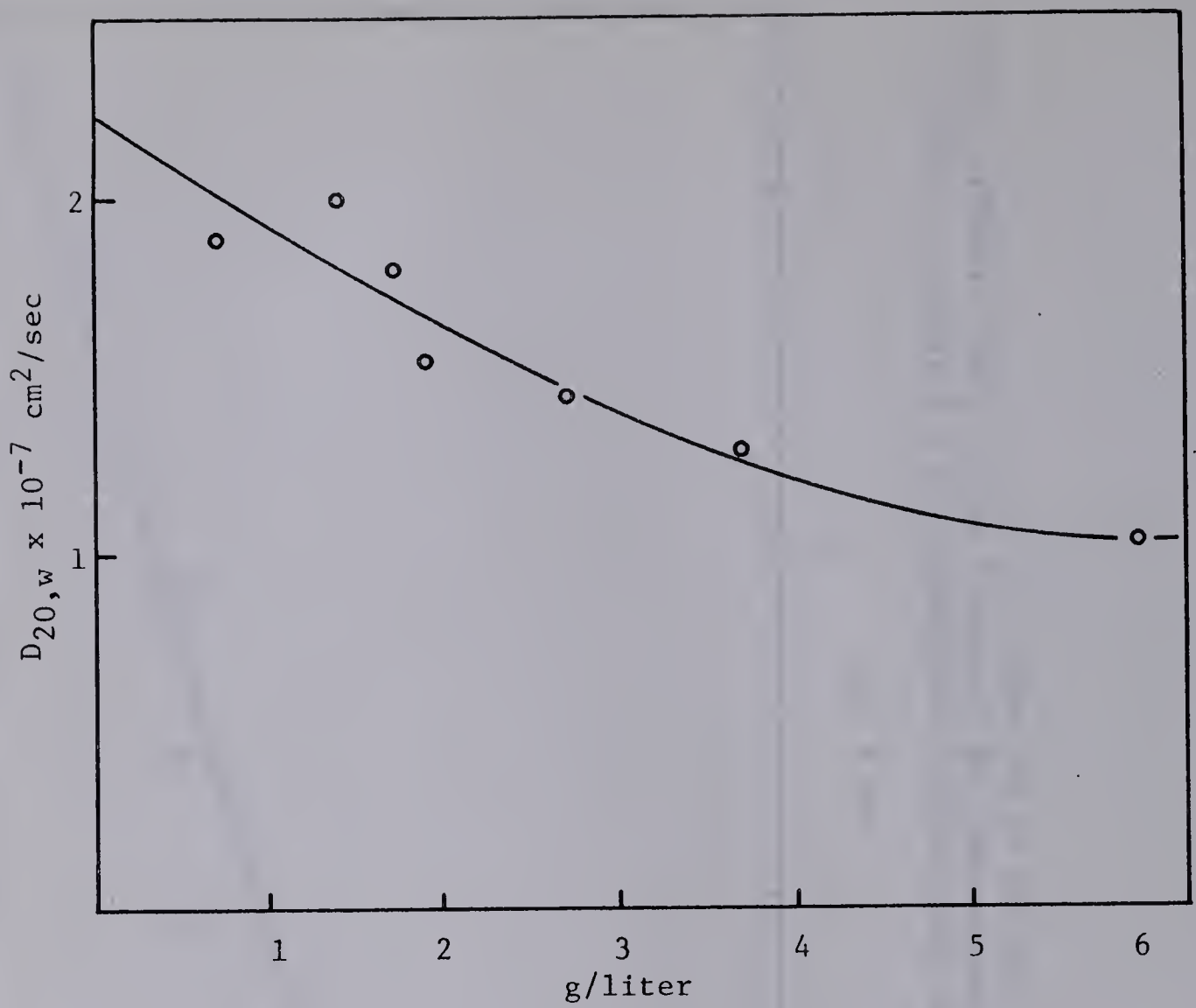


Figure 29

Diffusion coefficient of beef cardiac tropomyosin in 0.1 ionic strength buffer system (pH 7.0).

where ω = angular velocity
 r = distance of maximum ordinate from the axis of rotation
 t = time in seconds
 p = polydispersity coefficient
 D = diffusion coefficient.

It is assumed that this boundary spreading is caused solely by the diffusion of the solute, and that the effects of concentration and pressure on sedimentation velocity are negligible. For a homogeneous protein, the first term in equation (46) drops out, and a plot of $m_2^0(1 - \omega^2 st)$ against t yields a straight line relationship. The apparent diffusion constant is then obtained from one-half the slope of such a plot. Figure 28 illustrates application of the Baldwin and Williams treatment for a 0.44% beef cardiac tropomyosin solution at 0.1 ionic strength (pH 7.0). The data show a linearity in the plot of $m_2^0(1 - \omega^2 st)$ against t , with a slope that yields a value for the diffusion coefficient, $D_{20,w}$, of 1.98×10^{-7} cm²/sec. This diffusion value is in good agreement with that obtained experimentally under the same ionic strength conditions (see Figure 29).

The diffusion constant obtained by this method of analysis at ionic strength 0.1 is significantly lower than the value deduced for the same protein concentration at ionic strength 0.6 (see Figure 9). This suggests the presence of molecules larger than monomers in the system at low ionic strength, which are characterized by lower diffusion constants. These findings are additional confirmation of the concept of polymerization in low ionic strength media.

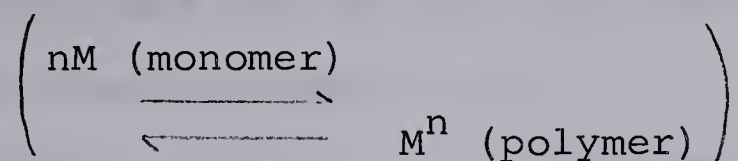
Table XI

Molecular Weight of Beef Cardiac Tropomyosin
(Archibald Method) from Top Portion of the
Cell at a Concentration of (a) 3.5 g/liter;
(b) 4.4 g/liter (both at ionic strength 0.1,
pH 7.0) .

Time (min.)	(a)	
	Molecular Weight	
	(at 8,225 rpm)	(at 14,290 rpm)
16	199,318	199,580
32	196,842	198,930
48	203,032	198,434
64	194,366	198,700
80	198,080	-
96	199,818	-
	(b)	
	(at 9,945 rpm)	(at 13,410 rpm)
32	210,353	208,943
48	216,608	214,791
64	218,574	222,702
80	214,805	212,506
96	212,847	-

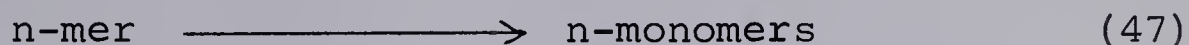
3. Reversibility of the Polymerization Process and Formulation of Expressions for the Nature of the Equilibrium State.

By knowing the molecular weight of the monomer and applying the mass law equation:



it is possible to calculate the equilibrium constant for the association reaction from the weight-average molecular weight at various protein concentrations. In this treatment, it was assumed that the partial specific volumes and the refractive index increments of the associating species were equal to those of the monomeric particle. Rao and Kegeles (113) have emphasized in their investigation of chymotrypsin polymerization that it must first be demonstrated that a system is at equilibrium before the mass law can be applied. To establish whether the tropomyosin monomer-n-mer system was in reversible equilibrium, experiments were conducted with different ultracentrifugal rotational speeds and times. Under the experimental conditions chosen (time and speed of centrifugation) c_m , the concentration at the meniscus, did not differ much from the original concentration. If the associating system were truly reversible, it could be predicted that the concentration of monomer and n-mer would be readjusted to the equilibrium state, as n-mers (polymers) were removed from the meniscus position and concentrated at the cell bottom under the influence of the centrifugal force. That this is the case may be seen from Table XI, where the molecular weight at ionic strength 0.1 is clearly insensitive to both rotational speed and time.

If the composition of the aggregating system is known, then the corresponding free energy of depolymerization may be calculated. This in fact was accomplished by Rao and Kegeles, who formulated an equation based on the mass law expression from which the depolymerization reaction from an n-mer to n-monomers may be characterized, viz.:



$$K = \frac{C_m^n}{C_p}$$

where K is the dissociation constant and C_p and C_m are the weight-concentrations of n-mer and monomer, respectively. If we have only monomers and n-mers in solution, then the weight average molecular weight, \bar{M}_w , may be expressed as:

$$\bar{M}_w = \frac{(C_m M_1) + (C_p M_n)}{C} \quad (48)$$

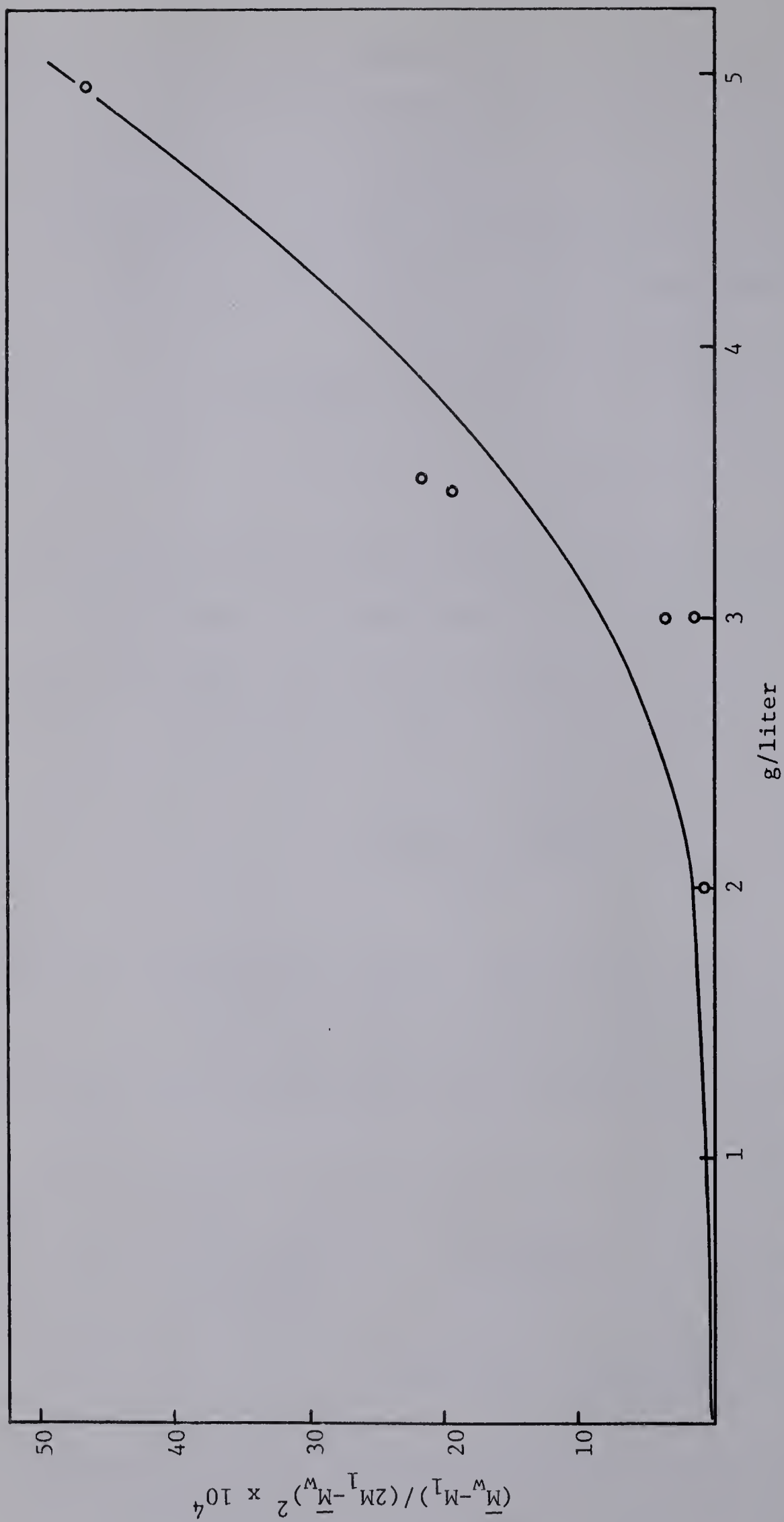
where M_1 and M_n are the molecular weight of monomer and n-mer and C is the total weight concentration ($C_m + C_p$).

Using these expressions, Rao and Kegeles set forth the following equation:

$$K_n^1 = \left\{ \frac{C}{(n-1)M_1} \right\}^{n-1} \times \frac{(nM_1 - \bar{M}_w)^n}{(\bar{M}_w - M_1)} \quad (49)$$

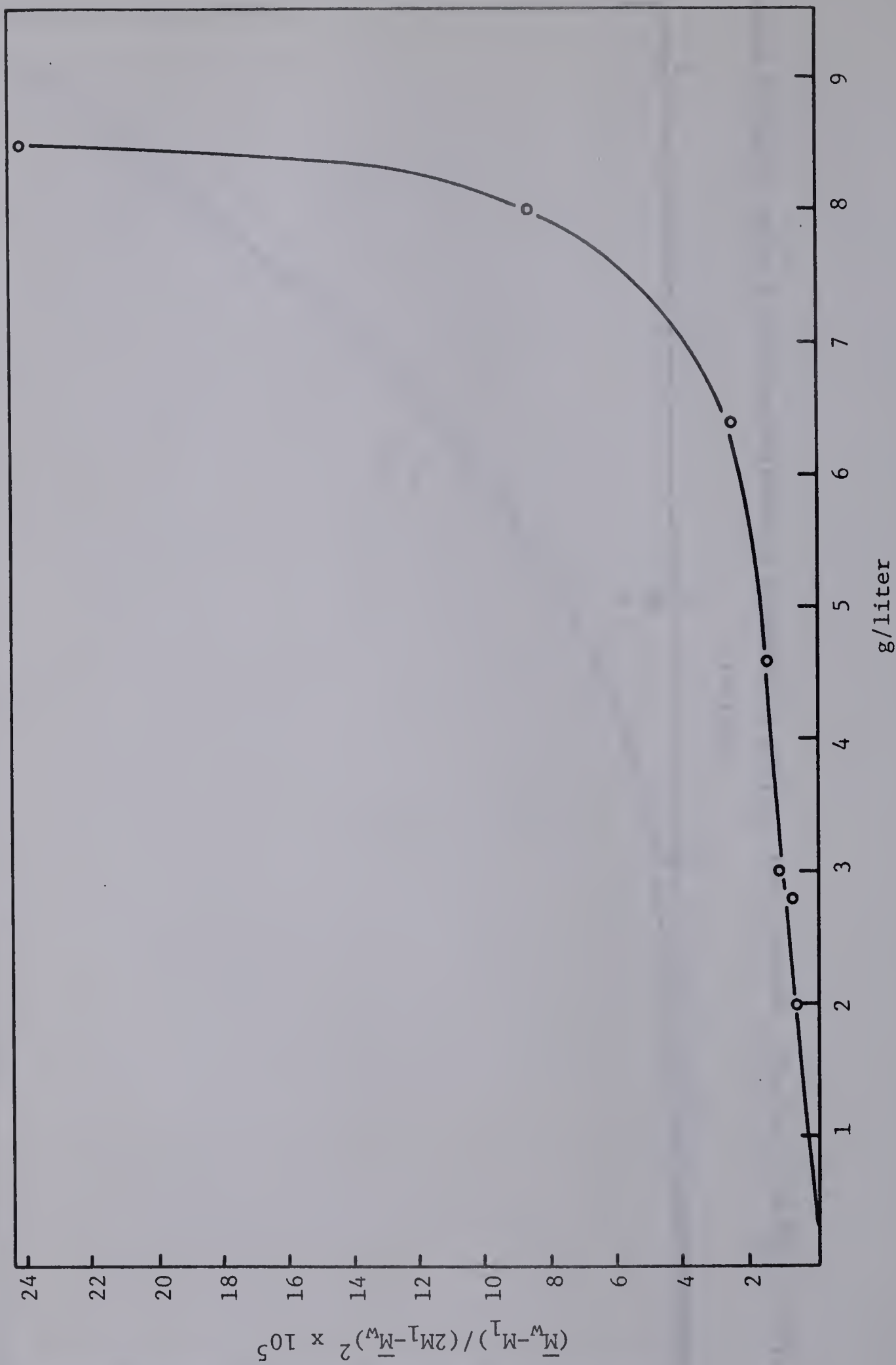
for the overall association reaction.*

*Note that the equation is written in the form of n-monomer \rightarrow n-mer where $K_n^1 = C_p/C_m^n$ on a gram/unit volume scale for the formation of polymer.



Plot of $(\bar{M}_w - M_l) / (2M_l - \bar{M}_w)^2$ against beef cardiac tropomyosin concentration in 0.1 ionic strength media.

Figure 30



Plot of $(\bar{M}_w - M_l) / (2M_l - \bar{M}_w)^2$ against beef cardiac tropomyosin concentration in 0.2 ionic strength media.

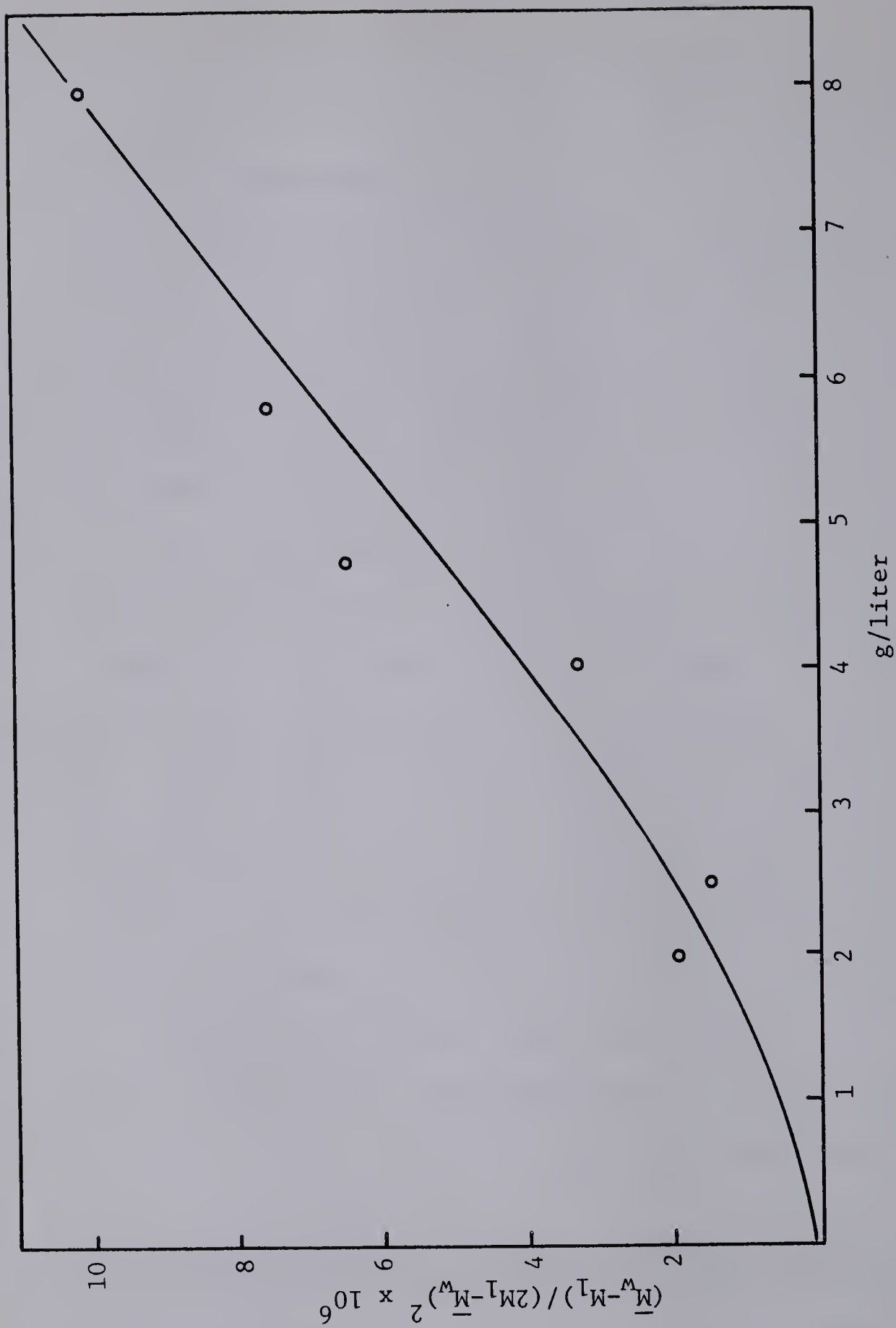
Figure 31

The terms in this expression are as follows: C is protein concentration in g/liter, M_1 is the monomer molecular weight, \bar{M}_w is the weight-average molecular weight and n the degree of association, 2 for dimers, 3 for trimers, etc. A plot of $(\bar{M}_w - M_1)/(2M_1 - \bar{M}_w)^2$ versus C should give a linear relationship if the system contains only monomers and dimers. If, however, trimers are also present, the plot should curve upward at higher protein concentrations where formation of trimers would be favored. This is because the value of the weight-average molecular weight (\bar{M}_w) becomes larger due to the inclusion of trimers as well as dimers and monomers in its expression. As a result, the term $(\bar{M}_w - M_1)$ has a higher value and $(2M_1 - \bar{M}_w)^2$ correspondingly a smaller value, leading to an overall larger numerical value for $(\bar{M}_w - M_1)/(2M_1 - \bar{M}_w)^2$.

If one plots $(\bar{M}_w - M_1)/(3M_1 - \bar{M}_w)^3$ versus C^2 , a linear relationship will only be realized if monomers and trimers are present. An upward curvature of the plot suggests higher n -mers, while a downward slope would imply that the species is predominantly dimeric.

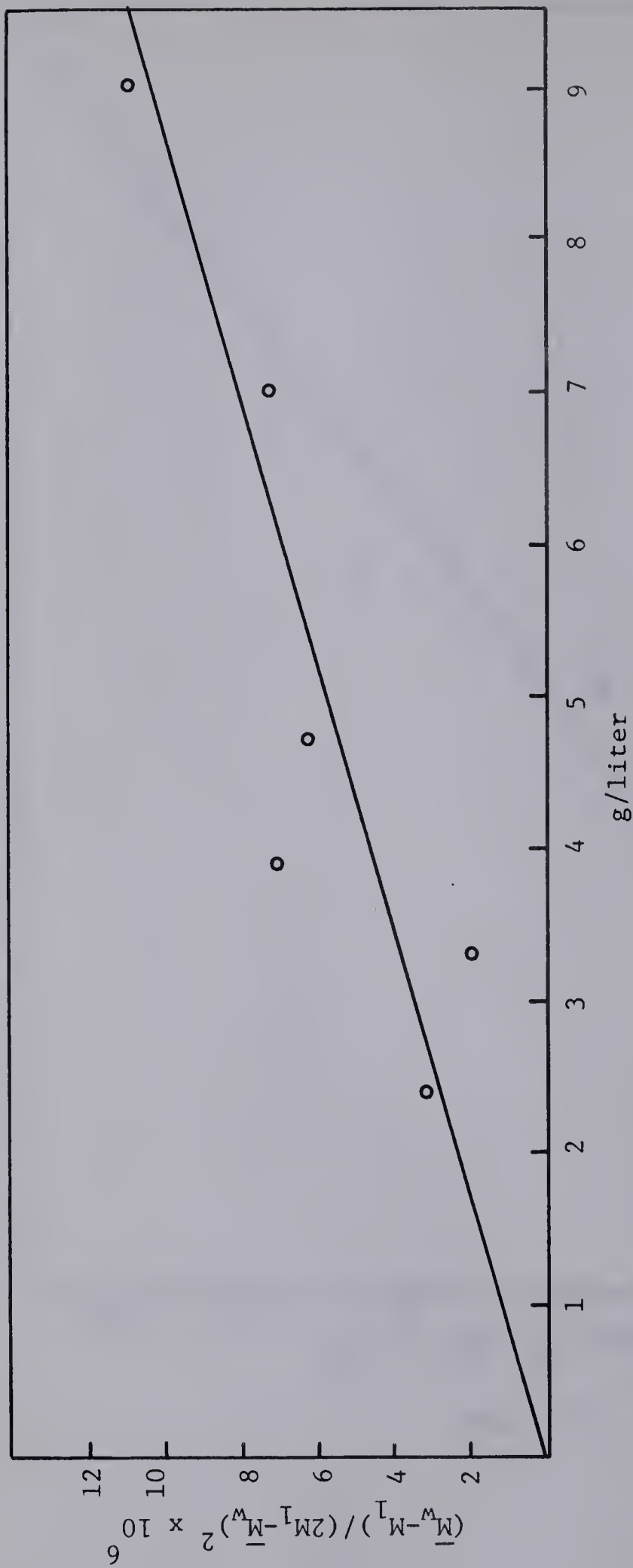
4. Extent of Polymerization of Beef Cardiac Tropomyosin over the Ionic Strength Range 0.1 to 0.4 all at pH 7.0.

The case of polymerization to the extent of dimer only (i.e., $n=2$) was considered first. In this situation, the values of $(\bar{M}_w - M_1)/(2M_1 - \bar{M}_w)^2$ were plotted against C as illustrated in Figures 29-32 for the beef system at 0.1 to 0.4 ionic strength inclusive. It is evident that a pronounced curvature in the plot for 0.1 and 0.2 ionic strength (Figs. 30, 31) occurs only at high concentration. This suggests that



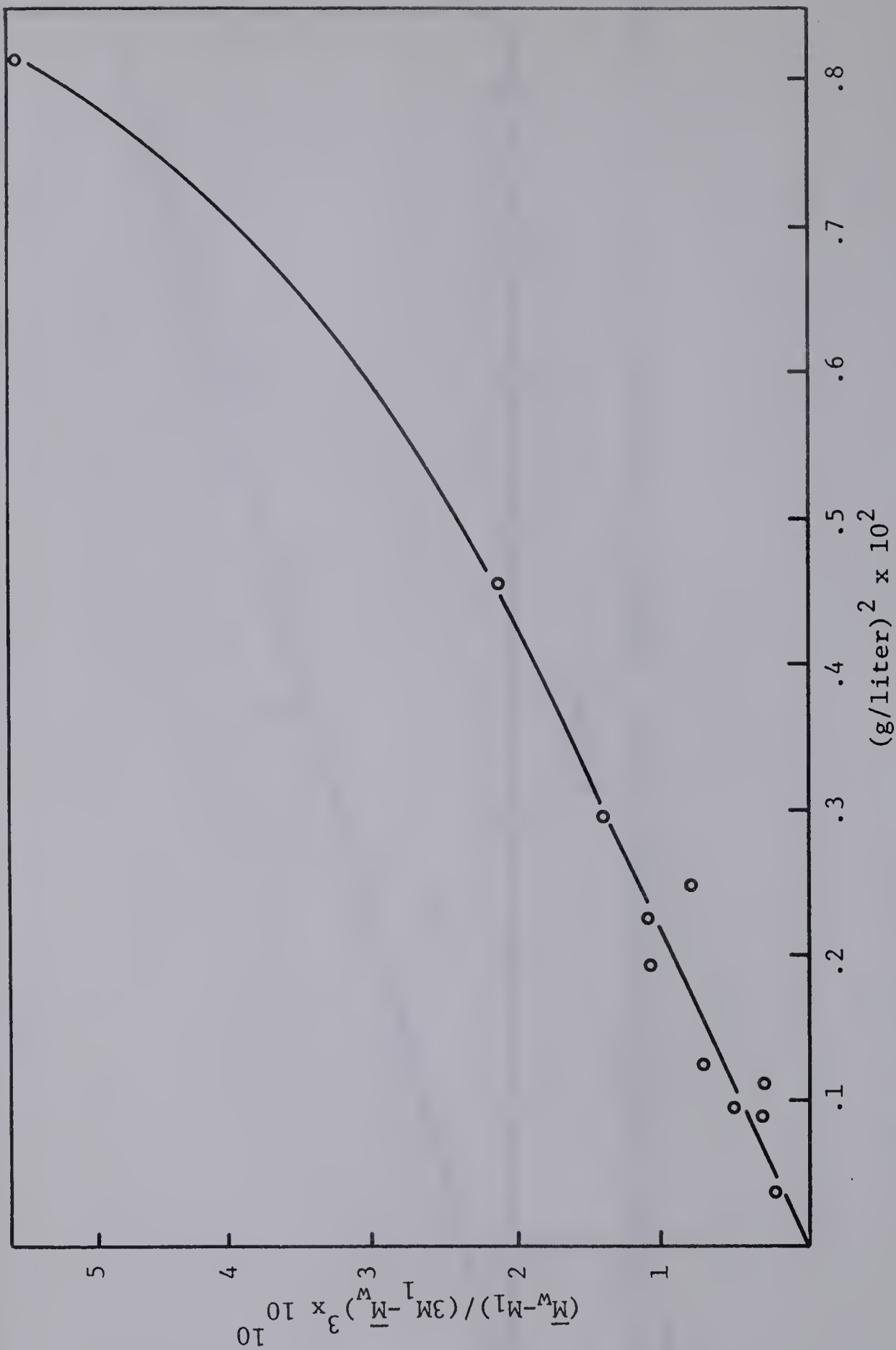
Plot of $(\bar{M}_w - M_l) / (2M_l - \bar{M}_w)^2$ against beef cardiac tropomyosin concentration in 0.3 ionic strength media.

Figure 32



Plot of $(\bar{M}_w - M_l) / (2M_l - \bar{M}_w)^2$ against beef cardiac tropomyosin concentration in 0.4 ionic strength media.

Figure 33



Plot of $(\bar{M}_w - M_l) / (3M_l - \bar{M}_w)^3$ against beef cardiac tropomyosin concentration (c^2) for 0.1 ionic strength media.

Figure 34

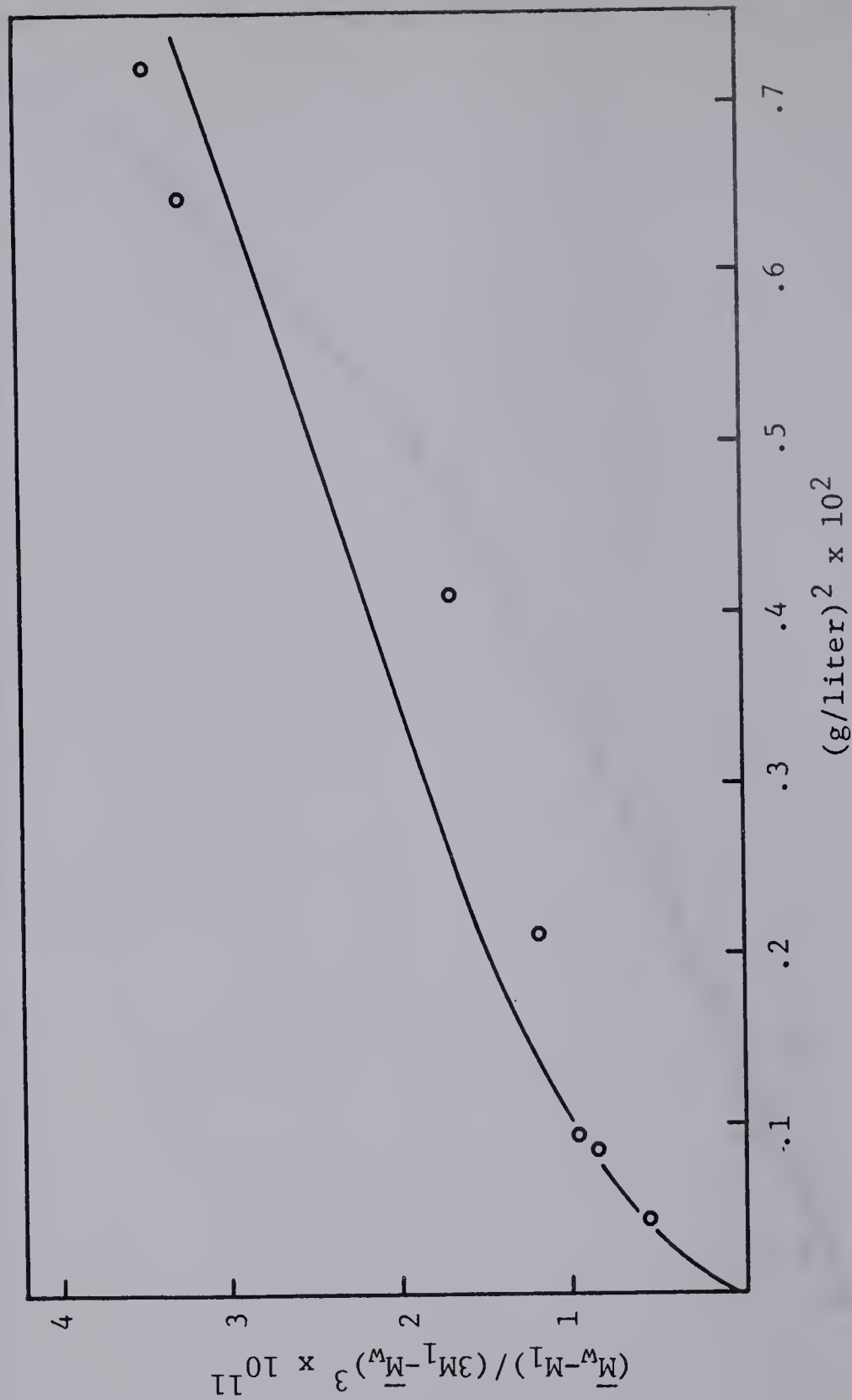


Figure 35

Plot of $(\bar{M}_w - M_l) / (3M_l - \bar{M}_w)^3$ against beef cardiac tropomyosin concentration (c^2) for 0.2 ionic strength media.

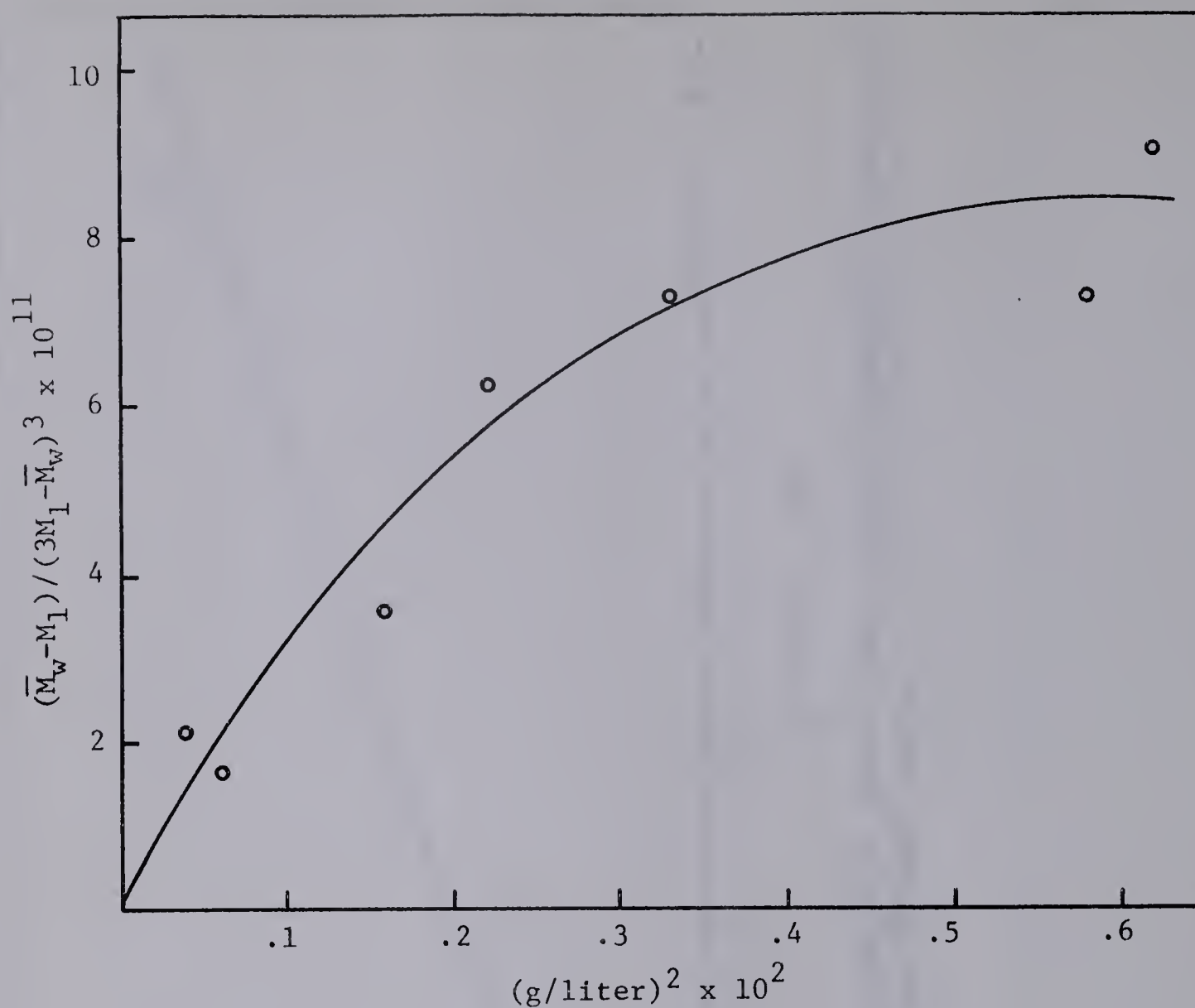


Figure 36

Plot of $(\bar{M}_w - M_1) / (3M_1 - \bar{M}_w)^3$ against beef cardiac tropomyosin concentration (c^2) for 0.3 ionic strength media.

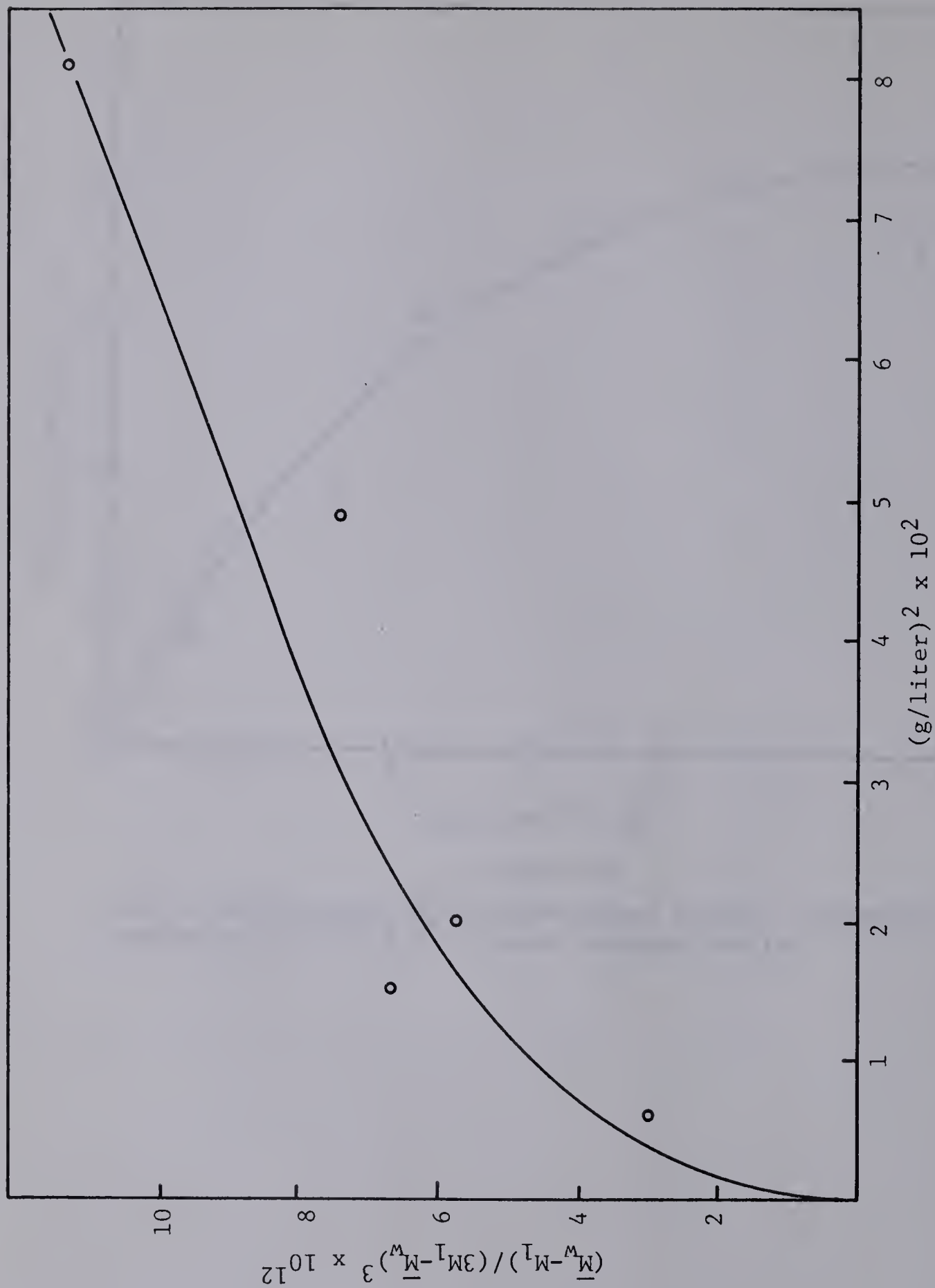


Figure 37

Plot of $(\bar{M}_w - \bar{M}_l) / (3\bar{M}_l - \bar{M}_w)^3$ against beef cardiac tropomyosin concentration $(c)^2$ for 0.4 ionic strength media.

the polymerization proceeded beyond dimerization at these high concentration levels; otherwise, one would have expected a straight line relationship throughout the entire concentration studied, if dimers were the only species present. This, in fact, seems to be the case only at low protein concentrations. At ionic strengths 0.3 and 0.4, the plot behaves linearly over a wider range of concentrations (Figures 32,33) suggesting that the degree of polymerization did not go beyond the dimer stage in these media.

Since the dimerization plots for ionic strength 0.1 and 0.2 suggest n-mers greater than dimers, it was interesting to extend the analysis to that of a system containing monomers and trimers exclusively. Here we plot: $(\bar{M}_w - M_1) / (3M_1 - \bar{M}_w)^3$ versus C^2 , as illustrated in Figures 34-37. In the case of the 0.1 ionic strength medium, it is evident that there is an upward curvature at a concentration greater than 7 (g/liter), whereas below this value, the plot behaves in linear fashion. This behaviour would be accounted for, if the system contained a mixture of monomers, trimers and higher n-mers at the higher concentration level, and only monomers and trimers at low concentration. However, the situation appears a bit more complex at ionic strength 0.2 where the plot shows a downward curvature at low concentration and a slight upward curve at higher concentration. This may be interpreted to indicate that the system is polymerized between trimer and monomer--that is, the dimer form, at concentrations no greater than 5 (g/liter), whereas trimer formation seems to occur at a concentration greater than 5 (g/liter). The plots for 0.3 and 0.4 ionic

strength show a definite downward curvature, suggesting that dimer formation is predominant at these ionic strength conditions.

These findings based on the assumption that the system contains only monomers and trimers (i.e., $n=3$) may be summarized by saying that at ionic strength 0.1, the system is a composite of monomer, trimer and higher n -mers at high concentration levels and only monomer and trimer at low and intermediate protein concentrations. On the other hand, at ionic strengths 0.3 and 0.4 the system is clearly monomer and dimer. The species present at ionic strength 0.2 are monomers and dimers at low concentration and monomers and trimers at higher concentration levels.

One may also use the Adams and Williams treatment for ideal aggregation systems (115) in order to evaluate the species composition of the tropomyosin system at various ionic strengths. A plot of

$$\frac{(1/2 AM_1 r) \frac{dc}{dr} - C}{C_a e^{\phi_1}}$$

against e^{ϕ_1} gives a horizontal line for a monomer-dimer association and an inclined line for monomer-dimer-trimer or monomer-trimer association. The terms of this equation are:

$$A = (1 - \bar{v} \rho) \omega^2 / 2RT$$

$$C = C_0 \text{ concentration}$$

$$r = \text{radial distance from the center of rotation}$$

$$\bar{v} = \text{partial specific volume of the monomer}$$

$$M_1 = \text{monomer molecular weight}$$

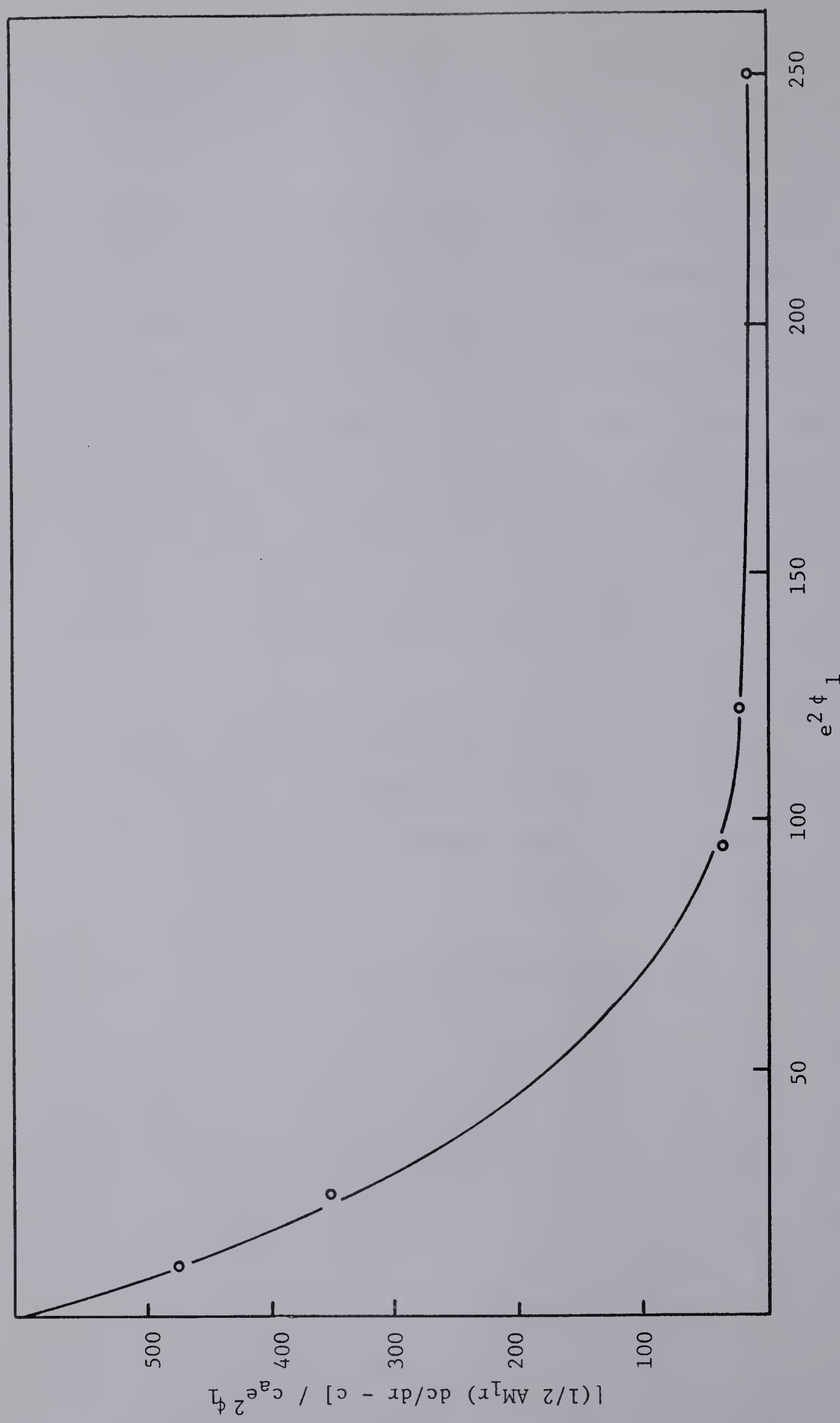


Figure 38

Plot of $[(1/2 AM_1r) dc/dr - c] / c_a e^{2\phi_1}$ versus $e^{2\phi_1}$ for beef cardiac tropomyosin in 0.2 ionic strength media (pH 7.0).

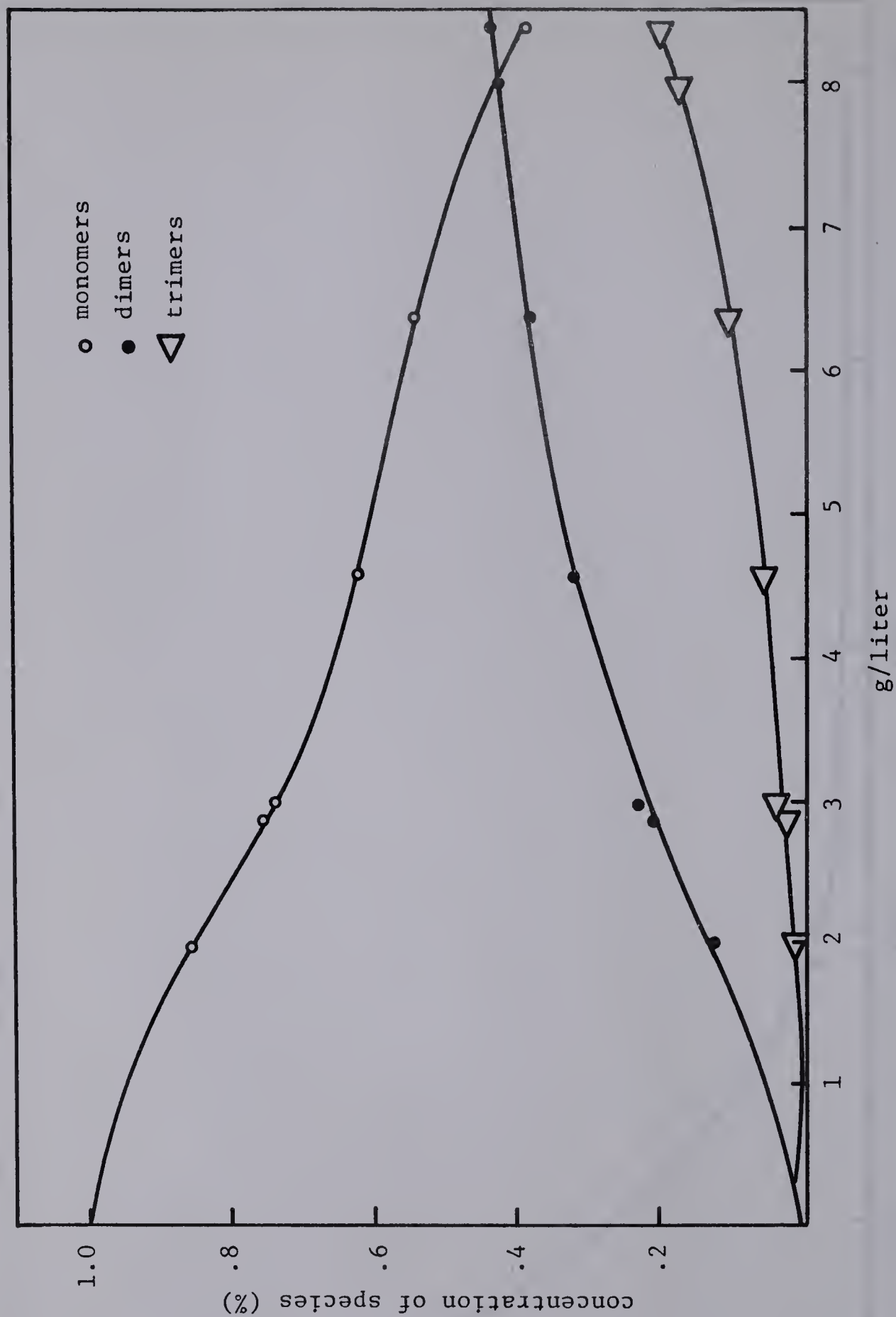
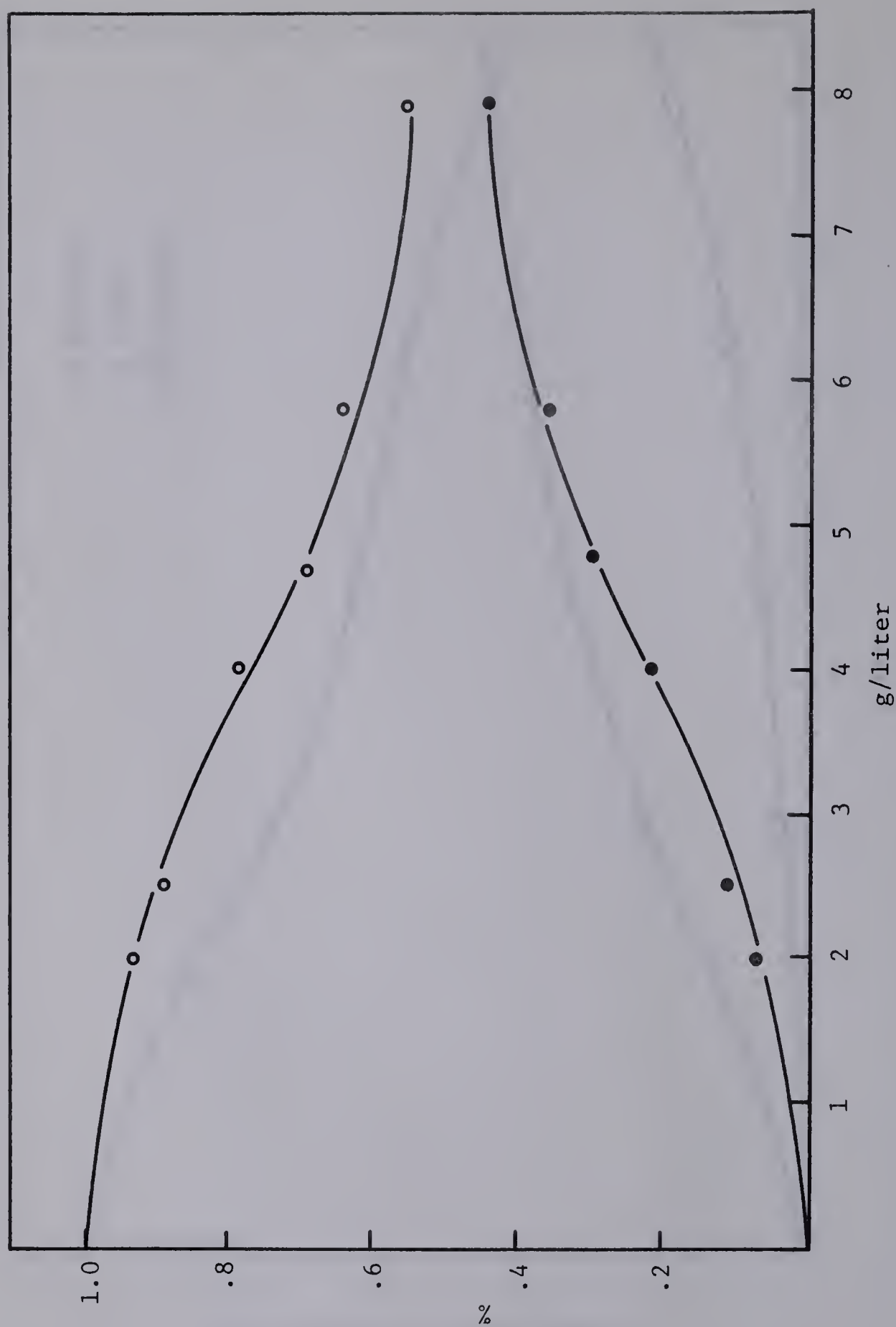


Figure 39

Percent composition of beef cardiac tropomyosin in the form of monomers ○, dimers ●, and trimers △ in 0.2 ionic strength media (pH 7.0).



Percent composition of beef cardiac tropomyosin in the form of monomers and dimers in 0.3 ionic strength media (pH 7.0).

Figure 40

ω = angular velocity of the rotor

C_a = the concentration at the meniscus

a = radial distance to the meniscus in the cell

$\emptyset_1 = AM_1 (r^2 - a^2)$

dc/dr = concentration gradient at the cell meniscus

The biphasic relationship obtained in Figure 38 suggests that the system at ionic strength 0.2 is composed of monomer-dimer-trimer or monomer-trimer constituents. Had the system been a monomer-dimer one exclusively, a linear relationship would have been anticipated. The agreement in the n-mer composition as revealed by these two methods may be considered as satisfactory.

The equilibrium constants may also be used to calculate the change of concentration of each species as the total concentration of protein is varied. Figures 39 and 40 illustrate plots of per cent of each species by weight against concentration of protein. It is evident from these plots that as the protein concentration is increased, the relative amounts of n-mers increase proportionally to the decrease of monomer species.

5. Determination of Equilibrium Constants for the Polymerization System at Ionic Strengths 0.2 and 0.3.

One means available for determining the equilibrium constants, K_2 (for dimers) and K_3 (for trimers), is the Steiner treatment (112), developed from light scattering, where the weight-average molecular weight, \bar{M}_w , of a heterogeneous species of n-mers may be expressed in the following form:

$$\bar{M}_w = \frac{1}{C} \left[C_1 M_1 + 2 \left(\frac{1}{K_2} \right) C_1^2 M_1 + 3 \left(\frac{1}{K_2 K_3} \right) C_1^3 M_1 + n \left(\frac{1}{K_2 K_3 \dots K_n} \right) C_1^n M_1 \right] \quad (50)$$

where

$$K_2 = C_1^2 / C_2$$

$$K_3 = C_2 C_1 / C_3$$

$$K_4 = C_3 C_1 / C_4$$

$$K_n = C_{n-1} C_1 / C_n$$

C_1 = concentration of monomer

C_2 = concentration of dimer

C_n = concentration of n-mer

C = total protein concentration

If we assume that only monomers, dimers and trimers are present in our reaction mixture, which seems to be the case in 0.2 and 0.3 ionic strength media, then the following equation may be derived from equation (50):

$$\left(\frac{\bar{M}_w - 1}{xM_1} \right) / (XC) = \frac{2}{K_2} + \frac{3}{K_2 K_3} (XC) \quad (51)$$

The symbol X denotes the concentration fraction of the monomer species; i.e.,

$$\begin{array}{ll} C_1 & = XC \\ \text{(monomer)} & \text{(fraction of total concentration),} \end{array} \quad (52)$$

and is derived from an integral equation developed by Steiner (112).

The equilibrium constants may be obtained graphically by plotting:

$[(\bar{M}_w / xM_1) - 1] / XC$ versus XC from which the values K_2 and K_3 are obtained from the intercept and slope terms,

Table XII

Free Energy Expressions for Dimer and Trimer Forms

$$\underline{I = 0.2}$$

dimer \longrightarrow 2 monomers;

$$\Delta F_2^0 = -RT \ln K_2 = -1642 \text{ cal/mole dimer}$$

trimer \longrightarrow monomer + dimer;

$$\Delta F_3^0 = -RT \ln K_3 = -719 \text{ cal/mole trimer}$$

trimer \longrightarrow 3/2 dimer;

$$\Delta F^0 F_3 - 1/2 F_2^0 = -102 \text{ cal/mole trimer}$$

$$\underline{I = 0.3}$$

dimer \longrightarrow 2 monomers;

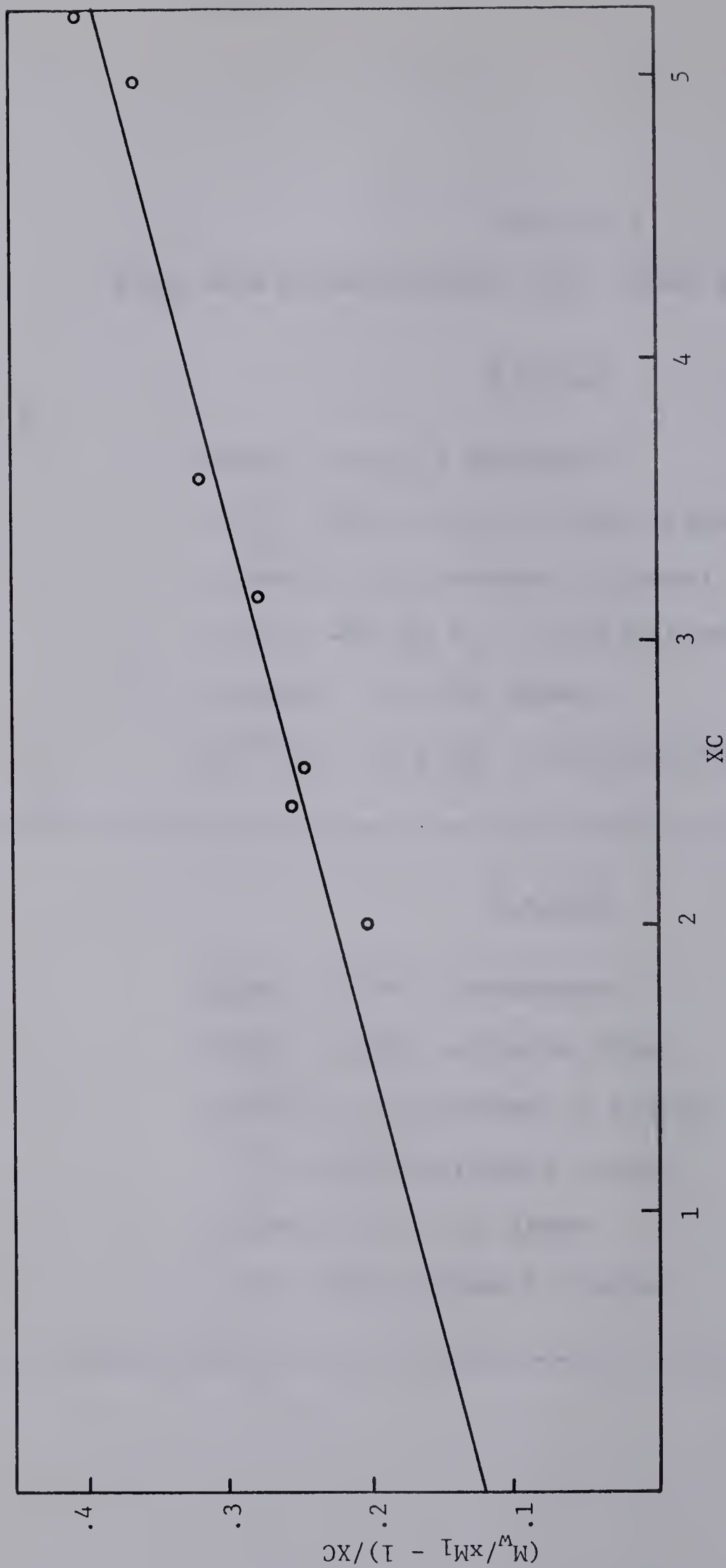
$$\Delta F_2^0 = -1812 \text{ cal/mole dimer}$$

trimer \longrightarrow monomer + dimer;

$$\Delta F_3^0 = -879 \text{ cal/mole trimer}$$

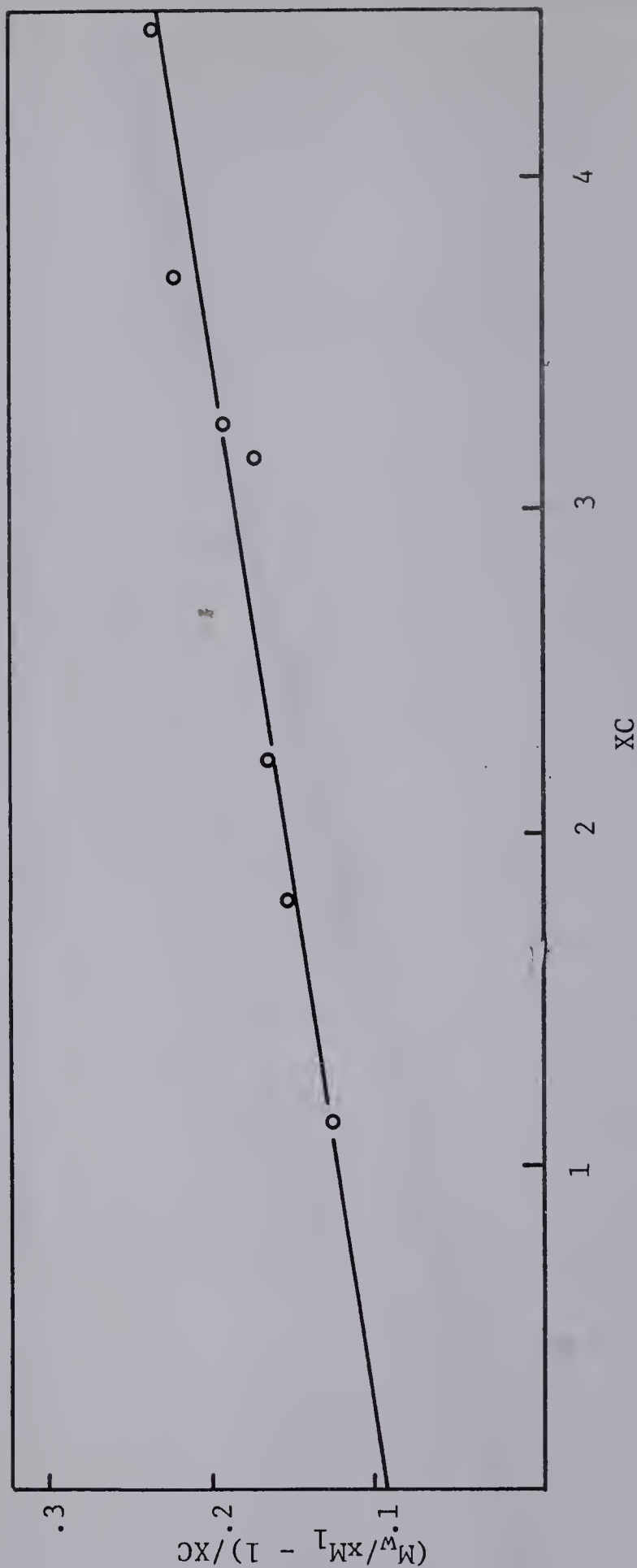
trimer \longrightarrow 3/2 dimer

$$\Delta F^0 = +27 \text{ cal/mole trimer}$$



Plot of $(\bar{M}_w / xM_1 - 1) / XC$ versus XC of beef cardiac tropomyosin in 0.2 ionic strength media, pH 7.0.

Figure 41



Plot of $(M_w/xM_1 - 1)/XC$ versus XC of beef cardiac tropomyosin in 0.3 ionic strength media, pH 7.0.

Figure 42

respectively. Figure 41 represents such a plot of the data for tropomyosin at ionic strength 0.2. The value of 16.7 g/liter was obtained for K_2 , whereas K_3 was evaluated as 3.4 g/liter. Similar treatment for the 0.3 ionic strength data yielded values of 22.2 and 4.5 g/liter for K_2 and K_3 , respectively (Figure 42).

The calculation of the free energy of dissociation expressions for dimers and trimers may now be made based on the dissociation constants (K values), from which the relative stability of dimers and trimers may be evaluated. The free energy expressions for the various reactions (based on the gram/liter concentration scale and unit activity coefficient) for 0.2 and 0.3 ionic strength, are depicted in Table XII in accordance with the format developed by Rao and Kegeles (113). The latter authors have presented these equations in this form in order to eliminate the standard free energy of the monomer.

The reaction constants deduced above imply that if we have a mixture containing trimers at a concentration level of 1 g per liter (the concentration used in the calculations), dissociation to dimers will occur with a net free energy change of -102 cal/mole trimer at an ionic strength of 0.2; while at ionic strength 0.3, the positive change of free energy obtained (+27 cal/mole trimer) implies that dissociation of trimer is not spontaneous. Insofar as the dimer is concerned in these reactions, it dissociates spontaneously into monomers with a free energy change of -1642 cal/mole dimer at ionic strength 0.2, while the value is -1812

cal/mole dimer at ionic strength 0.3. These values are comparable to those reported for other protein associating systems. For example, a ΔF_2^0 value of -1411 cal/mole dimer has been calculated for the dissociation of dimers to monomers for α -chymotrypsin (113) and -1280 cal/mole dimer for adrenocorticotropin (ACTH), dimer dissociation as determined by Squire and Li (116). The results reported here indicate that the influence of ionic strength from 0.3 to 0.2 is negligible in terms of the free energy change of dimers and trimers upon dissociation. This may not be the case for other protein systems. For example, Erlander et al. (117) have noted that the equilibrium constants for flagellin are shifted in the direction of dimer formation by an increase in ionic strength.

6. Optical Rotatory Dispersion Measurements on the Polymerization Process.

It was of interest to examine the influence of polymerization on the optical rotatory dispersion parameters, a_0 and b_0 , in the light of recent studies on aggregating systems (118). The possibility exists that one or the other of the dispersion parameters may undergo a marked change depending upon whether the polymerization process influences either the secondary and/or tertiary structure.

It has been reported that changes in side-chain group interaction resulting from separation of hydrophobic surfaces or rupture of side-chain hydrogen bonding or even a change in the polarizability of the environment of key chromophoric groups may lead to an apparent change in the a_0 term, which

Table XIII

Optical Rotatory Parameters for Beef Cardiac
Tropomyosin at Different Ionic Strength Conditions

Ionic Strength	pH	a _o	b _o	% helix
0.6	7.0	-16	-620	97
0.4	7.0	- 1	-619	97
0.3	7.0	-10	-618	96
0.2	7.0	- 9	-615	96
0.1	7.0	-10	-644	100
	Average	-9 (<u>±</u> 6)	-623 (<u>±</u> 8)	

is primarily sensitive to the tertiary structure, without changing the b_0 helix parameter (119-121). It is also possible for any one system to show a change in b_0 with or without any appreciable change in a_0 . Certainly protein systems undergoing helix \rightarrow random coil transitions fall in this class. However, it must be emphasized that deductions regarding conformational changes based on a_0 and b_0 variations are only tentative and a more rigorous interpretation must await a more complete understanding of both the theory of optical rotation and the structure of the protein under study.

It is relevant to note that recent dispersion studies, by Herskovits et al. (118) on β -lactoglobulin, and also by Schellman (122) on insulin, indicate that the dispersion parameter, a_0 , which is both a helix and an environmental term, undergoes large changes with changes in the state of aggregation of these systems, while at the same time, the b_0 parameter undergoes little variation. This was interpreted as due either to the formation of new "interior" (hydrophobic) regions or to the introduction of additional symmetry into the molecular aggregates.

On the basis of these observations, it was of interest to see whether beef cardiac tropomyosin exhibited any ORD changes associated with aggregation. Table XIII shows the ORD data (over a wavelength range of 600 to 300 $m\mu$) for beef cardiac tropomyosin over the ionic strength range 0.1 to 0.6 i.e., in the monomer to trimer range. These results lead to the conclusion that the degree of polymerization does not

significantly alter the helical parameters, a_0 and b_0 , for the tropomyosin system. They would also suggest that the association process does not involve any extensive reorganization of the secondary or tertiary structure of the tropomyosin molecule, consistent with the observation of Kay and Bailey (35) that the polymerization process is predominantly end-to-end. If the aggregation were side-to-side, one might well have anticipated changes at least in the tertiary structure, and these would have been reflected in a_0 .

7. Nature of the Polymerization Process.

The controlling element in the polymerization is not clear, but the investigations carried out by Asai (123) on rabbit skeletal tropomyosin using electrical birefringence measurements and Ooi et al. (124) using light scattering, have suggested that the charge pattern of tropomyosin is the important factor. This was based on the observation that polymerization was markedly decreased at pH values below 6 and higher than 9, although no major changes occurred in the secondary structure as deduced by optical rotation over the pH range 2-10 (11).

Chang and Tsao have suggested that -SH groups take part in the polymerization of rabbit skeletal tropomyosin since performic acid oxidation or blocking of -SH groups by metal ions or organic mercurials retards the polymerization process (125). In this connection, it is interesting to note the observations of Drabikowski and Novak (103) that auto-oxidation of -SH groups in tropomyosin (skeletal) had no influence on the viscosity of this protein, whereas some

organic mercurials led to an increased viscosity of tropomyosin in the absence of salt.

However, it was pointed out earlier in the Results section that both beef cardiac and rabbit cardiac tropomyosin possess no half-cystine residues as reflected in the amino acid analyses. This may indicate that the controlling element of the cardiac tropomyosin polymerization reaction is different from that operating in the skeletal system. On the basis of experiments carried out in this study, it would seem that the electrostatic interactions are the principal agents responsible for the polymerization reaction in cardiac tropomyosin. This does not mean that other forces, such as hydrophobic bonding and van der Waals interactions are non-existent, but that they may be overshadowed by the predominant electrostatic forces. Clearly the nature of the forces responsible for the polymerization process requires additional investigation.

IV. CONCLUSIONS

1. Hydrodynamic and Thermodynamic Parameters of Cardiac Tropomyosin.

It has been generally assumed that both cardiac and skeletal tropomyosin possess similar physico-chemical properties (34). However, this investigation has demonstrated that while the molecular properties of cardiac tropomyosin isolated from two different species (rabbit and beef) are similar, distinct differences are noted when tropomyosin prepared from heart muscle is compared with its skeletal homologue. A summary of the results arising from this study will now be presented.

(1) Both monomer beef and rabbit cardiac tropomyosin possess higher molecular weights ($\sim 100,000$) than the rabbit skeletal system ($\sim 55,000$), as deduced from Archibald and sedimentation-diffusion molecular weight measurements.

(2) In addition, light scattering measurements on beef cardiac tropomyosin reveal a molecular weight value consistent with those obtained by the above methods.

(3) Rabbit and beef cardiac tropomyosin solutions which contain 8M urea or 5M guanidine hydrochloride do not dissociate to lower molecular weight particles, as inferred from Archibald measurements. These observations are consistent with the premise that the cardiac tropomyosins are not dimeric forms of their skeletal counterparts.

(4) Additional differences between cardiac tropomyosin and rabbit skeletal tropomyosin are also reflected in the corresponding values obtained for the diffusion coefficients. The rabbit skeletal system is reported to have a much higher intrinsic $D_{20,w}$ (~ 4.5 F.U.) as opposed to the $D_{20,w}$ (~ 3.0 F.U.) for the cardiac system. In addition, the intrinsic viscosity values of 0.46 and 0.48 deciliters per gram for beef and rabbit cardiac tropomyosin are slightly greater than the value of 0.39 (dl/g) reported by Noelken for the rabbit skeletal system (92).

(5) Some of the hydrodynamic parameters investigated show a marked degree of similarity for the two systems. The sedimentation coefficients for the cardiac system are similar to that reported for skeletal tropomyosin, the intrinsic value being $\sim 3S$ in both cases.

(6) The amino acid analysis for beef and rabbit cardiac tropomyosin shows a close resemblance to the analysis reported for the skeletal system by Kominz et al. (89), Bailey (10), and Katz and Converse (34). It may be significant that the cardiac tropomyosins, like their skeletal counterparts, are made up of 65% polar amino acids, while the less helical muscle proteins (actin and heavy meromyosin) contain smaller amounts ($\sim 56\%$). Also both skeletal and cardiac tropomyosin possess no proline residues, unlike the muscle proteins of lower helical content such as actin and myosin. The major difference between rabbit skeletal and cardiac tropomyosin is that the latter do not contain any -SH groups.

(7) Optical rotatory dispersion measurements, carried out over both the ultraviolet and visible wavelength regions, do not reveal any large deviations in helical content between the cardiac and skeletal systems. Both proteins are markedly helical (85-95%) and this result has been corroborated by the independent method of deuterium-hydrogen isotope exchange.

2. Size and Shape of Cardiac Tropomyosin.

The close similarities of the hydrodynamic parameters of beef and rabbit cardiac tropomyosin provide strong evidence that these two proteins have similar basic structures. This has been verified by the use of appropriate models to evaluate the size and shape of the tropomyosin particles. The probable dimensions for both cardiac tropomyosins based on the axial ratios derived from the Scheraga-Mandelkern equation and the effective volumes for a prolate ellipsoid are approximately 36 Å wide and 510 Å long.

The 510 Å value for the length of the tropomyosin molecule was evaluated independently from three separate equations for prolate ellipsoids which emphasized either sedimentation, viscosity or diffusion parameters. This value in conjunction with the length derived from amino acid analysis favors, within the uncertainties involved in these calculations, a three-chain model. In addition, light scattering measurements on beef cardiac tropomyosin gave a length of 557 Å, assuming a prolate ellipsoid model. Calculations based on this value suggest that the tropomyosin molecule is made up of some 2.55 polypeptide chains. It may be that a more complicated packing involving the simultaneous

presence of three-chain regions and two-chain regions exists for the cardiac tropomyosin molecule.

It seems likely that in the tropomyosin molecule the specific arrangement of the polypeptide chains must be additionally stabilized along the entire length by hydrophobic bonding, or other interactions of the neighbouring helical chains. At the same time, the high content of polar amino acids in tropomyosin suggests that preservation of a completely helical conformation in aqueous media requires favorable interactions, not only between packed helical chains, but also between water and the still considerable protein surface that remains exposed to it.

As was demonstrated earlier, the application of the prolate ellipsoid model of Scheraga and Mandelkern results in an axial ratio of 14 for the cardiac tropomyosin system. In contrast, skeletal tropomyosin, based on viscosity increment calculations, possesses a value of 24 for the axial ratio. On the premise of a higher molecular weight and lower axial ratio for both cardiac tropomyosins, it might be anticipated that the $S_{20,w}^0$ value for these molecules would be higher than the 2.95 S reported for the skeletal system. Since both beef cardiac and rabbit cardiac tropomyosin possess similar sedimentation coefficients, this may be a reflection of a larger effective volume for the cardiac system. This was, in fact, found to be the case where the V_e values of rabbit cardiac and beef cardiac tropomyosin were calculated to be 2.11 ml/g and 2.02 ml/g respectively, as opposed to the anhydrous partial specific volume figure of 0.73 ml/g, suggesting an appreciably hydrated particle.

Table XIV

Molecular Weight and C-Terminal Data for Some Tropomyosins

Tropomyosin	Muscle Type	Molecular Weight	C-terminal amino acid residue end (129)*
rabbit	skeletal	55,000 (89)	Ileu-ser-
rabbit	cardiac	100,000	---
duck gizzard	smooth	153,000 (33)	Leu-leu-
prawn	skeletal	80,000 (33)	Ileu-Ileu-
sepia mantle	smooth	68,000 (33)	Leu-Thr-
pig	cardiac	89,000 (33)	Ileu-Ileu-
beef	cardiac	100,000	---
squid	smooth	62,000 (126)	---
pig	skeletal	---	Ileu-
pig bladder	smooth	---	Ser-
blow fly (adult)	---	65,000 (127)	---
blow fly (larval)	---	85,000 (127)	---
beef bladder	smooth	59,000 (89)	---
scallop adductor	skeletal	100,000 (128)	---

*Figures in parentheses refer to references.

The higher weight intrinsic viscosity, $[\eta]$, for both cardiac systems is probably due, in part, to the contribution of the larger effective volume.

3. Phylogenetic Relationships

It appears that there are variations in the tropomyosin molecule when a wide range of the evolutionary scale is considered. Table XIV illustrates the variability of molecular weights and C-terminal amino acid groups for some tropomyosins. While little is known of the significance of these differences, it may be speculated that they are a reflection of the observed physiological differences among cardiac, skeletal and smooth muscles. It seems that such alterations in molecular properties occur with respect to two time scales: that of the evolution of species and that of the development of the organism.

Of the two species studied, the beef, belonging to the Bovidea class, had its origin sometime in the latter part of the Miocene period, which is approximately 15 million years ago. On the other hand, rabbit, considered a member of the Logomorpha order, had its start some 40 million years ago in the Eocene period (130). This time differential between the two species apparently did not contribute to any differences in the molecular properties of the beef and rabbit cardiac tropomyosins. However, from the standpoint of organ development in the rabbit, it is apparent that significant molecular variation of tropomyosin occurs in the skeletal and cardiac muscle tissues. As was stated in the Introduction, distinct differences for the enzymatic and molecular properties of myosin have been reported by Stracher (29) and Kay and Brahms

Table XV

Composition of n-mer Species of Beef Cardiac Tropomyosin
at Various Ionic Strength Conditions

Ionic Strength	Concentration Range (g/liter)	Nature of n-mers
0.1	0 - 8	monomer-trimer
	8 - 9	monomer-trimer-n-mer
0.2	0 - 6.5	monomer-dimer
	6.5 - 8.5	monomer-trimer
0.3	0 - 8	monomer-dimer
0.4	0 - 9	monomer-dimer

(30) .

The variation between rabbit cardiac and rabbit skeletal tropomyosin, which has been described in this study, suggests that a particular molecular configuration may function most efficiently for a given set of physiological conditions. For example, cardiac muscle is characterized by undergoing a slower but constant contraction, whereas skeletal muscle contracts and relaxes more rapidly. As such, the differences in the tropomyosin molecules in these two tissues may have a direct bearing on the contraction rate of the myofibrils.

4. Association Reactions of the Cardiac Tropomyosins

The aggregation phenomena for cardiac tropomyosin were examined by means of the Archibald approach-to-sedimentation equilibrium technique. That the polymerization of tropomyosin is dependent on protein concentration and ionic strength is well-documented herein. Also this study has demonstrated that the formation of n-mers from monomer tropomyosin is greatly enhanced by an increase in protein concentration at any one ionic strength. Likewise, n-mers are favored at any one protein concentration when ionic strength is decreased. These changes are not only reflected in the molecular weight calculations, but also in the specific viscosity determination. The compositional variation of the system with ionic strength based on the analysis of monomers and dimers only on the one hand, and monomers and trimers only on the other, is summarized in Table XV.

That no drastic alterations occur in the secondary or tertiary structure of tropomyosin during polymerization is

evident from the optical rotatory parameters, a_o and b_o , which remain constant under varying degrees of ionic strength. This finding is consonant with the view that the aggregation process is primarily end-to-end, rather than side-to-side, since for the latter situation changes in at least the tertiary structure would have been anticipated.

The energetics of the association suggest that at 0.3 ionic strength, dissociation of trimers (concentration, 1 g/liter) is not spontaneous, but requires 27 cal/mole trimer. On the other hand, at ionic strength 0.2, the dissociation of trimers (1 g/liter) is spontaneous to the extent of -102 cal/mole trimer. Both these values for the free energy change are small suggesting that trimers and dimers exist at this total concentration. The dissociation of dimers at ionic strength 0.3 and 0.2 results in free energy changes of -1812 cal/mole dimer and -1642 cal/mole dimer respectively. This leads to the conclusion that the dissociation of dimers to monomers is spontaneous at this concentration level.

It has been pointed out by Tsao et al. (90) for the rabbit skeletal system that a portion of the interaction process appears to persist at salt concentrations high enough to suppress the electrostatic attractions. It may be that -SH groups play a role in this residual association for rabbit skeletal tropomyosin as suggested by Chang and Tsao (125). However, this explanation cannot be invoked with the cardiac systems in view of the absence of free -SH groups in their amino acid composition. The possibility of some hydrophobic interaction cannot be discounted in the polymerization reaction.

Depolymerization in higher ionic strength media may shed some light on the state of tropomyosin in the muscle. The initial extraction of tropomyosin requires a M-salt solution in order to solubize the protein from the fibrils. It is probable that the tropomyosin is ordinarily present in a polymeric form either as an n-mer or in conjugation with actin, and that the effect of salt is to depolymerize the molecule.

The interaction of tropomyosin with actin has been studied by Maruyama (15) using flow birefringence studies. He has reported that up to 25% of the tropomyosin is combined with F-actin. It may be that the present study on the characteristics of the polymerization process for beef cardiac tropomyosin will lead to a better understanding of the principles involved in the interaction of tropomyosin with actin. One can speculate that this interaction may play a major role in controlling or initiating contraction of the muscle fibers. Tropomyosin, by associating with the F-actin, may cause the actin molecule to become unavailable for combination with myosin, thus preventing contraction. Upon dissociation of tropomyosin from actin, the actin would be free to complex with myosin, forming actomyosin. It is this formation of actomyosin upon which depends one of the basic principles of the Huxley-Hanson sliding filament model for muscle contraction.

5. Suggestions for Further Investigation

In addition to further characterization of beef cardiac tropomyosin in the polymerized state, directed toward better understanding of its association reactions, other lines of investigation suggest themselves.

One of these is the use of light scattering and viscometry in order to obtain information on the relative size and shape of the dimers and trimers present at each ionic strength, and to propose suitable models for these species, based on the model already developed for the monomer. Another area for investigation is the influence of temperature and pH on the degree of polymerization, any changes to be monitored by viscosity, Archibald and optical rotatory dispersion measurements.

Influence of organic solvents, such as ethylene glycol, on the association process may provide information on whether other bonding forces play a significant role (i.e., hydrophobic bonding). It is to be noted that Chang and Tsao have reported that the polymerization of rabbit skeletal tropomyosin is decreased upon addition of urea, and that removal of urea causes restoration of the polymerization process (125). Since urea causes a decrease in the helicity of tropomyosin, it may be that the helical structure of tropomyosin is a necessary ingredient for the polymerization reaction.

It would be interesting to know whether or not other cardiac tropomyosins, such as dog and rabbit, behave similarly to beef cardiac, insofar as association and energetics are concerned. Additional information on these molecules will be useful, not only as model systems, but also to provide a possible clue to understanding the functional differences in various muscle types.

BIBLIOGRAPHY

1. Huxley, H.E., in *The Cell*, Vol. IV (J. Brachet and A.E. Mirsky, editors), Academic Press, Inc., N.Y. (1960) p. 365.
2. Perry, S.V., in *Comparative Biochemistry*, Vol. II (M. Florkin and H.S. Mason, editors), Academic Press, Inc., N.Y. (1960).
3. Bourne, G.H. (editor), *The Structure and Function of Muscle*, Vol. I, II and III, Academic Press, Inc., N.Y. (1960).
4. Paul, W.M., Daniel, E.E., Kay, C.M. and Moncton, G. (editors), *Muscle Physiology*, Pergamon Press, N.Y. (1965).
5. Szent-Györgyi, A.G., in *The Structure and Function of Muscle*, Vol. II (G.H. Bourne, editor), Academic Press, Inc., N.Y. (1960) p. 1.
6. Perry, S.V., in *Muscle Physiology* (W.M. Paul, E.E. Daniel, C.M. Kay and G. Moncton, editors), Pergamon Press, N.Y. (1965) p. 29.
7. Hanson, J. and Huxley, H.E., *Symposia Soc. Exptl. Biol.*, 9, 228 (1955).
8. Huxley, A.F. and Niedergerke, R., *Nature*, 173, 971 (1954).
9. Corsi, A. and Perry, S.V., *Biochem. J.*, 68, 12 (1958).
10. Bailey, K., *Biochem. J.*, 43, 271 (1948).
11. Knappeis, G.G. and Carlson, F., *J. Cell. Biol.*, 13, 323 (1962).
12. Huxley, H.E., *J. Mol. Biol.*, 7, 281 (1963).
13. Perry, S.V. and Corsi, A., *Biochem. J.*, 68, 5 (1958).
14. Martonosi, A., *J. Biol. Chem.*, 237, 2795 (1962).
15. Maruyama, K., *Arch. Biochem. Biophys.*, 105, 142 (1964).
16. Marechal, G. and Mommaerts, W.F.H.M., *Biochim. Biophys. Acta*, 70, 53 (1963).

17. Lowey, S. and Cohen, C., J. Mol. Biol., 4, 293 (1962).
18. Ruegg, J.C., Proc. Roy. Soc. (Lond.), B154, 224 (1961).
19. Johnson, W.H., Kahn, J. and Szent-Györgyi, A.G., Science, 130, 160 (1959).
20. Anfinsen, C.B., The Molecular Basis of Evolution, J. Wiley and Sons, N.Y. (1959).
21. Dixon, M. and Webb, E.G., The Enzymes (2nd edition), Academic Press, Inc., N.Y. (1964) p. 453.
22. Sutherland, E.W. and Wosilait, W.D., J. Biol. Chem., 218, 459 (1956).
23. Madsen, N.B. and Cori, C.F., J. Biol. Chem., 223, 1055 (1956).
24. Cohn, R., Kaplan, N.O., Levine, L. and Zwilling, E., Science, 136, 962 (1962).
25. Bailey, K., Biochem. J., 36, 121 (1942).
26. Brahms, J. and Kay, C.M., J. Mol. Biol., 5, 132 (1962).
27. Needham, D.M., Proc. Roy. Soc. (Lond.), B154, 517 (1961).
28. Perry, S.V. and Hartshorne, D., in The Effect of Use and Disuse on Neuromuscular Function (E. Gutman and P. Hnik, editors), Czechoslovak Academy of Sciences, Prague (1963).
29. Stracher, A., in Muscle Physiology (W.M. Paul, E.E. Daniel, C.M. Kay and G. Moncton, editors), Pergamon Press, N.Y. (1965) p. 85.
30. Kay, C.M. and Brahms, J., J. Biol. Chem., 238, 2945 (1963).
31. Burton, A., Am. Heart J., 54, 801 (1957).
32. Abbott, B.C. and Mommaerts, W.F.H.M., J. Gen. Physiol., 42, 533 (1959).
33. Tsao, T-C, Tan, P-H and Peng, C-M, Sci. Sinica, 5, 91 (1956).
34. Katz, A.M. and Converse, R.P., Circulation Res., 15, 194 (1964).

35. Kay, C.M. and Bailey, K., *Biochim. Biophys. Acta*, 40, 149 (1960).
36. Nichol, L.W., Bethune, J.R., Kegeles, G. and Hess, E.L., in *The Proteins*, Chap. 9, Vol. II (H. Neurath, editor), Academic Press, Inc., N.Y. (1964).
37. Huxley, H.E., in *Muscle Physiology* (W.M. Paul, E.E. Daniel, C.M. Kay and G. Moncton, editors), Pergamon Press, N.Y. (1960) p. 3.
38. Huxley, H.E., *Endeavour*, 15, 177 (1956).
39. Lowry, O.H., Rosebrough, N.J., Farr, A.L. and Randall, R.J., *J. Biol. Chem.*, 193, 265 (1951).
40. Street, H.S., Kenyon, A.E. and Watson, G.M., *Ann. App. Biol.*, 33, 1 (1946).
41. Kraemer, E.O., in *The Ultracentrifuge* (T. Svedberg and K.O. Pedersen, editors), Clarendon Press, Oxford (1940).
42. Cohn, E.J. and Edsall, J.T. (editors), *Proteins, Amino Acids and Peptides*, Reinhold Publishing Corp., N.Y. (1943).
43. Waugh, D.F. and Yphantis, D.A., *Rev. Sci. Instr.*, 23, 609 (1952).
44. Schachman, H.K., *Ultracentrifugation in Biochemistry*, Academic Press, Inc., N.Y. (1959) p. 75.
45. Schachman, H.K., in *Methods in Enzymology*, Vol. IV, Pt. 2 (S.P. Colowick and N.O. Kaplan, editors), Academic Press, Inc., N.Y. (1957) p. 32.
46. Schachman, H.K., *Ultracentrifugation in Biochemistry*, Academic Press, Inc., N.Y. (1959) p. 82.
47. Kay, C.M., *Biochim. Biophys. Acta*, 38, 420 (1960).
48. Green, W.A., PhD Thesis, The University of Alberta (1963) p. 53.

49. Archibald, W.J., J. Phys. and Colloid Chem., 51, 1204 (1947).
50. Pickels, E.G., Harrington, W.F. and Schachman, H.K., Proc. Natl. Acad. Sci., U.S., 38, 943 (1952).
51. Erlander, S.R. and Babcock, G.E., Biochim. Biophys. Acta, 50, 205 (1961).
52. Klainer, S.M. and Kegeles, C., Arch. Biochem. Biophys., 42, 596 (1956).
53. Moore, S., Spachman, D.H. and Stein, W.H., Anal. Chem., 30, 1185 (1958).
54. Moore, S. and Steins, W.H., in Methods in Enzymology, Vol. VI (S.P. Colowick and N.O. Kaplan, editors), Academic Press, Inc., N.Y. (1963) p. 819.
55. Yang, J.T., Advances in Protein Chemistry, 16, 327 (1961).
56. Kahn, D.S. and Polson, A., J. Phys. and Colloid Chem., 51, 816 (1947).
57. Bull, H.B., Physical Biochemistry, John Wiley and Sons, Inc., N.Y. (1943) p. 276.
58. Edsall, J.T., in The Proteins, Vol. I, Pt. B (H. Neurath and K. Bailey, editors), Academic Press, Inc., N.Y. (1953) p. 624.
59. Neurath, H., Chem. Revs., 30, 357 (1942).
60. Lundgren, H.P. and Ward, W.H., in Amino Acids and Proteins, Chap. 6 (D.M. Greenberg, editor), Charles C. Thomas, Springfield, Ill. (1951).
61. Longsworth, L.G., J. Am. Chem. Soc., 74, 4155 (1952).
62. Moffitt, W. and Yang, J.T., Proc. Natl. Acad. Sci., U.S., 42, 596 (1956).
63. Simmons, N.S., Cohen, C., Szent-Györgyi, A.G., Wtlauffer, D.B. and Blout, E.R., J. Am. Chem. Soc., 83, 4766 (1961).

64. Urnes, P.J. and Doty, P., in Advances in Protein Chemistry, Vol. XVI (C.B. Anfinsen, M.L. Anson, K. Bailey and J.T. Edsall, editors), Academic Press, Inc., N.Y. (1961) p. 401.
65. McCabe, W.J. and Yang, J.T., Biopolymers, 3, 209 (1965).
66. Linderstrøm-Lang, K.V., in Symposium on Peptide Chemistry Special Publication 2, The Chemical Society, London, (1955).
67. Linderstrøm-Lang, K.V., Symp. Protein Struct. (Paris), 1957, 23 (1958).
68. Ambrose, E.J. and Elliot, A., Proc. Roy. Soc., A205, 47 (1951).
69. Blout, E.R., DeLoze, C. and Asadourian, A., J. Am. Chem. Soc., 83, 1895 (1961).
70. Nielsen, S.O., Biochim. Biophys. Acta, 37, 146 (1960).
71. Nielsen, S.O., Bryan, W.P. and Mikkelsen, K., Biochim. Biophys. Acta, 42, 550 (1960).
72. Bryan, W.P. and Nielsen, S.O., Biochim. Biophys. Acta, 42, 552 (1960).
73. Stacey, K.A., Light Scattering in Physical Chemistry, Academic Press, Inc., N.Y. (1956).
74. Doty, P. and Edsall, J.T., Advances in Protein Chemistry, 6, 35 (1951).
75. Geiduschek, E.P. and Holtzer, A., Adv. Biol. and Med. Phys., 6, 431 (1958).
76. Lord Rayleigh, Phil. Mag., 41, 447 (1871).
77. Debye, P., J. Appl. Phys., 15, 388 (1944).
78. Debye, P., J. Phys. and Colloid Chem., 51, 18 (1947).
79. Zimm, B.H., J. Chem. Phys., 16, 1093 (1948).
80. Geiduschek, E.P. and Holtzer, A., Adv. Biol. and Med. Phys., 6, 444 (1958).

81. Yang, J.T., Technical Report No. RDD 1958-33, Laboratory Manual on Brice-Phoenix Light Scattering Photometer and Differential Refractometer, American Viscose Corp. (1958).
82. Alexander, P. and Stacey, K.A., Trans. Faraday Soc., 51, 299 (1955).
83. Oster, G., J. Polymer Sci., 9, 525 (1952).
84. Brice, B.A., Halwer, M. and Speiser, R., J. Opt. Soc. Am., 40, 768 (1950).
85. Tomimatsu, Y. and Palmer, K.J., Polymer Sci., 54, S21 (1961).
86. Tomimatsu, Y. and Palmer, K.J., Phys. Chem., 67, 1720 (1963).
87. Tomimatsu, Y., Biopolymers, 2, 275 (1964).
88. Kruis, A., Zeit. Phys. Chem., 34B, 13 (1936).
89. Kominz, D.R., Saad, F., Gladner, J.A. and Laki, K., Arch. Biochem. Biophys., 70, 16 (1957).
90. Tsao, T-C, Bailey, K. and Adair, G.S., Biochem. J., 49, 27 (1951).
91. Tsao, T-C, and Bailey, K., Discussions Faraday Soc., 13, 145 (1953).
92. Noelken, M.E., Dissertation Thesis, PhD, Washington University, St. Louis, Mo. (1962).
93. Kay, C.M. and Green, W.A., Circulation Res., 14, 38 (1964).
94. Huggins, M.L., J. Am. Chem. Soc., 64, 2716 (1942).
95. Riseman, J. and Ullman, R., J. Chem. Phys., 19, 578 (1951).
96. Kielly, W.W. and Harrington, W.F., Biochim. Biophys. Acta, 41, 401 (1960).
97. Scheraga, H.A. and Mandelkern, L., J. Am. Chem. Soc., 75, 179 (1953).
98. Cohen, C. and Szent-Györgyi, A.G., J. Am. Chem. Soc., 79, 248 (1957).

99. Narita, K., Katutani, Y and Imalori, K., The Fifth International Congress of Biochemistry, Moscow (1961).
100. Yang, J.T. and Doty, P., J. Am. Chem. Soc., 79, 761 (1957).
101. Schellman, J.A. and Schellman, C.G., Arch. Biochem. Biophys., 65, 58 (1956).
102. Kay, C.M., personal communication.
103. Drabikowski, W. and Novak, E., Acta Biochem. Poloneca, 12, 61 (1965).
104. Simha, R., J. Phys. Chem., 44, 25 (1940).
105. Perrin, F., J. Phys. Radium, 7, 7 (1936).
106. Svedberg, T. and Pedersen, K.O. (editors), The Ultracentrifuge, Clarendon Press, Oxford (1940).
107. Yang, J.T., in Advances in Protein Chemistry, Vol. XVI (C.B. Anfinsen, M.L. Anson, K. Bailey and J.T. Edsall, editors), Academic Press, Inc., N.Y. (1961) p. 344.
108. Lowey, S. and Cohen, C., J. Mol. Biol., 4, 293 (1962).
109. Holtzer, A.M., Lowey, S. and Schuster, T.M., in Molecular Basis of Neoplasia, Fiftieth Annual Symposium on Cancer Research, organized by the M.D. Anderson Hospital, Austin, University of Texas Press (1961) p. 259.
110. Latallo, Z.S., Fletcher, A.P., Alkjaersig, N. and Sherry, S., Am. J. Physiol., 202, 675 (1962).
111. Waugh, D.F., Wilhelmson, D.F., Commerford, S.J. and Sackler, M.L., J. Am. Chem. Soc., 75, 2529 (1953).
112. Steiner, R.F., Arch. Biochem. Biophys., 39, 333 (1952).
113. Rao, M.S.N. and Kegeles, G., J. Am. Chem. Soc., 80, 5724 (1958).
114. Baldwin, R.L. and Williams, J.W., J. Am. Chem. Soc., 72, 4325 (1950).

115. Adams, E.T., Jr. and Williams, J.W., J. Am. Chem. Soc., 86, 3454 (1964).
116. Squire, P.G. and Li, C-H, J. Am. Chem. Soc., 83, 3521 (1961).
117. Erlander, S.R., Koffler, H. and Foster, J.F., Arch. Biochem. Biophys., 90, 139 (1960).
118. Herskovits, T.T., Townsend, R. and Timasheff, S.N., J. Am. Chem. Soc., 86, 4445 (1964).
119. Tanford, C., De, P. and Taggart, V., J. Am. Chem. Soc., 82, 6028 (1960).
120. Williams, E.J. and Foster, J.F., J. Am. Chem. Soc., 81, 865 (1959).
121. Williams, E.J. and Foster, J.F., J. Am. Chem. Soc., 82, 242 (1960).
122. Schellman, J.A., Compt. rend. trav. lab. Carlsberg., Ser. chem., 30, 415 (1958).
123. Asai, H., J. Biochem. (Peking) 50, 182 (1961).
124. Ooi, T., Mihashi, K. and Kobayashi, H., Arch. Biochem. Biophys., 98, 1 (1962).
125. Change, Y. and Tsao, T-C, Sci. Sinica, 11, 1353 (1962).
126. Kubo, S., Mem. Fac. Fisheries, Hokkaido University, 9, 57 (1961) in Chem. Abst., 57, 12849 (1962).
127. Kominz, D.R., Maruyama, K., Levenbook, L. and Lewis, M., Biochim. Biophys. Acta, 63, 106 (1962).
128. Ruegg, J.C., cited by S.V. Perry in Comparative Biochemistry, Vol. II (M. Florkin and H.S. Mason, editors), Academic Press, Inc., N.Y. (1960) p. 245.
129. Vegotsky, A. and Fox, S.W., in Comparative Biochemistry, Vol. IV (M. Florkin and H.S. Mason, editors), Academic Press, Inc., N.Y. (1962) p. 185.

130. Gregory, W.K., Evolution Emerging, Vol. I, II, MacMillan Co., N.Y. (1951).
131. Katz, A.M. and Hall, E.J., Circulation Res., 13, 187 (1963).
132. Bailey, K., Biochim. Biophys. Acta, 24, 612 (1957).

APPENDIX 1

Estimates of diffusion coefficient constants were made from computations based on the maximum ordinate-area method, Rayleigh interference method and the second moment method. Calculations involving each of the three methods are illustrated:

A. Maximum ordinate-area method

$$D_{app} = \frac{A^2}{4\pi t (H_m)^2}$$

where

$$A = \text{area in cm}^2$$

$$t(H_m)^2 = \text{slope of the plot of time versus } 1/Y_m^2 \text{ (sec.)}$$

$$Y_m = \text{maximum ordinate height in cm.}$$

B. Rayleigh Interference Method

$$J = \text{total number of fringes}$$

$$j_K = \text{number of the different fringes up to a value less than } J/2$$

$$j_K^* = (2 j_K - J)/J$$

$$j_1 = \text{number of the different fringes up to a value greater than } J/2$$

$$j_1^* = (2j_1 - J)/J$$

$$\Delta H = \text{distance between paired fringes in cm.}$$

$$\frac{\Delta H}{\Delta h} = \text{magnification factor}$$

Sample Maximum-Ordinate Area Method Calculation for the Diffusion
Constant of Beef Cardiac Tropomyosin

Concentration = .47% Solvent = 0.5M KCl, 0.067M phosphate buffer, pH 7.0

Number	Time (min.)	Time (sec x 10 ³)	Y(cm)	Y ² (cm ²)	1/Y ² cm ⁻²
Zero			-	-	-
1A'	110.3	6.62	-	-	-
1B'	121.6	7.30	3.0237	9.143	.1094
2A''	284.0	17.04	2.2889	5.239	.1910
1A	3160.9	189.65	.8332	.6942	1.440
1B	4255.3	255.32	.7304	.5335	1.870
2A	4347.8	260.87	.7223	.5217	1.920
2A'	4347.8	260.87	.7215	.5206	1.930
2B	6072.2	364.33	.6247	.3903	2.560
4A	6072.8	364.37	.6246	.3901	2.560
4B	7064.3	423.86	.5806	.3371	2.970
3A	8505.7	510.34	.5259	.2766	3.620

Slope = $\frac{(510.3 - 7.3) \times 10^3 \text{ sec} = 1.4326 \times 10^5 \text{cm}^2 \text{sec}}{(3.620 - .109) \text{ cm}^{-2}}$ (see Figure 43) .

area² = 0.2246 (cm²)²

correction factor $\left(\frac{293}{273 + T} \right) \left(\frac{n_{\text{solv}}}{n_w} \right) \left(\frac{n_{t,w}}{n_{20,w}} \right) = 1.928$

D_{20,w} = 1.928 x $\frac{.2246 \text{ (cm}^2\text{)}^2}{12.57 \times 1.4326 \text{ cm}^2 \text{sec} \times 10^5} = 2.40 \times 10^{-7} \text{ cm}^2 \text{/sec}$

Diffusion of Beef Cardiac Tropomyosin in 0.5M KCl, 0.067M phosphate buffer, pH 7.0. Calculated by means of the Rayleigh interference method.

Number (#lB, protein concentration = .47%)

1*	2	3	4	5	6	7	8	9
j _K	j ^{*K} or $\frac{2j_K-j}{j}$	j _l	j _l [*] or $\frac{2j_l-j}{j}$	H (H _K -H _l)	X _K ^{**}	X _l ^{**}	$\frac{\Delta h}{(4Dt)^{1/2}}$	(4Dt) ^{1/2} $\frac{\Delta H}{\Delta h}$
							$\sum 6+7$	
1	.9048	11	.0952	.4508	1.1800	.0846	1.2646	.3578
2	.8095	12	.1905	.3895	.9257	.1705	1.0962	.3541
3	.7143	13	.2857	.3609	.7549	.2589	1.0138	.3559
4	.6190	14	.3810	.3458	.6195	.3516	.9711	.3561
5	.5238	15	.4762	.3403	.5035	.4508	.9543	.3565
6	.4286	16	.5714	.3431	.4002	.5597	.9599	.3562
7	.3333	17	.6667	.3516	.3045	.6841	.9886	.3557
8	.2381	18	.7619	.3733	.2143	.8342	1.0485	.3560
9	.1429	19	.8571	.4094	.1273	1.0360	1.1633	.3520
10	.0476	20	.9524	.5095	.0422	1.4010	1.4432	.3539

*Total number of fringes = 21.009.

$$D_{20,w} = D_{obs} \left(\frac{293}{273+T} \right) \left(\frac{n_{solv}}{n_w} \right) \left(\frac{n_{t,w}}{n_{20,w}} \right) = \frac{[(4Dt)^{1/2}]^2}{4 \times t \text{ in sec}} \times 1.928 = 2.38 \times 10^{-7} \text{ cm}^2/\text{sec}.$$

$$D_{20,w} = \frac{.1265}{4 \times 255.3 \times 10^3} \times 1.928$$

$$\frac{\Delta H}{\Delta h} = 1.00$$

$$\text{Avg.} = 0.3560$$

**From Tables of Probability Functions, Vol. 1, Federal Works Agency, Works Project Administration, Superintendent of Documents, Washington, D.C., 1941.

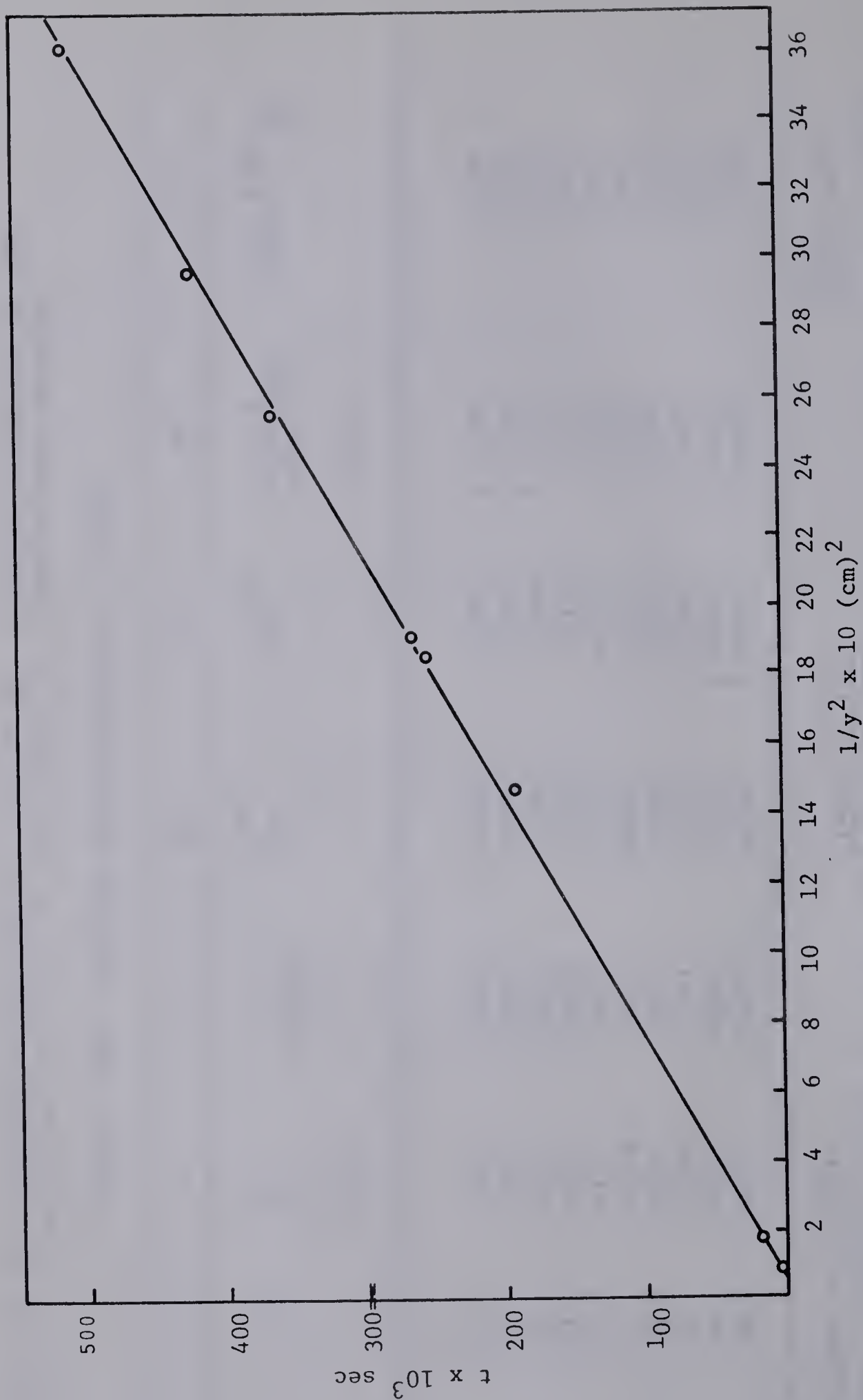


Figure 43

Plot of maximum ordinate-area method for determination of beef cardiac tropomyosin diffusion coefficient. Conditions: protein concentration, 0.47%; 0.5M KCl, 0.067M phosphate buffer, pH 7.0.

C. Statistical (second moment) Method

The diffusion curve is treated as a normal distribution curve by letting $Y = \frac{N}{\sigma \sqrt{2\pi}} e^{-(X-\bar{X})^2/2\sigma^2}$

where X = independent variable value

Y = dependent variable value usually called frequency, f

\bar{X} = mean value of X which is equal to $\frac{\sum f(X)}{N}$

N = number of observations in the distribution

$$= \sum f$$

σ = standard deviation (SD) which is equal to $\sqrt{\frac{\sum f(X-\bar{X})^2}{N}}$

M_2 = second moment of the curve about the central ordinate of the diffusion curve which equals σ^2

The diffusion constant, D_{app} , is related to σ by

$$D = \frac{\sigma^2}{2t} \quad \text{where } t \text{ is time in sec.}$$

$$M_2 = 18.08$$

The second moment thus calculated must be converted into absolute units by the expression:

$$M_2^O = M_2 w^2$$

where w^2 is the distance in cm. between successive vertical divisions.

$$\begin{aligned} M_2^O &= 18.08 (.06 \text{ cm})^2 \\ &= .06512 \text{ cm}^2 \end{aligned}$$

$$D_{app} = \frac{.06512 \text{ cm}}{2 \times 255.3 \times 10^3 \text{ sec}} = 1.275 \times 10^{-7} \text{ cm}^2/\text{sec}$$

$$\begin{aligned} D_{20,w} &= 1.275 \times 10^{-7} \text{ cm}^2/\text{sec} \times 1.928 \\ &= 2.45 \times 10^{-7} \text{ cm}^2/\text{sec.} \end{aligned}$$

Second moment calculation for the diffusion constant
of beef cardiac tropomyosin
(Sample 1B; see Figure 44)

X	f	f (x)	Σ f	dev
0	0	0	0	-11.533
1	.0441	.0441	.0441	-10.533
2	.0744	.1488	.1185	- 9.533
3	.1138	.3414	.2323	- 8.533
4	.1639	.6556	.3962	- 7.533
5	.2280	1.1400	.6242	- 6.533
6	.3100	1.8600	.9342	- 5.533
7	.4022	2.8154	1.3364	- 4.533
8	.5355	4.2840	1.8719	- 3.533
9	.6260	5.6340	2.4979	- 2.533
10	.7019	7.0190	3.1998	- 1.533
11	.7386	8.1246	3.9384	- .533
12	.7097	8.5164	4.6481	+ .467
13	.6627	8.6151	5.3108	+ 1.467
14	.5892	8.2488	5.9000	+ 2.467
15	.4916	7.3740	6.3916	+ 3.467
16	.4021	6.4336	6.7937	+ 4.467
17	.3124	5.3108	7.1061	+ 5.467
18	.2411	4.3398	7.3472	+ 6.467
19	.1756	3.3364	7.5228	+ 7.467
20	.1270	2.5400	7.6498	+ 8.467
21	.0871	1.8291	7.7369	+ 9.467
22	.0592	1.3024	7.7961	+10.467
	7.7961	89.9133		

$$\overline{X} = \frac{\sum f(x)}{N} = \frac{89.9133}{7.7961} = 11.533$$

$$\frac{N}{SD} = 1.833 \qquad SD = \sqrt{\frac{f (X-\overline{X})^2}{N}} = \underline{+4.253}$$

$(dev)^2$	$f (dev)^2$	dev/SD	Ordinate	Actual Ordinate
133.010	0.000	2.712	.0100	.0183
110.944	4.8926	2.477	.0200	.0367
90.878	6.7613	2.241	.0324	.0594
72.812	8.286	2.006	.0535	.0981
56.746	9.3007	1.771	.0833	.1527
42.680	9.7310	1.536	.1228	.2257
30.614	9.4903	1.301	.1714	.3142
20.548	8.2644	1.066	.2263	.4148
12.482	6.6841	.831	.2827	.5182
6.416	4.0164	.596	.3342	.6126
2.350	1.6495	.360	.3739	.6854
.284	.210	.125	.3958	.7255
.218	.155	.110	.3965	.7268
2.152	1.4261	.345	.3758	.6888
6.086	3.5859	.580	.3372	.6181
12.020	5.9090	.815	.2862	.5246
19.954	8.0235	1.050	.2299	.4214
29.888	9.3370	1.285	.1747	.3202
41.822	10.0833	1.521	.1257	.2304
55.756	9.7908	1.756	.0855	.1567
71.690	9.1046	1.991	.0551	.1010
89.624	7.8063	2.226	.0335	.0614
109.558	6.4853	2.461	.0194	.0356
140.9931				

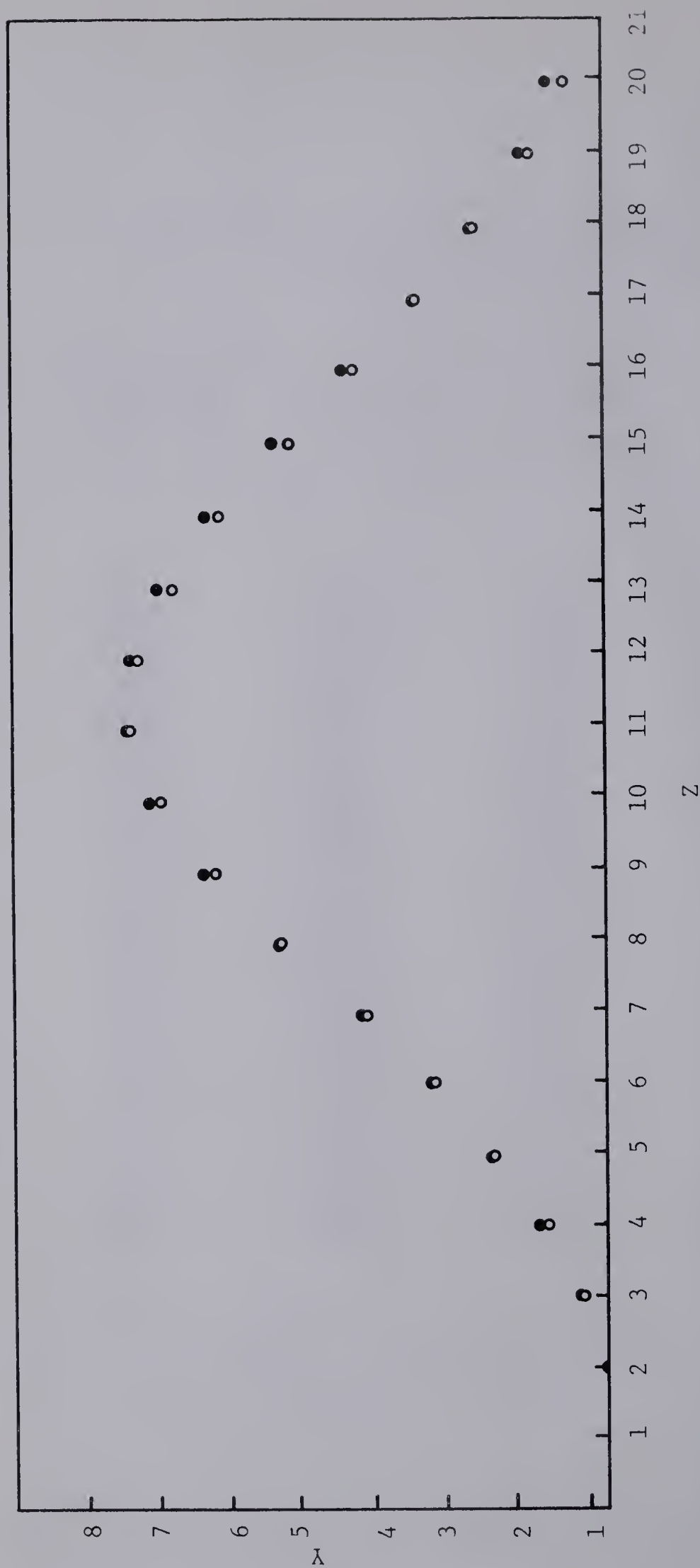


Figure 44

Comparison of a normal distribution curve \bullet with the experimental diffusion curve \circ obtained from measurements on 0.47% beef cardiac tropomyosin at pH 7.0. Solvent conditions: 0.5M KCl, 0.067M phosphate buffer.

θ	F_{θ}	\overline{G}_{θ}	$\frac{F_{\theta} G_{\theta}}{F_{\theta} G_0}$	$\left(\frac{F_{\theta} G_{\theta}}{F_{\theta} G_0} \right)_{\text{solv.}}^{(1)}$
0	1, 2, 3, 4	69.5		
35	3, 4	94.5	168.75×10^{-3}	4.41×10^{-3}
45	1, 2, 4	55.7	84.99	2.00
60	2, 4	54.0	41.19	1.23
75	1, 4	69.7	26.40	1.54
90	1, 4	54.3	20.57	0.97
105	1, 4	56.2	21.28	1.31
120	1, 4	67.5	25.57	1.25
135	1, 4	99.7	37.76	2.11

(1) Solvent scattering was measured in the same way as that of the solution.

APPENDIX 2

Measurements of light scattering of beef cardiac
tropomyosin in 0.5M KCl, 0.067M phosphate buffer, pH 7.0.

Light Scattering Computations

C = .00201 gm/ml
cylindrical cell #1

$\lambda = 436 \text{ m}\mu$

$\Delta \left(\frac{F_o G_e}{F_e G_o} \right)$	$J_e^{(2)}$	Kc/R_e	$\sin^2 \frac{\theta}{2} + 1000c$
164.34x10 ⁻³	58.17x10 ⁻³	2.235x10 ⁻⁵	2.100
82.99	40.08	3.244	2.150
39.96	28.11	4.626	2.260
24.86	22.59	5.755	2.381
19.60	19.43	6.690	2.510
19.98	17.62	7.380	2.639
24.32	15.77	8.247	2.760
35.66	14.92	8.713	2.864

$$(2) \quad J_{e(\text{uncorrected})} \Delta \left(\frac{F_o G_e}{F_e G_o} \right) \frac{\sin \theta}{1 + \cos^2 \theta}$$

$$J_{e(\text{corrected for back reflection})} = 1.045 [J_{e \text{ observed}}^* - 0.045 J_{180-e \text{ observed}}^*] \quad (81)$$

*Since cylindrical cell was used, back reflection correction was necessary according to the Tomimatsu-Palmer procedure (87).

F_e = filters at angle θ

\overline{G}_e = average recorder reading

θ = angle of measurements

Tomimatsu-Palmer Reflection Corrections for
Cylindrical Light-Scattering Cells (87)

R_e/R_{180+e}	R_e corrected	R_{180+e} corrected
-----------------	-----------------	-----------------------

1.00	1.006	1.006
1.25	1.282	.981
1.50	1.559	.956
1.75	1.835	.931
2.00	2.111	.906
3.00	3.217	.807
4.00	4.322	.707
5.00	5.427	.608
7.00	7.638	.459
10.00	10.954	.311

$$\begin{aligned}
 K &= \frac{2 \pi^2 \eta_o^2}{N_o \lambda_o^4} \left(\frac{dn}{dc} \right)^2 \\
 &= \frac{2 \pi^2 (1.330) (.1885)^2}{6.06 \times 10^{23} \times (4.36 \times 10^{-5})^4} \\
 &= 5.590 \times 10^{-7}
 \end{aligned}$$

Here, $\eta_o = 1.330$ for 0.5M KCl, 0.067M phosphate buffer,
and

$dn/dc = 0.1885$ ml/g for beef cardiac tropomyosin.

R_θ = Brice constant x working standard constant "a" x cell
constant x J_θ (corrected).

$$= 0.1650 \times .0391 \times 1.340$$

$$= .008644 J_\theta \text{ (corrected)}.$$

$$\text{Brice constant} = \frac{TD}{1.045 h \pi} \left(\eta_o^2 \frac{R_w}{R_c} \right) = .1650.$$

Values for (TD), h and $\eta_o^2 R_w / R_c$ were obtained from the
photometer manual.

From the Zimm plot:

$$\left(K_c / R_\theta \right)_{\substack{c=0 \\ \theta=0}} = 1.01 \times 10^{-5}$$

$$\text{Thus, } M_w = 99,000$$

$$(\text{slope})_{\theta=0} = 5.0 \times 10^{-5}. \text{ Thus, } B = 2.5 \times 10^{-5}.$$

$$(\text{slope})_{c=0} = 7.43 \times 10^{-7}. \text{ Thus,}$$

$$R_g = \frac{\sqrt{3 \lambda}}{4 \pi \eta_o} \sqrt{\frac{(\text{slope})_{c=0}}{(\text{intercept})_{\substack{c=0 \\ \theta=0}}}} = 124.7 \text{ \AA}$$

$$\text{Rod model } L = \sqrt{12} \text{ \AA}. R_g = 432 \text{ \AA}.$$

$$\text{Coil model } L = \sqrt{6} \text{ \AA}. R_g = 306 \text{ \AA}.$$

$$\text{Ellipsoidal model } L = \sqrt{20} \text{ \AA}. R_g = 557 \text{ \AA}.$$

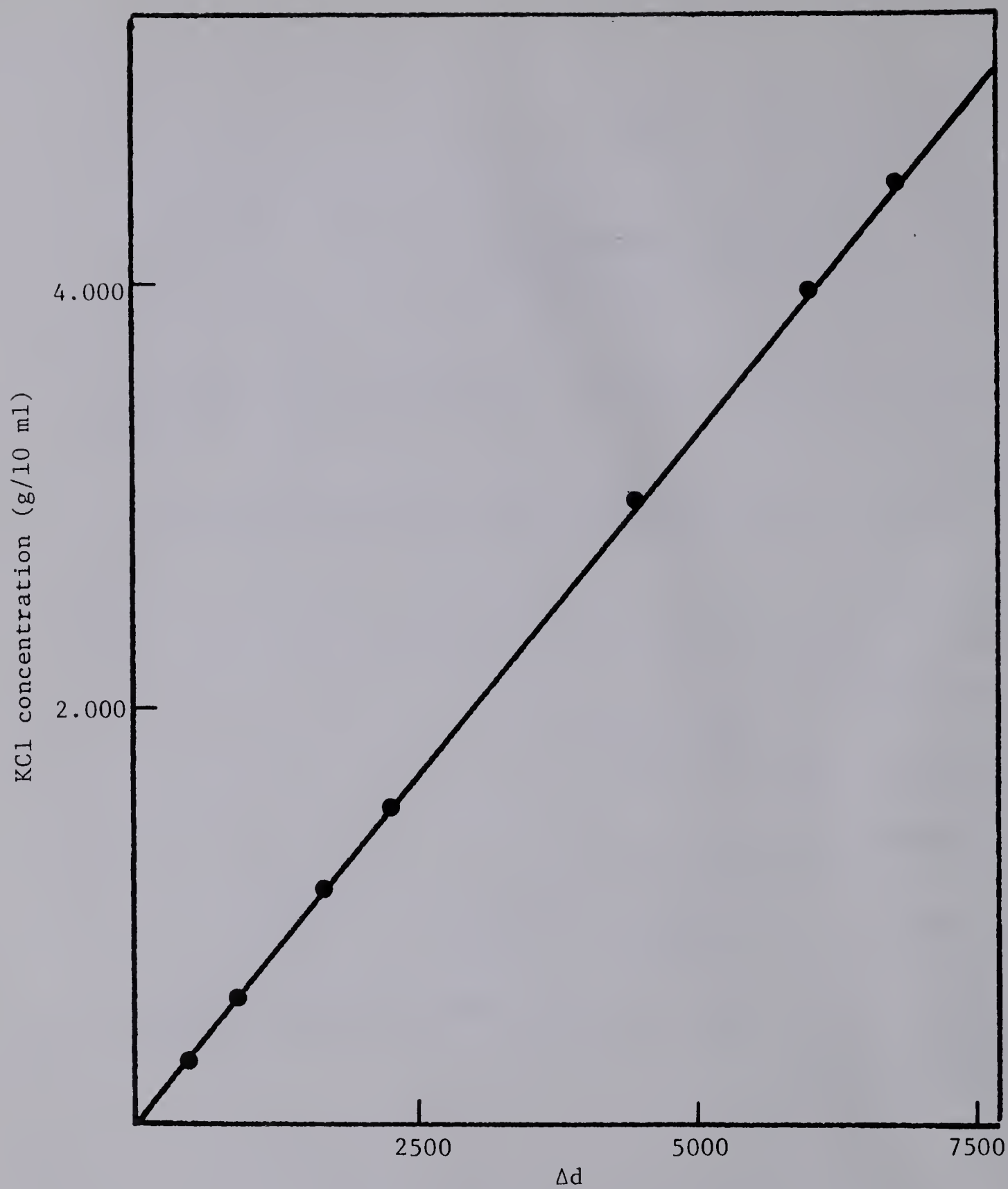


Figure 45

Δd versus concentration of KCl at $\lambda = 435.8 \text{ m}\mu$.

APPENDIX 3

Refractive Index Increment Measurements

A. Instrument calibration at $\lambda = 435.8 \text{ m}\mu$ and 25°C .

KCl g/100 ml	$\Delta n \times 10^3$ ⁽¹⁾ (refractive index difference in comparison to water)	$\Delta d \times 10^{-3}$ ⁽²⁾ (light beam displacement)	$k \times 10^6$ ⁽³⁾ (instrument constant)
.5964	0.845	.9009	.9380
1.0794	1.521	1.6305	.9328
1.4911	2.093	2.2476	.9312
2.9821	4.135	4.4017	.9394
		Average	.9350

(1) Obtained from the data of Kruis (88).

(2) Obtained from a least square plot of KCl concentration (gm/10 ml) against Δd (see Figure 45).

(3) $k = \Delta n / \Delta d$.

B. Refractive index increment measurements for beef cardiac tropomyosin in 0.5M KCl, 0.067M phosphate buffer solution, pH 7.0.

% Protein Concentration	$\Delta d \times 10^{-3}$ ⁽⁴⁾	(dn/dc) ml/gm
.785	1.588	.1888
.440	.892	.1881
.265	.532	.1875
.123	.249	.1897
	Average	.1885

(4) $\Delta d = (d_{2 \text{ Protein}} - d_{1 \text{ Solvent}}) - (d_{2 \text{ solvent}} - d_{1 \text{ Solvent}})$
(zero correction)

from which $\Delta n = k \Delta d$ and $dn/dc = \Delta n/c$.

B29841